2014

Linking Cell Cycle Delays to Apoptosis in Cancer Cells

Victoria Caruso Silva
Lehigh University

Linking Cell Cycle Delays to Apoptosis in Cancer Cells

by

Victoria Caruso Silva

A Dissertation

Presented to the Graduate and Research Committee

of Lehigh University

in Candidacy for the Degree of

Doctor of Philosophy

in

Cell and Molecular Biology

Lehigh University

May 19, 2014

Approved and recommended for acceptance as a dissertation in partial fulfillment of the requirements for the degree of Doctor of Philosophy

Victoria Caruso Silva
Linking Cell Cycle Delays to Apoptosis in Cancer Cells

April 16, 2014

Defense Date

Lynne Cassimeris, Ph.D.
Committee Chair

Approved Date

Committee Members:

Robert Skibbens, Ph.D.

Linda Lowe-Krentz, Ph.D.

Frank Luca, Ph.D.

ACKNOWLEDGMENTS

I would like to express my deepest gratitude to my advisor, Dr. Lynne Cassimeris for all of the guidance she has offered throughout my thesis work. I thank her for challenging me and encouraging me to ask big questions. It is greatly because of Lynne's support that I have found and had the courage to pursue my most passionate interests. Lynne's scientific merit is only outshined by her fantastic sense of humor and good heart. I am so fortunate to have had the opportunity to learn from and work with her.

I wish to thank my committee members, Drs. Robert Skibbens, Linda Lowe-Krentz and Frank Luca for their great enthusiasm, guidance, honest critique and support that each of them offered me over the years. I would also like to recognize all of the faculty, staff and graduate student members in the Department of Biological sciences. I thank all them for their friendship, advice and general collegiality that have made my time at Lehigh University so positive and rewarding.

I would also convey to my family and friends how integral they have been to the completion of this degree. I thank my wonderful grandparents, Anthony and Mildred for countless trips to the library, helping with my first science fair project and their general interest and unconditional support. I thank my parents Ed and Millicent for their sacrifice, loving guidance and unwavering faith in me. To my mother and father in-law, John and Sue, thank you both being so interested and completely wonderful to me over the years.

Finally, I wish to acknowledge my husband, Justin, who has been my sounding board, counselor and cheerleader. His support and encouragement through the long hours and weekends spent studying or working on research have kept me sane. He is my best friend and the person to whom I dedicate this work.

TABLE OF CONTENTS

List of Figures vi

Abstract 1

Chapter 1: Introduction

Control of Cell Fate 4

Division Cycle 4

Microtubules and the Cell Cycle 6

Microtubules at Mitotic Entry 8

Stathmin and Mitotic Entry 10

Stathmin and Cell Fate 10

Programmed Cell Death 11

cFLIP and p53 Dependent Death 13

References 16

Chapter 2:Stathmin and Microtubules Regulate Mitotic Entry in Hela Cells by Controlling Activation of both Aurora A Kinase and PLK1

Abstract 20

Introduction 21

Results 24

Discussion 37

Conclusions 41

Materials and Methods 41

References 47

Figures 56

Chapter 3: Mechanistic basis for p53-deficient cell death triggered by a mitotic entry delay

Introduction 73

Results 74

Discussion 81

Materials and Methods 84

References 89

Figures 93

Chapter 4: Conclusions and Future Directions

Future Directions 101

Stathmin and PLK1 Recruitment 101

Stathmin and AURKA Distribution 103

Caspase 8 Activation 104

Conclusions 107

References 109

Vita 111

LIST OF FIGURES

Figure 2.1: Active Aurora A at the centrosome is reduced in stathmin-depleted Hela cells.

Figure 2.2: Stathmin depletion from Hela cells decreased the level of active CDC25

Figure 2.3: P53 was restored by depletion of HPV E6 protein from Hela cells.

Figure 2.4: Inhibition of AURKA does not delay mitotic entry

Figure 2.5: Active Plk1 on chromatin is decreased in stathmin-depleted cells

Figure 2.6: Partial inhibition of both AURKA and Plk1 delays mitotic entry.

Figure 2.5: MTs are required for AURKA activation

Figure 2.8: MT depolymerization restores active Plk1 in stathmin-depleted cells without reversing the delay in Plk1 localization to centrosomes

Figure 2.9: Stathmin overexpression decreased Plk1, but not AURKA, activation level

Figure 2.11: Stathmin is phosphorylated by AURKA and inhibits Plk1 autophosphorylation in vitro

Figure 2.12: Summary of MT and stathmin regulation of AURKA and Plk1 activation

Figure 2.10: Exogenous stathmin expression restores normal MT number and mitotic entry timing

Figure 3.1: A mitotic entry delay triggers cell death in p53 deficient cells

Figure 3.2: A Wee 1 inhibitor relieved both the stathmin depletion-induced cell cycle delay and cell death Figure 3.3: A mitotic entry delay triggers caspase 8 activation

Figure 3.3: A mitotic entry delay triggers caspase 8 activation

Figure 3.4: Stathmin depletion and cFLIP regulate caspase 8 activity

ABSTRACT

For any cell within a multicellular organism, a multitude of environmental signals influence cell fate. The context and timing of these often redundant and overlapping signaling cascades govern whether a cell will differentiate, reproduce or die. Some of these signaling networks form checkpoints that sense and respond to the needs of the individual cell. In cancer, often one or more of these signals is missing or mutated which results in uncontrolled cell growth, usually to the detriment of the organism. Understanding the signaling events that normally control cell proliferation and death is important for controlling and eliminating cancerous cells. Microtubule targeting drugs have been used to disrupt mitotic progression and cause cell death in cancer cells because of their typically high proliferation rates. However, these drugs kill normal dividing cells and damage healthy tissues. Therefore, there have been great efforts to find selective ways to target cancerous cells without harming normal cells.

One of the major regulators of genomic stability in cells is p53. Mutations or gene deletions of p53 are present in over half of all cancers. Many studies have demonstrated that p53-deficient cells are uniquely vulnerable to depletion of a microtubule regulator protein called stathmin. Stathmin depletion slows proliferation via a mitotic entry delay (including results presented in Chapter 2) and increases cell death in p53-deficient cells. Research presented in this dissertation addresses the mechanisms by which stathmin loss delays mitotic entry and triggers cell death.

In order to know why cells are slow to enter mitosis we investigated the activity of the enzymes that govern mitotic entry. We previously found stathmin-depleted cells have decreased active CDK1. The level of active CDC25, which removes CDK1

inhibition, was also reduced in these cells. However, none of the upstream regulators that might inhibit CDC25 activation were changed upon stathmin depletion. Therefore, we hypothesized that loss of stathmin directly affects the core enzymes in the mitotic entry complex. We found that stathmin depletion decreases activation of Aurora A kinase (AURKA) and Polo-like Kinase 1 (PLK1), two key enzymes of the mitotic entry feedback loop that control CDK1 activation kinetics.

Since stathmin depletion delays mitotic entry and causes apoptotic cell death, we hypothesized that the cell cycle delay and cell death were linked. We found that inducing a mitotic entry delay with the use of enzyme inhibitors to AURKA and PLK1 was sufficient to trigger cell death but only in cells lacking functional p53. To understand the mechanism of the cell death in these cells we looked for activation of initiator caspases 8 and 9, the primary drivers of apoptosis. We found caspase 8 activation in both stathmin-depleted and mitotic entry-delayed cells. Additionally, we were able to rescue viability of these cells by inhibiting caspase 8 activity indicating that cell death occurs via a caspase 8 dependent pathway. CDK1 is known to inhibit a number of caspases including caspase 8 via a protective phosphorylation. We found that phosphorylation of caspase 8 at Serine 387 was decreased in stathmin-depleted cells, suggesting an increased sensitivity of caspase 8 to activation.

In order to understand the role of p53 for survival in stathmin depletion we hypothesized that p53 may regulate a caspase 8 inhibitor. We found the level of cFLIP, a major inhibitor of caspase 8, to be decreased in the absence of p53, consistent with the observations of others. We were able to rescue viability of stathmin-depleted cells by restoring cFLIP level. Therefore we concluded that in the absence of p53, decreased

cFLIP levels lower the threshold for caspase 8 activation. The absence of stathmin and p53 results in loss of two inhibitors of caspase 8. The sum of inhibition may be sufficient to either stochastically trigger cell death or increase susceptibility to other death signals. Regardless of the mechanism, modulating stathmin or disrupting mitotic entry directly represents a potential selective and potent means of targeting p53 deficient cancers.

Chapter 1: Introduction

Control of Cell Fate

For multicellular organisms, a full grown adult is comprised of trillions of cells that invariably arose from a single cell. For each cell, whether it is a zygote or part of a larger tissue or organ system, a complex array of signals determine its fate. The choice for each cell is to differentiate, reproduce or die, a decision regulated by myriad inputs that are continuously read and interpreted. Disturbances in the system of checks and balances results in inappropriate cell growth or death and can lead to degenerative disorders or cancer. Cancer cells missing these checks and balances are able to out compete their neighboring cells, outgrow their environmental boundaries and destroy normal tissue function. All of the signaling layers including feedback mechanisms and pathway cross-talk that govern cell fate remain to be fully understood. Research results contained in this dissertation describe novel layers of regulation that control timing of cell division and cell fate.

Cell Division Cycle

All proliferating cells go through the cell division cycle, during which they increase in volume and make more cell components and duplicate their genetic material. A new daughter cell exits mitosis into G1 phase where it awaits growth factor and mitogen signals, which will trigger growth of the cell and commit the cell to divide. In the absence of DNA damage or other stress, the cell will then duplicate its genome only once, as well as its centrosomes, the microtubule organizing centers, in S phase. After successful duplication, the cell prepares for division by confirming that all components

are undamaged, of appropriate number and at the right intracellular location. These checks include proper fragmentation of the Golgi apparatus, release of focal adhesions, re-localization of key signaling molecules as well as the integrity of the DNA. If all is within a normal range, the cell then prepares for mitosis where the genetic material, now condensed chromatin, as well as cytoplasmic components, organelles and various membranes segregate between the two forming cells. The transition between G2 and mitosis is highly regulated and involves multiple and redundant safeguard mechanisms to ensure that cell division occurs correctly and at the appropriate time.

The preparation for mitosis is principally an enzymatic process occurring at distinct subcellular locations. During G2, cyclin B protein level gradually rise and associate with cyclin dependent kinase 1, CDK1, at centrosomes to form mitotic cyclin dependent kinase complexes. The association of the CDK with its cyclin causes the T-loop in the kinase, which would otherwise block kinase activity, to change conformation. Phosphorylation by CAK (CDK Activating Kinase- CDK7 complexes with cyclin H) on Threonine 160 further extends the T-loop resulting in a fully active kinase. However, prior to the activating phosphorylation by CAK, another kinase, Wee1, phosphorylates at two sites, threonine 14 and tyrosine15, which inhibit full kinase activity. The result is a cyclin dependent kinase that is primed for activation.

However, like all enzymatic processes within the cell, there are rapid state changes, which result in short-lived active cyclin CDK1 without inhibitory phosphorylations present. Active CDK1 complexes can activate Polo-like kinase 1 (PLK-1) and Aurora A kinase (AURKA), which phosphorylate (activate) CDC25, a dual specificity phosphatase, to remove inhibitory phosphorylations from other cyclin

B/CDK1 complexes. In addition, CDK1 also directly phosphorylates Wee 1 kinase and inhibits its activity. These two phosphorylation events occur gradually until some critical active CDK1 concentration is reached that gives rise to a rapid and nearly complete hyperphosphorylation of both Wee1 and CDC25. The result of this hypersensitivity of Wee1 and CDC25 is an all or nothing requirement for mitotic entry, the mitotic switch (Trunnel 2011).

Following this switch, a rapid amplification of CDK1 activity results in phosphorylation of target proteins that drive a number of cellular events. Endoplasmic reticulum and Golgi membranes fragment to facilitate subsequent segregation of the organelles to new daughters. Phosphorylation of histones and condensins drive chromatin condensation. Phosphorylated nuclear lamins and nuclear envelope proteins promote the disassembly of the nuclear envelope, which is necessary for the association of chromatin with the spindle poles. In addition, microtubule associated proteins, MAPs, are also phosphorylated to facilitate reorganization of the microtubule array into the mitotic spindle (Kline-Smith 2004).

Microtubules and the Cell Cycle

Along with the accumulation of cellular signals, necessary changes occur in the microtubule cytoskeleton in order to allow the formation of the mitotic spindles, which will separate the chromatin and assist in cytokinesis. Microtubules are polar polymers consisting of alternating subunits of alpha and beta tubulin proteins that assemble from soluble heterodimer pools in the cytoplasm. Both alpha and beta tubulin have GTP in binding pockets but only the site on beta tubulin is accessible for hydrolysis. These

protofilaments, usually a set of thirteen, form hollow tubes, lending to their name, microtubules. Microtubule assembly most often begins at a microtubule organizing complex (MTOC), typically a centrosome, where several molecules of gamma tubulin with other proteins form a ring complex. This complex referred to as gamma-Tubulin Ring Complex, gamma- TURC, nucleates microtubule growth by providing both a point of nucleation for subunit addition as well a template for the appropriate pitch of the helix. Microtubule assembly is driven by the concentration of free subunits of tubulin dimers. Subunit addition takes place primarily at plus ends since in vertebrate cells the minus ends are anchored to the MTOC. Initially a new microtubule forms a sheet-like lattice, which rolls up into a cylinder once it has grown enough. As new subunits are added, the GTP in beta tubulin already incorporated into the polymer hydrolyzes, a process that is actually stimulated by the longitudinally adjacent alpha-tubulin. GDP-beta tubulin has a curved formation that opposes the stable straight structure of the cylinder. The remaining GTP-beta tubulin at the plus ends prevents disassembly of the polymer by holding the protofilaments in a straight conformation and is referred to as the GTP cap. Hydrolysis of these GTP-tubulins leads to loss of the GTP cap, an event called catastrophe, allowing the protofilaments, which make up the microtubule to peel outward from the central axis of the cylinder. Tubulin subunits are lost and the microtubule shortens until complete disassembly or a new GTP-cap can form, an event defined as rescue. The fate of the caps and the longevity of each microtubule can also be affected by microtubule associated proteins, MAPs, which can either promote or decrease stability of the cylinder.

Within many interphase cells, there are typically two populations of microtubules, a population that is stable and a larger one that exhibits this dynamic instability. The

dynamic microtubules are able to search the intracellular space and interact with peripheral proteins that link them to other cellular structures such as actin filaments as well as to position the centrosome within the cell (Wade 2009, Akhmanova 2008).

The traditional view of microtubule dynamics holds that changes in dynamics are driven by cellular signals originating both inside and outside of the cell. Most research has focused on the effect signaling molecules have on the cytoskeleton; however, there are also many examples of how changes within the microtubule array can result in changes in activation or locations of signaling molecules. For example, Rho guanine exchange factor, HEF1, binds microtubules but upon nocodazole treatment, it becomes unbound and can activate Rho (Chang 2008). This example and others demonstrate how signaling can arise in an inside-out fashion. The microtubule state can relay cellular signals by controlling the location and availability of key signaling molecules.

At mitotic entry the characteristics and number of microtubules changes drastically. This change is brought on by changes to the microtubule associated proteins that are regulated by CDK1. The long, stable microtubules that persist during interphase must be disassembled rapidly in order to form the mitotic spindle.

Microtubules at Mitotic Entry

The microtubule transition between interphase and mitosis occurs at the end of prophase at nuclear envelope breakdown. Work by the Borisy lab group characterized the key events that occurred in the microtubule array at this point of the cell cycle. The two possibilities for rearranging the microtubule skeleton were that the network was reorganized, keeping the majority of polymer together like the established mitosis/G1

transition or that the microtubules were first disassembled and then rebuilt from individual subunits. Using fluorescence redistribution after photoactivation to measure MT turnover, they discovered that there was a steep drop in polymer near the time of nuclear envelope breakdown (NEB) and a corresponding increase in soluble tubulin. There is a shift in microtubule arrangement, the long cytoplasmic microtubules that spanned the radius of the cell disappear and in their place are short microtubules distributed out of the centrosome early in prometaphase, or the forming spindle. By metaphase, the majority of microtubules originate in the spindle and are oriented toward the aligned chromatids; few astral microtubules also exist. In order for a new interphase array to form once mitosis is complete, there is no disassembly of the mitotic array, as indicated by no drop in polymer level, the tubulin is reorganized among the existing microtubules (Zhai 1996).

Further work by the Wadsworth lab characterized the complete reorganization of microtubules at NEB by looking at individual microtubules. They found that the depolymerization that takes place is due to an increase in the incidence of catastrophe, a decrease in pausing and a decrease in rescue frequency. They divided collapse of the array into two mechanisms. The first is the increase in dynamic instability of individual microtubules. The second mechanism arose from observations of short microtubule bundles moving along individual microtubules towards the centrosome. They determined that cytoplasmic dynein was predominantly responsible for the minus end directed motion of these bundles. It is likely that both of these mechanisms are necessary for complete remodeling of the microtubule array to form a spindle (Rusan 2002).

Stathmin and Mitotic Entry

Work by a number of labs revealed a requirement for a microtubule regulatory protein, stathmin, in proliferation and survival of certain cancer cells. Initial studies using stathmin-targeted ribozymes or survivin-promoter driven siRNA expression vector, identified that loss of stathmin leads to an accumulation of G2/M cells, loss of clonogenicity and increased apoptosis in a prostate cancer cell line and slowed proliferation and increased cell death in cancerous but not in non-cancerous cell lines (Mistry 2005, Zhang 2006). Small interfering RNA targeting stathmin also increased sensitivity to treatment with chemotherapeutic taxanes, making stathmin an attractive candidate for cancer therapies (Alli 2002, Wang, 2007). Stathmin transcription and subsequent protein level are negatively regulated in part by p53 (Murphy 1999). Work by the Hait lab attempting to restore some function to p53 deficient cells by depleting stathmin discovered that stathmin loss in p53 deficient cells caused slowed proliferation and apoptotic cell death (Alli 2007). Alli et al. suggested that loss or mutation of p53 specifically in combination with stathmin depletion gave rise to two unique phenotypes, a G2/M arrest and apoptosis. If this model were correct it would suggest that loss of stathmin, perhaps via microtubule changes, and loss of p53 signaling are read and summed by individual cells to negatively influence cell fate.

Stathmin and Cell Fate

Stathmin acts as a microtubule destabilizer by both sequestering free tubulin and promoting catastrophe of existing microtubules (Howell 1999, Larsson 1999, Belmont and Mitchison 1996). Phosphorylation of stathmin at four serine sites renders stathmin

functionally off with respect to tubulin, a modification that occurs during mitosis and in response to various stresses such as heat shock, changes in cellular calcium, and through ASK1, p38 and JNK signaling (Beretta 1995, Larsson 1999, Gradin 1997, Hu 2010, Mizumura 2006). It was initially proposed that stathmin, from the Greek "stathmos" meaning "station" acts as a cellular relay to regulate cellular proliferation, differentiation and function (Sobel 1991). Therefore stathmin's name seems particularly fitting given what we now know about stathmin's role in cell proliferation and survival, which is presented in Chapter's 2 and 3 of this dissertation.

Previous research from the Cassimeris Lab revealed that stathmin depletion leads to slowed proliferation caused by a mitotic entry delay (Carney 2012) and that interaction of stathmin and tubulin are necessary for timely mitotic entry (Carney *unpublished)*. The cell death observed in stathmin-depleted cells appeared to be apoptosis, based on observed cell morphology, presence of cleaved PARP and involvement of caspase 3 activity and was confirmed to be dependent on the absence of p53 as restoration of the p53 rescued cells from death (Carney 2010, 2012). As described in Chapter 2 of this dissertation, stathmin depletion delays mitotic entry via decreased activation of mitotic kinases AURKA and PLK1, which slows kinetics of CDK1 activation. Decreased CDK1 activity at mitotic entry as is found with stathmin depletion is sufficient to induce cell death in cells missing p53, demonstrated in Chapter 3 of this dissertation.

Programmed Cell Death

When it comes to cells there are many ways to die including: necrosis, entosis, mitotic catastrophe and autophagy, perhaps the most studied however, is apoptosis, a

form of programmed cell death. Apoptosis is characterized by distinct morphological changes and enzymatic events involving signal cascades by caspases. Cells undergoing programmed cell death typically undergo blebbing to form apoptotic bodies that *in vivo* will be engulfed by phagocytic cells such as macrophages. The signal that initiates apoptotic cell death can originate from within the cell or from the external environment. Loss of mitochondrial outer membrane integrity (MOMP) allows release of cytochrome c, which facilitates oligomerization of APAF, which recruits and dimerizes/activates caspase 9. Activation of caspase 9 to form the apoptosome triggers cleavage and activation of executioner caspases 3 and 7, leading to cleavage of other substrates that lead to the chemical and physical changes associated with apoptosis (Green 2005). These changes include nuclear fragmentation, exposure of phosphatidylserine on the outer plasma membrane and formation of microvesicle or apoptotic bodies.

Apoptosis can also be initiated from external signals and may or may not include MOMP. Extracellular death ligands such as Fas ligand or TNFα bind to death receptors and induce oligomerization and recruitment of adaptor proteins such as FADD or TRADD respectively. Death domain association facilitates binding of procaspase 8 and autolytic cleavage to produce active caspase 8. Caspase 3 and 7 are activated by caspase 8 and apoptosis proceeds by the same pathway as described with caspase 9 activation (Wang 2008). New findings have also uncovered unconventional roles for caspase 8 activity both in cell death and survival that can be independent of death signaling (Day 2008). In the absence of a caspase activator, removal of apoptotic inhibitors such as occurs in genotoxic stress can be sufficient to induce caspase 8 dependent cell death (Tenev 2011). Additionally, the autoprocessing of caspase 8 is also inhibited by

phosphorylation by CDK1/cyclin B and ERK, which elevate the threshold necessary for a cell's response to extrinsic death signals. (Matthess 2010).

In addition to caspase 8, CDK1/cyclin B also regulates and inhibits activation of Caspase 1, 2, 4, 5, and 9 (Andersen 2009, Harley 2010). Clearly cells at mitosis are strongly protected against cell death perhaps due to their inherent vulnerability during this portion of the cell cycle. During division cells undergo loss of attachment and mitochondrial fission that may otherwise trigger death from anoikis response or accidental cytochrome c release (Andersen 2009). As described in Chapter 3, caspase 8 phosphorylation at Serine 387 by CDK1 is significantly reduced in both stathmin depletion and direct CDK1 inhibition, translating to a lowered threshold for caspase 8 activation in these cells.

cFLIP and p53 Dependent Death

Cellular FLICE Protein, cFLIP, is an anti-apoptotic regulator that binds to FADD and/or caspase 8, 10 (Safa 2012). Caspase 8 activation and cleavage occurs in two steps. Upon homodimerization, caspase 8 autoproteolysis produces two cleavage products, a p43 and p10 subunit from each procaspase 8. Each p43 subunit is further cleaved to produce a p18 subunit that complexes with p10 subunit. Two p18 and p10 subunits oligomerize to form a fully active caspase 8 complex. At certain cellular concentrations, cFLIP promotes initial autocatalytic processing to p43 from procaspase 8 but inhibits further cleavage required for fully active caspase 8, p18/p10 complex formation (Budd 2006, Krueger 2001). However, cells are sensitive to changing levels of cFLIP protein and at low or high concentrations cFLIP can promote death by dimerizing with caspase 8

resulting in full caspase activation (Chang 2002). cFLIP's specific role in caspase 8 regulation and ultimate cell fate decisions is complicated and still incompletely described. However, siRNA to cFLIP sensitizes cells to other apoptotic triggers such as TRAIL signaling (Safa 2012, Galligan 2005).

Intracellular levels of cFLIP are regulated in part by p53, which has been suggested to control cFLIP transcription and/or degradation (Bartke 2010, Fukazawa 2001). Mutations and deletions of p53 therefore correlate with changes in cFLIP levels that increase susceptibility of cells to caspase 8 dependent death. As described in Chapter 3 of this dissertation, in the absence of p53, cFLIP levels are decreased which in conjunction with CDK1 inhibition is sufficient to trigger cell death. Restoring cFLIP levels in stathmin-depleted cells restores cell viability indicating a role for cFLIP in inhibition of caspase 8 activation. The combinatorial effect of reduced caspase 8 phosphorylation and loss of cFLIP inhibition sums to alter the probability of apoptosis.

Cell to cell variability in total levels of caspases, cFLIP and other apoptotic regulators as well as the concentration of membrane localized death receptors likely accounts for the unpredictability in death timing. For each cell, these ratios are likely unique which accounts for the unpredictability of time of death observed in stathmin-depleted or CDK1 inhibited cells. As described in Chapter 3, activation of a cell death pathway is stochastic, occurring not during the mitotic entry delay but rather hours to days following the initial delay. The only time cell death is rarely observed is during mitosis as almost all cell death occurs at some point during interphase. These cells die at variable times following mitotic exit suggesting that death is not triggered by a specific cell cycle event.

These findings suggest that targeting stathmin or mitotic entry are attractive therapeutic strategies for p53 null and loss of function mutations as they cause no or minimal mitotic disruption and selectively favor death in p53 deficient cells. AURKA or PLK1 inhibitors are currently in clinical phase I and II clinical trials. Either inhibitor at established effective doses yields a distinct mitotic arrest with abnormal spindles, which leads to mitotic slippage and cell death or aneuploidy (Steegmaier 2007, Lu 2010, Hoar 2007). However, combination therapy of lower concentrations AURKA and PLK1 inhibitors has the potential to only effect mitotic entry. Thus proper titration of combined inhibitors may allow mitosis to proceed normally avoiding adverse effects on normal dividing cells as well as aneuploidy. Alternatively, small molecule inhibitors or viral mediated knockdown of stathmin in tumor cells may offer greater selectivity and success as prospective therapies, particularly in combination with low doses of other effective compounds such as taxanes (Miceli 2013, Mistry 2007, Alli 2002). Research described in this dissertation suggests interrupting mitotic entry as a novel therapeutic approach for the selective targeting of the majority of cancer cells.

References:

1. Soussi T (2000) The p53 tumor suppressor gene: from molecular biology to clinical investigation. Annals of the New York Academy of Sciences 910:121-137; discussion 137-129.
2. Green DR & Kroemer G (2009) Cytoplasmic functions of the tumour suppressor p53. Nature 458(7242):1127-1130.
3. Matoba S, et al. (2006) p53 regulates mitochondrial respiration. Science 312(5780):1650-1653.
4. Nantajit D, et al. (2010) Cyclin B1/Cdk1 phosphorylation of mitochondrial p53 induces anti-apoptotic response. PloS one 5(8):e12341.
5. Vecil GG & Lang FF (2003) Clinical trials of adenoviruses in brain tumors: a review of Ad-p53 and oncolytic adenoviruses. Journal of neuro-oncology 65(3):237-246.
6. Prabhu VV, et al. (2012) Therapeutic targeting of the p53 pathway in cancer stem cells. Expert opinion on therapeutic targets 16(12):1161-11
7. Martin L, et al. (2014) Identification and characterization of small molecules that inhibit nonsense mediated RNA decay and suppress nonsense p53 mutations. Cancer research.
8. Reaper PM, et al. (2011) Selective killing of ATM- or p53-deficient cancer cells through inhibition of ATR. Nature chemical biology 7(7):428-430.
9. Schoppy DW & Brown EJ (2012) Chk'ing p53-deficient breast cancers. The Journal of clinical investigation 122(4):1202-1205.

10. Jemaa M, et al. (2012) Selective killing of p53-deficient cancer cells by SP600125. EMBO molecular medicine 4(6):500-514.
11. Liu X, Lei M, & Erikson RL (2006) Normal cells, but not cancer cells, survive severe Plk1 depletion. Molecular and cellular biology 26(6):2093-2108.
12. Mistry SJ, Bank A, & Atweh GF (2005) Targeting stathmin in prostate cancer. Molecular cancer therapeutics 4(12):1821-1829.
13. Belletti B & Baldassarre G (2011) Stathmin: a protein with many tasks. New biomarker and potential target in cancer. Expert opinion on therapeutic targets 15(11):1249-1266.
14. Zhang HZ, et al. (2006) Silencing stathmin gene expression by survivin promoter-driven siRNA vector to reverse malignant phenotype of tumor cells. Cancer biology & therapy 5(11):1457-1461.
15. Alli E, Bash-Babula J, Yang JM, & Hait WN (2002) Effect of stathmin on the sensitivity to antimicrotubule drugs in human breast cancer. Cancer research 62(23):6864-6869.
16. Wang R, et al. (2007) Inhibiting proliferation and enhancing chemosensitivity to taxanes in osteosarcoma cells by RNA interference-mediated downregulation of stathmin expression. Mol Med 13(11-12):567-575.
17. Alli E, Yang JM, Ford JM, & Hait WN (2007) Reversal of stathmin-mediated resistance to paclitaxel and vinblastine in human breast carcinoma cells. Molecular pharmacology 71(5):1233-1240.

18. Carney BK & Cassimeris L (2010) Stathmin/oncoprotein 18, a microtubule regulatory protein, is required for survival of both normal and cancer cell lines lacking the tumor suppressor, p53. Cancer biology & therapy 9(9):699-709.
19. Silva VC & Cassimeris L (2013) Stathmin and microtubules regulate mitotic entry in HeLa cells by controlling activation of both Aurora kinase A and Plk1. Molecular biology of the cell 24(24):3819-3831.
20. Carney BK, Caruso Silva V, & Cassimeris L (2012) The microtubule cytoskeleton is required for a G2 cell cycle delay in cancer cells lacking stathmin and p53. Cytoskeleton (Hoboken) 69(5):278-289.
21. Green DR (2005) Apoptotic pathways: ten minutes to dead. Cell 121(5):671-674.
22. Andersen JL, et al. (2009) Restraint of apoptosis during mitosis through interdomain phosphorylation of caspase-2. The EMBO journal 28(20):3216-3227.
23. Matthess Y, Raab M, Sanhaji M, Lavrik IN, & Strebhardt K (2010) Cdk1/cyclin B1 controls Fas-mediated apoptosis by regulating caspase-8 activity. Molecular and cellular biology 30(24):5726-5740.
24. Fukazawa T, et al. (2001) Accelerated degradation of cellular FLIP protein through the ubiquitin-proteasome pathway in p53-mediated apoptosis of human cancer cells. Oncogene 20(37):5225-5231.
25. Galligan L, et al. (2005) Chemotherapy and TRAIL-mediated colon cancer cell death: the roles of p53, TRAIL receptors, and c-FLIP. Molecular cancer therapeutics 4(12):2026-2036.

26. Grinshtein N, et al. (2011) Small molecule kinase inhibitor screen identifies polo-like kinase 1 as a target for neuroblastoma tumor-initiating cells. Cancer research 71(4):1385-1395.
27. Hirai H, et al. (2009) Small-molecule inhibition of Wee1 kinase by MK-1775 selectively sensitizes p53-deficient tumor cells to DNA-damaging agents. Molecular cancer therapeutics 8(11):2992-3000.
28. Vassilev LT, et al. (2006) Selective small-molecule inhibitor reveals critical mitotic functions of human CDK1. Proceedings of the National Academy of Sciences of the United States of America 103(28):10660-10665.

Chapter 2:

Abstract

Depletion of stathmin, a microtubule destabilizer, slows cell proliferation and delays cells during G2. We find that mitotic entry is delayed in these cells through reduced activation of CDC25 and its upstream activators, Aurora A and Plk1. Reduced activation of both Aurora A and Plk1 is likely responsible for the cell cycle delay since treatment with chemical inhibitors to both enzymes, but not to either kinase alone, delayed mitotic entry with timing similar to that in stathmin-depleted cells. Aurora A localization to the centrosome required an intact microtubule cytoskeleton and stathmin depletion spread its localization beyond that of γ-Tb at the centrosome, indicating a microtubule-dependent regulation of Aurora A activation. Plk1 was inhibited by excess stathmin, detected using in vitro assays and in cells overexpressing stathmin-CFP. Recruitment of Plk1 to the centrosome was delayed in stathmin-depleted cells; this delayed localization was independent of microtubules. Depolymerizing microtubules with nocodazole abrogates the stathmin-depletion induced cell cycle delay (Carney et al., 2012) and restored Plk1 activity to near normal levels, demonstrating that microtubules also contribute to Plk1 activation. These data demonstrate that stathmin regulates mitotic entry, partially via microtubules, to control localization and activation of both Aurora A and Plk1.

Introduction

Several current cancer therapies are aimed at halting cell division and most do so by disrupting the microtubule (MT) cytoskeleton (Jordan and Wilson, 2004). However, these therapies also damage normal tissue and therefore have widespread toxicity. More selective approaches are being developed that target MT accessory proteins and/or exploit possible synergies between new and current therapies (Jordan and Kamath, 2007*;* Mitra *et al.,* 2011; Leinung *et al.,* 2012).

The microtubule regulatory protein, stathmin, has been implicated in survival of certain cancer cell lines, including those missing a functional p53 protein. Depleting cells of stathmin leads to slowed growth (Zhang *et al.,* 2006; Chen *et al.,* 2007; Wang *et al.,* 2007; Carney and Cassimeris, 2010; Carney *et al.,* 2012), an accumulation of cells with 4N DNA content (Alli *et al.,* 2002; Mistry *et al.,* 2005) and an increased occurrence of apoptosis (Alli *et al.,* 2007; Belletti *et al.,* 2011). However, the mechanisms slowing proliferation and causing cell death have not been defined but at least in some cases depend on loss of both p53 and stathmin (Carney and Cassimeris, 2010). Interpretations by others suggest that stathmin depletion leads to a G2/M (Johnsen *et al.,* 2000; Polager *et al.,* 2003) or mitotic block (Alli *et al.,* 2007*)* however, stathmin is phosphorylated during mitosis at four serine sites by CDKs and other protein kinases and is functionally off with respect to MT regulation (Larsson *et al.,* 1997; Holmfeldt *et al.,* 2009). We previously demonstrated that stathmin depletion in Hela cells leads to an accumulation of cells in the G2 cell cycle stage (Carney and Cassimeris, 2010) and an increase in the interphase duration without a change in the timing of mitosis (Carney *et al.,* 2012). Based

on these data we hypothesized that stathmin-depleted cancer cells were slowed in G2 prior to mitotic entry.

The commitment to enter mitosis relies on integration of various environmental and cellular inputs that either drive or slow progression into mitosis by regulating the activation state of cyclin B/CDK1. Beginning in early G2, cyclin B level rises in the cytosol and by mid-G2 cyclin B accumulates on centrosomes in complex with CDK1, forming what is historically known as the maturation-promoting factor (Linqvist *et al.,* 2009). The cyclinB-CDK1 complex is both negatively and positively regulated by phosphorylations by Wee1 kinase at threonine 14 and tyrosine 15 and by CAK1 at threonine 160, respectively. CDC25 B/C phosphatases remove the inhibitory phosphorylation allowing for full kinase activity. Accumulation of active CDC25, a key component of the "mitotic trigger", occurs rapidly (Trunnel *et al.,* 2011). The events leading to maximal activation of CDK1 are highly regulated. Positive and negative feedback pathways ensure that the commitment to enter mitosis, including nuclear envelope breakdown, only occurs when all checkpoints have been satisfied (Reider, 2011). DNA damage, defects in Golgi fragmentation, perturbations of proteins functioning in cell adhesion and activation of cellular stress pathways such as those involving p38 can arrest cells in G2 until the stressor or damage is addressed (Ando *et al.,* 2007; Persico *et al.,* 2010; Molli *et al.,* 2010; Reinhardt *et al.,* 2010; Michal *et al.,* 2012). Most of these inhibitory signals directly or indirectly converge at the level of CDK1 via CDC25 phosphatase activation at the centrosome (Perry and Kornbluth, 2007).

The centrosome serves as the major localization site for enzymes controlling mitotic entry in addition to its role as the microtubule-organizing center of the cell

(Kramer *et al*., 2004). There is evidence to support overlap of these processes, in particular mitotic enzymes such as Plk1 and Aurora A Kinase (AURKA) regulate MT nucleation and assembly at centrosomes (Kang *et al.,* 2006; Katayama *et al.,* 2008; Xu and Dai, 2011; Toya *et al.,* 2011). Therefore, it is likely that MTs may in turn also affect activity and/or localization of these molecules.

The MT cytoskeleton also functions in signal transduction, acting either through MT dynamics or through sequestration of MT interacting proteins (Gunderson and Cook, 1999; Reider and Cole, 2000; Ezratty *et al.,* 2005; Efimov and Kaverina, 2009). Stathmin binds tubulin dimers and/or MTs to control partitioning of tubulin between the soluble and polymer pools (Holmfeldt *et al.,* 2007; Sellin *et al.,* 2008). Stathmin also regulates MT nucleation at centrosomes and therefore sets MT number (Howell *et al.,* 1999; Ringhoff and Cassimeris 2009).

From our previous results showing that cells depleted of stathmin were delayed in the G2 phase of the cell cycle, we concluded that stathmin was necessary for timely progression through G2 and entry into mitosis (Carney and Cassimeris*,* 2010). Additionally, we found that the delay induced by stathmin depletion could be abrogated by treatment with nocodazole to depolymerize MTs, suggesting that stathmin's role is carried out via microtubules, a new function for the MT cytoskeleton in mitotic entry (Carney *et al.,* 2012). In order to determine the cause of delayed mitotic entry induced by stathmin depletion, we examined the signaling pathways that converge on cyclin-B/CDK1 activation. We found that levels of active AURKA and Plk1 were significantly decreased in stathmin-depleted prophase cells and that a G2 delay could be induced by treatment with chemical inhibitors to not one, but to both AURKA and Plk1 enzymes.

These data support a model where decreased stathmin level delays mitotic entry by inhibiting both of these enzymes. To test whether AURKA and Plk1 were regulated by stathmin via MTs, we treated stathmin-depleted cells with nocodazole and were able to partially restore activity of Plk1, but not of AURKA. We discovered that AURKA localization at the centrosome and subsequent activation was abolished by nocodazole treatment, indicating a role for MTs in AURKA recruitment to the centrosome. Plk1 recruitment to centrosomes was delayed in stathmin-depleted cells, and this delayed recruitment was independent of MTs. Collectively these data indicate that stathmin, at least partially through its effects on MTs, regulates mitotic entry by controlling activation of both AURKA and Plk1, a novel role for MTs in cell cycle progression.

Results:

Common G2 checkpoint pathways are not activated by stathmin depletion

To determine why loss of stathmin delays mitotic entry, we first asked whether stathmin depletion activated upstream checkpoint pathways that ultimately reduce CDK1 activation. SiRNA transfection reduced stathmin protein level to approximately 25% of that in cells transfected with a non-targeting siRNA. Protein depletion was detected within 24 hours and knockdown was maintained beyond 48 hours post transfection (Figure 1 B; note that an shRNA targeting a second region in stathmin produced the same knockdown and delay in G2, Carney and Cassimeris, 2010). We had previously shown that stathmin depletion increased the population of cells staining positive for CDK1(Y15P) (inhibitory phosphorylation) indicating that cyclinB-CDK1 complexes were present, but less active in these cells (Carney and Cassimeris, 2010). The inhibitory

phosphorylation is removed by CDC25 phosphatases (Figure 2.1, A). We found that active CDC25, marked by phosphorylation at T48, a modification necessary for full phosphatase activity (Izumi and Maller, 1993) was reduced in stathmin-depleted cells (Figure 2.2). Several G2 checkpoint pathways converge at the level of CDC25's, where activation of a checkpoint inhibits CDC25 activation. We examined several G2 checkpoint proteins for modifications that could lead to decreased CDC25 activation. We did not find evidence to support activation of these upstream pathways, including: p38 (via phosphorylation on T180 or Y182), DNA damage responsive pathways (via CHK1 phosphorylation on S317) or Wee 1 kinase (predominantly regulated by protein level). Additionally, cyclin B protein levels accumulated normally in these cells (data not shown) indicating that the delayed mitotic entry was not due to disruption of an earlier event. Because we saw diminished activation of CDC25 phosphatase, without activation of several upstream pathways that respond to signals and inhibit CDC25, we next examined the activation of AURKA and Plk1, two enzymes able to activate CDC25.

Stathmin depletion reduces active Aurora A kinase on centrosomes

Since AURKA plays a major role in activation of CDC25 and is part of a positive feedback loop including Plk1 and CDC25 that fully activates CDK1/cyclin B (Dutertre *et al*., 2004; Figure 2.1, A), we examined the levels of active AURKA in stathmin-depleted Hela cells. In late G2, AURKA is recruited to the centrosome where it is activated following its dimerization, which facilitates autophosphorylation at T288 (Eyers *et al.,* 2003; Joukov *et al.,* 2010). Phosphorylation of T288 is typically used as a convenient marker of active AURKA (Ohashi *et al,.* 2006). We found that the amount of active

AURKA kinase at the centrosomes of Hela cells was reduced to ~ 50% of control levels as determined by quantitative immunofluorescence using an antibody specific for AURKA T288P (Figure 2.1, E and F). This reduced activation was not due to a reduction in total AURKA protein level (Figure 2.1, C and D).

Our previous data indicated that loss of both stathmin and p53 was necessary for slowed cell proliferation (Alli *et al.,* 2007; Carney and Cassimeris, 2010), so we also asked whether p53 protein level contributed to the decline in active AURKA, or whether the inhibition was strictly dependent on stathmin. Hela cells normally lack detectable levels of p53 because the HPV viral protein E6, present in these cells, targets p53 for proteasomal degradation (Scheffner *et al.,* 1990). Depletion of viral protein E6 in Hela cells allowed p53 to accumulate (Koivusalo *et al.,* 2005, Figure 2.3). Restoring p53 did not change the levels of either total or active AURKA at centrosomes (Figure 2.1, C, E and F). We also found that regardless of p53 level, stathmin depletion was sufficient to decrease AURKA T288P levels, indicating that stathmin, and not p53, controls activation of AURKA at the centrosome (Figure 2.1, E and F) in these cells.

Inhibiting AURKA with specific kinase inhibitor S 1451 is not sufficient to slow mitotic entry

We next asked whether partial inhibition of AURKA was sufficient to delay mitotic entry by treatment with a chemical inhibitor. Using a specific inhibitor to AURKA, S 1451, which blocks phosphorylation of AURKA on T288 (Yuan *et al.,* 2012), we treated Hela cells with 300 nM S 1451 and measured the phosphorylation states of AURKA and Plk1. The inhibitor concentration was chosen based on published IC50

values (Aliagas-Martin *et al.,* 2009) and confirmed in cell proliferation assays (our unpublished data). We found that the level of AURKA T288P at centrosomes in S 1451 treated Hela cells was reduced to 50% of DMSO-treated cells (Figure 2.4, A), which matches the reduction in active AURKA measured after stathmin depletion (see Figure 2.1 E and F). We found that treatment with S 1451 did not change the level of active Plk1 (T210P) (data not shown), which was surprising since AURKA activity is necessary for Plk1 activation (Seki *et al.,* 2008). It is possible that the residual 50% active AURKA is sufficient to activate Plk1.

To ask whether AURKA inhibition was sufficient to delay progression through interphase, we followed individual cells by phase contrast microscopy, collecting images at 5 minute intervals for up to 72 hours. Interphase and mitotic durations were measured as described in Methods. Treatment of Hela cells with 300nM S 1451 did not increase interphase duration but rather shortened interphase by approximately 30 minutes compared to DMSO treated controls (Figure 2.4, B). Mitotic duration in S 1451 treated cells was significantly increased by an average of 1 hour (Figure 2.4, C) as others have reported (Hoar *et al*., 2007). These chemical inhibitor studies indicate that stathmin depletion cannot delay mitotic entry only by partial inhibition of AURKA.

Stathmin depletion leads to decreased levels of active Plk1 within the nucleus

Plk1 is necessary for G2 checkpoint maintenance and recovery from checkpoint activation through its phosphorylation (activation) of CDC25 (Tsvetkov and Stern, 2004; Macurek *et al.,* 2008). We hypothesized that the cell cycle delay induced by stathmin depletion also involved reduced activation of Plk1. We found that total levels of Plk1 do

not change with stathmin depletion as measured by western blot (Figure 2.5, A) or immunofluorescence (Figure 2.5, B). However, active Plk1 within the nucleus, as measured by quantitative immunofluorescence of phosphorylation on T210 (Lowery *et al.,* 2005), was reduced in stathmin-depleted cells to 30% of control levels (Figure 2.5, C and D), and confirmed by western blot (Figure 2.5, E). We observed Plk1 (T210P) predominantly within the nucleus, consistent with a previous report (Lee *et al.,* 2008). We did not consistently observe phosphorylated Plk1 (T210P) on centrosomes, unlike what some have observed (Kishi *et al.,* 2009), therefore we confined our measurements to nuclear-localized, active Plk1. It is likely that centrosome-localized phospho-Plk1 was not detected by the antibody used here since we clearly observed Plk1 on centrosomes with an antibody recognizing the protein independent of its phosphorylation state, as described below.

Consistent with previous reports, we confirmed that p53 restoration in Hela cells reduced total Plk1 protein level (Figure 2.5, A) concomitant with p53's role in Plk1 transcription inhibition (McKenzie *et al.,* 2010). Restoring p53 by depletion of E6 also reduced the level of active Plk1 on chromatin (T210P level; Figure 2.5 C and D). The decreased activation of Plk1 in these cells is likely due, at least in part, to reduced Plk1 expression. Taken together, these data indicate that p53 controls Plk1 expression while stathmin depletion reduces Plk1 activation.

Since stathmin depletion led to a reduction in both active AURKA and Plk1, it is possible that either partial inhibition of Plk1, or the combined partial inhibition of both AURKA and Plk1 was responsible for the delayed mitotic entry observed in stathmin-depleted cells. We next used chemical inhibitors to test these possibilities.

Inhibiting Plk1 with inhibitor BI 2536 is not sufficient to slow mitotic entry

If the G2 delay induced by stathmin depletion were due to reduced Plk1 activation, then we would expect that chemical inhibition of Plk1 would delay mitotic entry. To inhibit Plk1 we used a specific inhibitor, BI 2536, at a concentration based on published IC50 values (Steegmaier *et al.,* 2007) and confirmed in cell proliferation assays (our unpublished data). We treated Hela cells with 0.8 nM BI 2536 and measured cell cycle times. Inhibition of Plk1 with BI 2536 increased interphase duration by approximately 2.5 hours (Figure 2.6, A) and increased mitotic duration by about eleven minutes (Figure 2.6, B). Although the increased time in mitosis was modest, the lengthening of mitosis was statistically significant compared to DMSO-treated controls. The Plk1 inhibitor used here blocks the enzyme's ATP binding pocket but does not prevent phosphorylation at T210 (Scutt *et al.,* 2009), typically used as a marker of enzyme activation. Therefore we could not use T210P as a measure of Plk1 inhibition.

Although Plk1-inhibited cells took longer to progress through interphase, this delay could reflect either a delay in mitotic entry or earlier in the cell cycle since Plk1 was recently reported to function in late G1 by regulating firing of replication origins (Song *et al.,* 2012). To test whether the small interphase delay observed in BI 2536 treated cells was due to delayed mitotic entry, we synchronized cells with a double thymidine block and released them into media containing 0.8nM BI 2536. Mitotic index was determined at 2-hour intervals for 12 hours after release. We found that Hela cells synchronized at the G1/S border and released into Plk1 inhibitor, BI 2536, entered mitosis with normal timing compared to control cells released into DMSO (Figure 2.6,

C). These data demonstrate that Plk1 inhibition alone is not sufficient to delay mitotic entry.

Simultaneous Inhibition of both AURKA and Plk1 delays mitotic entry

Inhibition of either AURKA or Plk1 alone did not mimic the G2 delay induced by stathmin depletion and we therefore hypothesized that partial inhibition of both enzymes was necessary to produce a cell cycle delay. We treated asynchronously growing Hela cells with a combination of 300 nM S 1451 and 0.8 nM BI 2536 to inhibit both AURKA and Plk1 kinases. Cells treated with both inhibitors were delayed significantly in mitosis and many died by apoptosis (detected by changes in cell morphology) and as such we were not able to calculate interphase durations in these cells. To avoid possible effects of a prolonged preceding mitosis and loss of cell number due to death, we synchronized cells at the G1/S border using a double thymidine block, released cells into media containing both 300nM S 1451 and 0.8nM BI 2536 and determined mitotic index at 2 hour intervals for 12 hours. The combination of inhibitors delayed the peak of mitotic entry by 4 hours; shifting from 8 hours to 12 hours post release compared to DMSO-treated control cells (Figure 2.6, C). This delay is similar to the 4.6 hour delay measured in stathmin-depleted cells (Carney *et al*., 2012). We then wanted to confirm that stathmin depletion delays cells by partial inhibition of AURKA and PLK1 and not some other parallel pathway governing mitotic entry. To address this possibility we, treated synchronized control transfected or stathmin-depleted cells with a double thymidine block, released them into media containing DMSO or a combination of 300nM S1451 and BI2536 and then determined mitotic index at timepoints for the next 14 hours. We found that control transfected cells released into S1451 and BI2536, stathmin-depleted

cells released into DMSO and stathmin-depleted cells released into S1451 and BI2536 all had a peak of mitotic entry at 12 hours post release versus control transfected cells released into DMSO at 8 hours post release (Figure 2.6, C). Combined depletion of stathmin and chemical inhibition of AURKA and PLK1 does not augment the duration of the delay caused by either treatment alone. These data demonstrate the combined partial inhibition of AURKA and Plk1 is sufficient to delay mitotic entry, indicating that stathmin depletion slows cell cycle progression by the combined inhibition of two enzymes.

MTs are required for AURKA centrosomal localization and activation

Previously we demonstrated that the interphase delay caused by stathmin depletion required MTs since nocodazole-induced MT depolymerization alleviated the delay during G2 (Carney *et al.,* 2012). The results described above indicate that stathmin depletion reduced the amount of active AURKA and Plk1 enzymes, and that partial inhibition of the two enzymes was sufficient to delay mitotic entry. To probe whether MTs serve as a signal relay between stathmin and these enzymes, we first examined whether MTs were required for activation of AURKA in cells expressing stathmin at endogenous levels. Hela cells were incubated in 33 μM nocodazole for 3 h prior to fixation, sufficient to depolymerize all MTs (data not shown). Surprisingly, AURKA centrosomal localization and activation were blocked significantly by MT depolymerization. AURKA was clearly visible in the cytoplasm but did not accumulate on centrosomes in Hela cells treated with nocodazole (Figure 2.5, A, upper). We also did not detect active AURKA, as marked by T288P (Figure 2. 5, A, lower) in nocodazole-

treated cells. Since we found that AURKA required MTs to localize at the centrosome and become active, it was not surprising that AURKA activity was not restored by nocodazole treatment of stathmin-depleted cells (data not shown). These data indicate that AURKA requires an intact MT cytoskeleton for centrosome localization and activation, independent of stathmin level.

Stathmin depletion increases MT polymer level in a number of cell types (Howell *et al.*, 1999; Holmfeldt *et al.,* 2007; Sellin *et al.,* 2008, see below), and this increased polymer could interfere with AURKA activation at centrosomes by slowing its translocation to the centrosome in G2 or by interfering with its proper localization to centrosomes. To test the first possibility, we measured the percentage of centrosomes staining positive for AURKA in cells fixed at various times after release from a double thymidine block. The timing of AURKA localization to centrosomes was unaffected by stathmin depletion indicating that trafficking of AURKA to the centrosome is not altered by stathmin depletion (Figure 2.5 B). In measuring AURKA levels at centrosomes, we consistently observed a wider distribution of AURKA in the centrosome region of stathmin-depleted cells. Quantitative measurements of the width of AURKA or active AURKA (T288P) localization confirmed this impression (Figure 2.5, C and D). While γ-tubulin distribution was identical in control-transfected and stathmin-depleted cells (Figure 5 E and F), AURKA, or the active enzyme, was spread over a significantly wider area in stathmin-depleted cells. This localization included puncta that likely represent MT-bound enzyme. In C. *elegans*, AIR-1 (AURKA homolog) is also localized to both MTs and centrosomes (Toya *et al.,* 2011). Assuming that AURKA is distributed in a

spherical shape near the centrosome, our data indicate that the widening of AURKA localization is equivalent to an ~ 2 fold dilution in local concentration.

Microtubule depolymerization restores Plk1 activation in stathmin-depleted cells

We next asked whether Plk1 activation is regulated by MTs, beginning with cells expressing stathmin at endogenous levels. Cells were incubated in 33 μM nocodazole for 3 h to depolymerize MTs and levels of active Plk1 measured with an antibody specific for Plk1 phosphorylated at T210. Active Plk1 levels were unchanged by MT depolymerization compared to DMSO treated cells, indicating that MT depolymerization did not contribute significantly to Plk1 activation (Figure 2.8 A).

We previously showed that MT depolymerization abrogates the G2 cell cycle delay caused by stathmin depletion (Carney *et al*., *2012*). Therefore, we next asked whether MT depolymerization abrogates the delay by restoring active Plk1. We depleted stathmin in Hela cells and approximately 45 hours after transfection treated cells with 33 μM nocodazole for 3 hours, a concentration and time period previously determined sufficient to depolymerize all MTs and restore the population of cells in G2 to the level measured in siGLO treated control cells (with or without an intact MT cytoskeleton; Carney *et al.*, 2012). Nocodazole treatment partially rescued activation of Plk1 in stathmin-depleted cells. We found that Plk1 T210P was reduced to 35% of control level after stathmin depletion, and that incubation with nocodazole restored activity to 82% of the control value (Figure 2.8, B). It is likely that the restored Plk1 activity was sufficient to abrogate the G2 cell cycle delay since it is only when both enzymes were inhibited that a delay was observed.

Plk1 recruitment to centrosomes was delayed in stathmin-depleted cells

The data presented above indicate that stathmin depletion reduced active Plk1, at least partially via the MT cytoskeleton. Reduced activation of Plk1, measured within the nucleus, could result from either loss of centrosome localization where it is activated (Lens *et al.,* 2010), or reduced nuclear import and/or nuclear retention of the active kinase. Nuclear import and/or nuclear retention of active Plk1 do not appear dependent on stathmin levels since the ratio of active Plk1 in the nucleus vs. the cytoplasm was the same in control-transfected and stathmin-depleted cells (Figure 2.8, C). In contrast, Plk1 localization to the centrosome was delayed by about 3 h, measured by fixing cells at various times after release from a double thymidine block and staining with an antibodies to Plk1 and g-tubulin (Figure 2.8, D). Delayed translocation of Plk1 from the cytoplasm to centrosomes could result from MT-based tethering to retain the enzyme in the cytoplasm. We tested this possibility by MT depolymerization, shown above to restore active Plk1 to near control levels. Surprisingly, MT depolymerization (3 h incubation in 33 μM nocodazole) had no effect on the delayed localization of Plk1 to centrosomes, measured by the percent of centrosomes staining positive for Plk1 at 9 or 12 h post-release from a double thymidine block (Figure 2.8, E). Taken together with our data showing near complete restoration of active Plk1 in stathmin-depleted cells treated with nocodazole, these data indicate that Plk1 activation can occur in the absence of MTs and without centrosome localization. To date, the mechanism of Plk1 activation at the centrosome is poorly understood (Soung *et al.,* 2009), and alternative activation pathways are not yet known.

Stathmin overexpression decreased Plk1 activation

Activation of AURKA and Plk1 in G2 are partially inhibited by stathmin depletion and/or the resulting increase in MTs. To probe whether either enzyme's activation is dependent on stathmin level over a broad range of concentrations, we next asked whether stathmin over-expression leads to greater or lesser activation of AURKA and Plk1 compared to cells expressing stathmin at endogenous levels. We depleted stathmin in Hela cells using siRNA targeting its 5' untranslated region and exogenously expressed stathmin from a plasmid encoding stathmin-GFP or CFP (Ringhoff and Cassimeris, 2009). Western blots of Hela cells transfected with stathmin siRNA and/or STMN-GFP (or CFP) plasmid showed that stathmin level is reduced significantly after transfection with the 5' UTR-targeted siRNA and that stathmin-CFP is expressed at a greater level than endogenous stathmin with or without concomitant knockdown of the endogenous protein (Figure 2.9, A and B). MT density was proportional to stathmin level, yet modest since MTs retained their typical interphase organization (Figure 2.10, A and B).

Stathmin overexpression did not effect AURKA activation, and expression of stathmin-CFP was sufficient to restore active AURKA to control levels in cells depleted of endogenous stathmin (Figure 2.9, C). Interestingly, Plk1 activation was significantly decreased by stathmin overexpression, as well as by stathmin depletion, indicating that full Plk1 activation requires stathmin expression within certain limits. Stathmin-CFP expression in cells depleted of endogenous stathmin was sufficient to restore Plk1 activation and to restore normal timing for mitotic entry, as measured by the proportion of cells staining positive for several G2 markers (Figure 2.9 D).

Stathmin interacts with AURKA and Plk1 in vitro

Our data indicate that stathmin expression level acts upstream to regulate AURKA and Plk1 activation at mitotic entry, and that this upstream signal pathway is at least partially relayed via MTs. To probe whether stathmin is also a downstream target of these enzymes, as expected if these proteins function in a negative feedback loop, we examined whether purified, active kinases can phosphorylate stathmin in vitro. Stathmin contains 4 serine phosphorylation sites and two of these, S16 and S63, contain a consensus sequence for AURKA phosphorylation (Sardon *et al.,* 2010 and Gadea and Ruderman, 2006). In vitro, purified stathmin was phosphorylated by AURKA and this phosphorylation was lost when Serine 16 and Serine 63 were mutated to alanine, indicating that one or both of these sites were phosphorylated by AURKA (Figure 2.11, A and B).

While stathmin is readily phosphorylated by AURKA, it is not a substrate for Plk1 (Figure 2.11, C) consistent with negative results from phospho-proteomic screens to identify all Plk1 targets (Santamaria *et al.,* 2011 and Grosstessner-Hain *et al.,* 2011). In the course of our in vitro experiments, we routinely saw that active Plk1 underwent autophosphorylation and incorporated radioactive phosphate, but that samples containing stathmin inhibited this autophosphorylation reaction. Inhibition of Plk1 autophosphorylation was dependent on stathmin concentration and was most easily detected at high molar ratios of stathmin/Plk1 (Figure 2.11, D). The concentration of Plk1 in Hela cells is not known, but is likely considerably lower than that of stathmin (500 - 1000 ng/mg total protein has been measured in transformed cells (Brattsand *et al.,* 1993) and the molar ratios tested here are feasible ratios within cells.

Discussion:

Stathmin depletion reduces AURKA and Plk1 activation

Cells depleted of stathmin are slower to proliferate (Zhang *et al.,* 2006; Chen *et al.,* 2007; Wang *et al.,* 2007; Carney and Cassimeris, 2010) and are delayed during G2 (Carney and Cassimeris, 2010; Carney *et al.,* 2012). Here we explored the mechanism responsible for this delay and found that stathmin depletion leads to less active CDC25 by reducing the activation of both AURKA and Plk1. Chemical inhibition of AURKA and Plk1 separately or in combination demonstrated that both enzymes must be partially inhibited to significantly delay cells during G2.

Previous studies suggested that reduced levels of both stathmin and p53 were required for delayed cell proliferation, which represents a combination of slower cell cycle progression and cell death (Alli *et al*., 2007, Carney and Cassimeris, 2010). Our current study indicates that increased p53 expression (by restoring p53 in Hela cells) reduced Plk1 expression (see also, McKenzie *et al.,* 2010) but did not reduce AURKA expression or activation. Therefore, we conclude that stathmin depletion, and not loss of p53, is responsible for delayed mitotic entry. In contrast, cell death likely requires loss of both stathmin and p53 (Alli *et al*., 2007, Carney and Cassimeris, 2010).

Chemical inhibitor studies support the idea that simultaneous inhibition of both AURKA and Plk1 delays mitotic entry (Van Horn *et al.,* 2010), while inhibition of a single enzyme does not (Lenart 2007; Van Horn *et al.,* 2010). Either inhibitor is sufficient to block cells in mitosis (Steegmaier *et al.,* 2007; Gleixner *et al.,* 2010; Grinshtein *et al.,* 2011; Hoar *et al.,* 2007; Fu *et al.,* 2012; Yuan *et al.,* 2012). Computer

simulations support the idea that partial inhibition of both AURKA and Plk1 synergistically inhibit CDK1 activation (Zou *et al.,* 2011). Given the feedback loops among enzymes driving mitotic entry, combinations of other enzymes regulating cell cycle progression should slow mitotic entry, as predicted in simulations combining Plk1 inhibition and a DNA damage response (Kesseler *et al.,* 2013).

Several other factors also slow entry into mitosis by inhibiting activation of AURKA, Plk1 or both enzymes. *Clostridium difficile* Toxin B inhibits Rho GTPase activity, delays AURKA activation and prolongs G2, but Plk1 activation was not measured (Ando *et al.,* 2007). Disruption of Golgi fragmentation also delayed cells in G2 and reduced AURKA recruitment to centrosomes (Persico *et al.,* 2010), but whether diminished recruitment causes the delay is unknown (Cervigni et al. 2011). Finally, knockdown of G Protein Coupled Receptor Kinase 5 reduced MT nucleation from the centrosome, delayed mitotic entry, and inhibited both AURKA and Plk1 (Michal *et al.,* 2012).

Stathmin regulates AURKA and Plk1 partially via MTs

While stathmin depletion inhibits activation of AURKA and Plk1, it does not appear to activate known checkpoint pathways that can inhibit mitotic entry, making it unlikely that stathmin depletion acts upstream of these pathways. It is possible that stathmin functions as a downstream relay, communicating inhibitory signals from an activated checkpoint to reduce the activities of AURKA, Plk1 and CDC25. Stathmin depletion decreased AURKA and Plk1 activation via a process partially dependent on MTs (summarized in Figure 2.12 and discussed below) since we previously showed that

MT depolymerization, by a 3 h incubation in nocodazole, was sufficient to remove the G2 cell cycle delay induced by stathmin depletion (Carney *et al*., 2012).

Diagrams in Figure 2.12 summarize the MT and stathmin dependent regulation of AURKA and Plk1. MT depolymerization (at endogenous stathmin levels) inhibited AURKA localization to the centrosome and subsequent activation. Plk1 was activated normally under these conditions. Both AURKA and Plk1 were also activated normally in cells treated with 10 nM paclitaxel (our unpublished observations). This low concentration of paclitaxel is sufficient to block cells at metaphase (Jordan et al. 1993) but allows MTs to remain dynamic (our unpublished observations) and does not slow mitotic entry (Carney et al., 2012). Stathmin depletion inhibited both AURKA and Plk1 activation, while stathmin overexpression inhibited Plk1 activation, likely through a direct interaction. Thus, stathmin depletion is unique in inhibiting both AURKA and Plk1, and it is only under these conditions that we measure a delayed entry into mitosis.

The MT-based regulation of AURKA is demonstrated by the MT-dependent localization and subsequent activation of AURKA at the centrosome. Stathmin depletion also inhibits AURKA activation, but not recruitment to the centrosome. Stathmin depletion increases centrosomal MT nucleation rate, increases MT polymer (Larsson *et al., 1997;* Ringhoff and Cassimeris 2009; Carney and Cassimeris, 2010), and increases the density of MTs near the centrosome (Cassimeris, unpublished observations). The distribution of AURKA across a wider area near the centrosome in stathmin-depleted cells is likely a consequence of excess MTs, given the MT requirement for AURKA localization. This broadening of AURKA distribution is equivalent to protein dilution; reducing local AURKA concentration should reduce dimer formation and limit

autophosphorylation reactions, as shown experimentally in vitro (Joukov *et al.* 2010) and by computational modeling (Zou *et al.,* 2011).

Plk1 activation also depends on both stathmin and MTs. Stathmin depletion inhibited Plk1 activation and delayed Plk1 recruitment to centrosomes. Curiously MT depolymerization did not prevent Plk1 binding to centrosomes, and did not rescue the time delay in Plk1 arrival at the centrosomes of stathmin-depleted cells, yet restored active Plk1 in cells depleted of stathmin. These data indicate that Plk1 recruitment and retention at centrosomes is not solely dependent on MTs. Purified stathmin inhibited Plk1 autophosphorylation in vitro, as did stathmn-CFP overexpression, demonstrating that stathmin can directly regulate Plk1.

The mechanisms underlying Plk1 localization to the centrosome and activation at this site are still poorly understood. In Drosophila, Plk1 is tethered to interphase MTs through its binding to MAP205, a MAP4 homolog (Archambault *et al.,* 2008). Release from MTs/MAP205 then allows Plk1 activation. Stathmin depletion could decrease Plk1 activation via increased tethering to MTs. While this mechanism would explain the ability of MT depolymerization to restore Plk1 activity to near control levels in stathmin-depleted cells, it does not explain the MT-independent delay in Plk1 localization to centrosomes. How Plk1 is recruited or targeted to centrosomes has not been studied thoroughly, but involves anchoring proteins, which are themselves regulated by CDK1 (Soung *et al.,* 2009). MT depolymerization restores Plk1 activity sufficiently to relieve the delay in G2, but does not also restore timely centrosome recruitment, implying that the activation step is more complex than currently thought.

Conclusions

In summary, our results demonstrate a previously unrecognized communication between stathmin and the MT cytoskeleton with the enzymes AURKA, Plk1 and CDC25 that drive CDK1/cyclin B activation for timely entry into mitosis. While stathmin depletion likely regulates AURKA and Plk1 in part via MT polymers, the precise mechanism regulating each enzyme is not yet clear. The MT-dependent signal relay cannot simply reflect a general MT stability since paclitaxel at nanomolar concentrations stabilizes MTs to some extent (Jordan *et al.,* 1993; our unpublished observations) but does not slow interphase progression (Carney *et al., 2012*). Therefore, small molecule inhibitors (Liang *et al.,* 2008) or ribozymes to decrease stathmin expression (Mistry *et al.,* 2005) should target cell processes distinct from those targeted by paclitaxel.

Materials and Methods:

Cell Culture and Plasmid Transfections: Hela cells were grown in DMEM (Sigma) supplemented with 10% fetal bovine serum (FBS; Invitogen) and 1X antibiotic/antimycotic (Sigma). In some experiments, Hela cells were synchronized through a double thymidine block by overnight incubation in 5mM thymidine (in DMEM), 8 h release in DMEM after 5 washes in warm PBS and then 16 h incubation in 5mM thymidine (in DMEM). Cells were transferred to DMEM following 5 washes with warm PBS and fixed at time points. For RNAi in synchronized cells, transfections were performed during the first 8 h release of the double thymidine block.

In some experiments Hela cells were transfected with plasmids for expression of stathmin-GFP or stathmin-CFP (Ringhoff and Cassimeris, 2009) using X-tremeGENE HP DNA Transfection Reagent (version 1.0; Roche Diagnostics, Indianapolis, IN) according to the manufacturer's protocol. When transfected with both siRNA and plasmids, plasmid transfection was performed 5 hours after siRNA and samples were fixed 43 hours after the second transfection.

Drugs and Reagents: Chemical inhibitors to Plk1 (BI 2536, Grinshtein *et al.,* 2011), and AURKA (S 1451, Yuan *et al.,* 2011) were purchased from Selleckchem. All other reagents were from Sigma unless noted otherwise.

RNA Interference and Transient Transfection: Cells were grown in 35mm dishes and transfected with siRNAs using GeneSilencer (Genlantis) 1-2 days after plating according to the manufacturer's protocol. Cells were serum starved from the time of transfection to four hours post-transfection to improve efficiency. siRNA oligonucleotides (Thermoscientific/Dharmacon) used were SMTN1 (Op18-443), 5'-CGUUUGCGAGAGAAGGAUAdtdt-3', STMN1 5'UTR CCCAGUUGAUUGUGCAGAAUU and HPV E6 (18E6-385), 5'-CUAACACUGGGUUAUACAAdtdt-3' (restores p53 by depleting the HPV E6 protein) (Koivusalo *et al.,* 2005). SiGlo Risc-Free siRNA (Dharmacon) or siGenome non-targeting siRNA (Thermoscientific/Dharmacon) were used as control siRNA sequences for these experiments.

Indirect Immunofluorescence and confocal microscopy: Hela cells were grown on glass coverslips and treated as described above. They were either fixed with 4% Paraformaldehyde (Electron Microscopy Services)/20% glycerol in PEM (100 mM Pipes, 1 mM $MgSO_4$, 2 mM EGTA, pH 6.9) for 10 minutes at room temperature or with methanol supplemented with 1mM EDTA at -20^{o}C for 10 minutes. Cells fixed with paraformaldehyde/glycerol were permeabilized with methanol at -20^{o}C for 10 minutes. Fixed cells were incubated with blocking reagent (10% FBS in phosphate buffered saline, PBS) for 30 minutes at 37^{o}C followed by a 45-minute incubation with primary antibody at 37^{o}C. Cells were then washed with PBS and incubated with secondary antibody and 1.5 μM propidium iodide for an additional 45 minutes at 37^{o}C. Antibodies used included: anti-phospho-Aurora A (T288) (1:1000, Cell Signaling), anti-phospho-Plk1 (T210) (1:1000, BD Pharmingen), anti-Aurora A (1:100, Cell Signaling), anti-Plk1 (Millipore) and Goat anti-mouse or anti-rabbit Alexa Fluor 488 or 568 (1:50, Invitrogen). Coverslips were then washed with PBS and mounted on slides with Vectashield (Vector Labs). Cells were imaged as described previously (Piehl and Cassimeris, 2003) using 63X/1.4 numerical aperture plan apo objective on an inverted microscope (Zeiss Axiovert 200M).

For synchronized cells mitotic index was determined by staining with propidium iodide and counting cells with condensed chromatin as a percent of total cells. At least ten fields (coverslip positions, > 100 cells per time point) were counted for each treatment group. For time course studies, cells were stained for either AURKA or Plk1 along with γ-tubulin (to label centrosomes) and TO-PRO 3 (to label DNA, Invitrogen). The percent of cells with visible centrosomes positive for AURKA or Plk1 were counted

for at least 5 fields (coverslip positions, >100 cells per time point) for each treatment group.

For quantitative measurement of fluorescence, maximum intensity projections were made from Z-stacks in Zeiss LSM viewer and exported as tiff files to MetaMorph. Fluorescence intensity from standard regions of interest (ROIs) was integrated and background intensity (average of 2 standard areas outside of ROI) subtracted. Values were normalized by setting the average control value to 100 for each individual experiment. Normalized data were then pooled for all experiments. For distribution measurements of AURKA and γ-tubulin, intensities along a line scan of the centrosome region of the cell were recorded. Values along the line that were continuously two-fold over background were used to determine width of AURKA and γ-tubulin distribution.

Western Blotting: Soluble cell extracts were prepared as described previously (Carney and Cassimeris, 2010) and protein concentrations were measured by Bradford assay. Lysates were diluted in PAGE sample buffer, 10 μg total protein per lane was typically loaded and resolved in 10% polyacrylamide gels and transferred to Immobilon Membranes (Millpore, Billerica, MA). Membranes were blocked with 5% non-fat milk or 5% BSA (for phospho-antibodies) in Tris-buffered saline with 0.1% Tween and then probed with primary antibodies: anti-Aurora A (1:1000 Cell Signaling), anti-Plk1 (1:1000, Millipore), anti-Plk1 T210P (1:1000, BD Pharmingen) or anti-stathmin (1:2000, Sigma) followed by secondary antibodies, anti-mouse (1:2000; Abcam) or anti-rabbit (1:10,000, BD Biosciences) horseradish peroxidase-linked IgG. Immunoreactive bands were developed using enhanced chemiluminscence (GE Amersham). Membranes were

reprobed with anti-α-tubulin (1:1000, Sigma) or GAPDH (1:1000, Abcam) as a loading control.

Live Cell Imaging: To follow cell fates over several days, Hela cells were plated on Mattek dishes and imaged using a Nikon Biostation IM as described previously (Carney *et al.,* 2012). Cells were imaged with phase contrast optics using a 20X objective and images were collected at 5-minute intervals for 24-72 hours. Cell fates were tracked from image series. Mitotic entry was marked either by the first image showing loss of the nuclear envelope or by significant cell rounding. Mitotic exit was marked as the first image showing formation of cleavage furrow, indicating the start of cytokinesis.

In vitro protein expression and kinase assays: Sequences encoding stathmin-FLAG, stathmin-S16,63A-FLAG, stathmin-S25,38A-FLAG, stathmin- Δ5-25-FLAG, and stathmin-Δ100-147-FLAG (each including Nco1 and BamH1 restriction sites) were generated by total gene synthesis and inserted into the Nco1 and BamH1 sites of the pET-28a plasmid (gene synthesis, cloning and sequence verifications performed by Genewiz, South Plainfield, NJ). Plasmids were transfected into E. coli and protein expression induced with 1 mM IPTG for 1-3 hours. Cells were pelleted and resuspended in TBS, 0.1% NP-40, protease inhibitor cocktail (ThermoScientific) and PMSF. E. coli were lysed by sonication, clarified, boiled for 10 minutes, and the final clarified supernatants frozen at -20°C. Stathmin is heat stable and the final supernatant fraction was > 90% stathmin based on Coomassie Blue stained SDS gels and confirmed by immunoblots probed with anti-stathmin (a combination of rabbit antibodies recognizing the C terminus (Sigma) and

a region around amino acid 38 (Cell Signaling) to detect all mutants) and anti-FLAG (M2, Sigma).

For in vitro kinase assays, purified stathmin-FLAG or mutants (7.6 μM when used as an enzyme substrate or 0.1 - 3 μM for Plk1 inhibition experiments) in kinase buffer (20 mM HEPES, 10 mM $MgCl_2$, 10 mM KCl, 1 μM DTT, 100 μg/mL BSA, 0.01% NP-40) were incubated with 5 μM ATP, 5 μCi [^{32}P]-ATP (Perkin Elmer, 6000 Ci/mmol), and either active AURKA (0.6 nM; from Millipore (Dundee, UK) or Prospec-Tany TechnoGene Ltd. (Ness Ziona, Israel)) or active Plk1 (70-140 nM; Signal Chem, British Columbia, Canada) for 30 m at 30°C. In additional experiments, dephosphorylated casein (Sigma) was used as a Plk1 substrate (Steegmaier *et al.,* 2007). The final concentration of casein in these reactions was 3 μM. The BSA concentration in the standard reaction mixture was 1.5 μM; where noted the BSA concentration was raised to 7.5 μM to test whether excess protein inhibits Plk1 activity. Reactions were stopped by adding 5X SDS sample buffer and heating to 70°C for 10 m. Proteins were separated on 10% PAGE-gels, stained with Coomassie Blue, wet gels were exposed to phosphorImager screens for 1 - 5 hours and imaged with a Storm 840 PhosphorImager (Amersham Biosciences).

Data Analysis: Statistical analysis of fluorescence intensity and cell cycle durations were performed using unpaired t-tests with GraphPad Software (www.graphpad.com/quickcalcs/ttest1.cfm).

References:

1. Aliagas-Martin *et al.* (2009). A class of 2,4-bisanilinopyrimidine Aurora A inhibitors with unusually high selectivity against Aurora B. Journal of medicinal chemistry *52*, 3300-3307.
2. Alli, E., Bash-Babula, J., Yang, J.M., and Hait, W.N. (2002). Effect of stathmin on the sensitivity to antimicrotubule drugs in human breast cancer. Cancer research *62*, 6864-6869.
3. Alli, E., Yang, J.M., Ford, J.M., and Hait, W.N. (2007). Reversal of stathmin-mediated resistance to paclitaxel and vinblastine in human breast carcinoma cells. Molecular pharmacology *71*, 1233-1240.
4. Ando, Y., Yasuda, S., Oceguera-Yanez, F., and Narumiya, S. (2007). Inactivation of Rho GTPases with Clostridium difficile toxin B impairs centrosomal activation of Aurora-A in G2/M transition of HeLa cells. Molecular biology of the cell *18*, 3752-3763.
5. Archambault, V., D'Avino, P.P., Deery, M.J., Lilley, K.S., and Glover, D.M. (2008). Sequestration of Polo kinase to microtubules by phosphopriming-independent binding to Map205 is relieved by phosphorylation at a CDK site in mitosis. Genes & development *22*, 2707-2720.
6. Belletti, B., and Baldassarre, G. (2011). Stathmin: a protein with many tasks. New biomarker and potential target in cancer. Expert opinion on therapeutic targets *15*, 1249-1266.
7. Brattsand, G., Roos, G., Marklund, U., Ueda, H., Landberg, G., Nanberg, E., Sideras, P., and Gullberg, M. (1993). Quantitative-analysis of the expression and regulation of an activation-regulated phosphoprotein (oncoprotein 18) in normal and neoplastic-cells. Leukemia *7*, 569-579.
8. Carney, B.K., Caruso Silva, V., and Cassimeris, L. (2012). The microtubule cytoskeleton is required for a G2 cell cycle delay in cancer cells lacking stathmin and p53. Cytoskeleton (Hoboken) *69*, 278-289.

9. Carney, B.K., and Cassimeris, L. (2010). Stathmin/oncoprotein 18, a microtubule regulatory protein, is required for survival of both normal and cancer cell lines lacking the tumor suppressor, p53. Cancer biology & therapy *9*, 699-709.
10. Cervigni, R.I., Barretta, M.L., Persico, A., Corda, D., and Colanzi, A. (2011). The role of Aurora-A kinase in the Golgi-dependent control of mitotic entry. Bioarchitecture *1*, 61-65.
11. Chen, Y., Lin, M.C., Yao, H., Wang, H., Zhang, A.Q., Yu, J., Hui, C.K., Lau, G.K., He, M.L., Sung, J., and Kung, H.F. (2007). Lentivirus-mediated RNA interference targeting enhancer of zeste homolog 2 inhibits hepatocellular carcinoma growth through down-regulation of stathmin. Hepatology *46*, 200-208.
12. Dutertre *et al.*, (2004). Phosphorylation of CDC25B by Aurora-A at the centrosome contributes to the G2-M transition. Journal of cell science *117*, 2523-2531.
13. Efimov, A., and Kaverina, I. (2009). Significance of microtubule catastrophes at focal adhesion sites. Cell adhesion & migration *3*, 285-287.
14. Eyers, P.A., Erikson, E., Chen, L.G., and Maller, J.L. (2003). A novel mechanism for activation of the protein kinase Aurora A. Current biology : CB *13*, 691-697.
15. Ezratty, E.J., Partridge, M.A., and Gundersen, G.G. (2005). Microtubule-induced focal adhesion disassembly is mediated by dynamin and focal adhesion kinase. Nature cell biology *7*, 581-590.
16. Fu, S., Li, Y., Huang, J., Liu, T., Hong, Z., Chen, A., Bast, R.C., Kavanagh, J.J., Gershenson, D.M., Sood, A.K., and Hu, W. (2012). Aurora kinase inhibitor VE 465 synergistically enhances cytotoxicity of carboplatin in ovarian cancer cells through induction of apoptosis and downregulation of histone 3. Cancer biology & therapy *13*, 1034-1041.
17. Gadea, B.B., and Ruderman, J.V. (2006). Aurora B is required for mitotic chromatin-induced phosphorylation of Op18/Stathmin. Proceedings of the National Academy of Sciences of the United States of America *103*, 4493-4498.
18. Gleixner, K.V. *et al.* (2010). Polo-like kinase 1 (Plk1) as a novel drug target in chronic myeloid leukemia: overriding imatinib resistance with the Plk1 inhibitor BI 2536. Cancer research *70*, 1513-1523.

19. Grinshtein, N., Datti, A., Fujitani, M., Uehling, D., Prakesch, M., Isaac, M., Irwin, M.S., Wrana, J.L., Al-Awar, R., and Kaplan, D.R. (2011). Small molecule kinase inhibitor screen identifies polo-like kinase 1 as a target for neuroblastoma tumor-initiating cells. Cancer research *71*, 1385-1395.
20. Grosstessner-Hain *et al.* (2011). Quantitative phospho-proteomics to investigate the polo-like kinase 1-dependent phospho-proteome. Molecular & cellular proteomics : MCP *10*, M111 008540.
21. Gundersen, G.G., and Cook, T.A. (1999). Microtubules and signal transduction. Current opinion in cell biology *11*, 81-94.
22. Hoar, K., Chakravarty, A., Rabino, C., Wysong, D., Bowman, D., Roy, N., and Ecsedy, J.A. (2007). MLN8054, a small-molecule inhibitor of Aurora A, causes spindle pole and chromosome congression defects leading to aneuploidy. Molecular and cellular biology *27*, 4513-4525.
23. Holmfeldt, P., Stenmark, S., and Gullberg, M. (2007). Interphase-specific phosphorylation-mediated regulation of tubulin dimer partitioning in human cells. Molecular biology of the cell *18*, 1909-1917.
24. Holmfeldt, P., Sellin, M.E., and Gullberg, M. (2009). Predominant regulators of tubulin monomer-polymer partitioning and their implication for cell polarization. Cellular and molecular life sciences : CMLS *66*, 3263-3276.
25. Howell, B., Larsson, N., Gullberg, M., and Cassimeris, L. (1999). Dissociation of the tubulin-sequestering and microtubule catastrophe-promoting activities of oncoprotein 18/stathmin. Molecular biology of the cell *10*, 105-118.
26. Izumi, T., and Maller, J.L. (1993). Elimination of cdc2 phosphorylation sites in the cdc25 phosphatase blocks initiation of M-phase. Molecular biology of the cell *4*, 1337-1350.
27. Johnsen, J.I., Aurelio, O.N., Kwaja, Z., Jorgensen, G.E., Pellegata, N.S., Plattner, R., Stanbridge, E.J., and Cajot, J.F. (2000). p53-mediated negative regulation of stathmin/Op18 expression is associated with G(2)/M cell-cycle arrest. International journal of cancer. Journal international du cancer *88*, 685-691.

28. Jordan, M.A., Toso, R.J., Thrower, D., and Wilson, L. (1993). Mechanism of mitotic block and inhibition of cell proliferation by taxol at low concentrations. Proceedings of the National Academy of Sciences of the United States of America *90*, 9552-9556.
29. Jordan, M.A., and Wilson, L. (2004). Microtubules as a target for anticancer drugs. Nature reviews. Cancer *4*, 253-265.
30. Jordan, M.A., and Kamath, K. (2007). How do microtubule-targeted drugs work? An overview. Current cancer drug targets *7*, 730-742.
31. Joukov, V., De Nicolo, A., Rodriguez, A., Walter, J.C., and Livingston, D.M. (2010). Centrosomal protein of 192 kDa (Cep192) promotes centrosome-driven spindle assembly by engaging in organelle-specific Aurora A activation. Proceedings of the National Academy of Sciences of the United States of America *107*, 21022-21027.
32. Kang, Y.H., Park, J.E., Yu, L.R., Soung, N.K., Yun, S.M., Bang, J.K., Seong, Y.S., Yu, H., Garfield, S., Veenstra, T.D., and Lee, K.S. (2006). Self-regulated Plk1 recruitment to kinetochores by the Plk1-PBIP1 interaction is critical for proper chromosome segregation. Molecular cell *24*, 409-422.
33. Katayama, H., Sasai, K., Kloc, M., Brinkley, B.R., and Sen, S. (2008). Aurora kinase-A regulates kinetochore/chromatin associated microtubule assembly in human cells. Cell Cycle *7*, 2691-2704.
34. Kesseler, K.J., Blinov, M.L., Elston, T.C., Kaufmann, W.K., and Simpson, D.A. (2013). A predictive mathematical model of the DNA damage G2 checkpoint. Journal of theoretical biology *320*, 159-169.
35. Kishi, K., van Vugt, M.A., Okamoto, K., Hayashi, Y., and Yaffe, M.B. (2009). Functional dynamics of Polo-like kinase 1 at the centrosome. Molecular and cellular biology *29*, 3134-3150.
36. Koivusalo, R., Krausz, E., Helenius, H., and Hietanen, S. (2005). Chemotherapy compounds in cervical cancer cells primed by reconstitution of p53 function after short interfering RNA-mediated degradation of human papillomavirus 18 E6 mRNA: opposite effect of siRNA in combination with different drugs. Molecular pharmacology *68*, 372-382.

37. Kramer, A., Lukas, J., and Bartek, J. (2004). Checking out the centrosome. Cell Cycle *3*, 1390-1393.
38. Larsson, N., Marklund, U., Gradin, H.M., Brattsand, G., and Gullberg, M. (1997). Control of microtubule dynamics by oncoprotein 18: dissection of the regulatory role of multisite phosphorylation during mitosis. Molecular and cellular biology *17*, 5530-5539.
39. Lee, K.S., Oh, D.Y., Kang, Y.H., and Park, J.E. (2008). Self-regulated mechanism of Plk1 localization to kinetochores: lessons from the Plk1-PBIP1 interaction. Cell division *3*, 4.
40. Leinung, M., Cuny, C., Diensthuber, M., Stover, T., and Wagenblast, J. (2012). Small molecules in combination with conventional chemotherapeutic drugs: Light at the end of the tunnel? Oncology letters *4*, 1043-1046.
41. Lenart, P., Petronczki, M., Steegmaier, M., Di Fiore, B., Lipp, J.J., Hoffmann, M., Rettig, W.J., Kraut, N., and Peters, J.M. (2007). The small-molecule inhibitor BI 2536 reveals novel insights into mitotic roles of polo-like kinase 1. Current biology : CB *17*, 304-315.
42. Lens, S.M., Voest, E.E., and Medema, R.H. (2010). Shared and separate functions of polo-like kinases and aurora kinases in cancer. Nature reviews. Cancer *10*, 825-841.
43. Liang, X.J., Choi, Y., Sackett, D.L., and Park, J.K. (2008). Nitrosoureas inhibit the stathmin-mediated migration and invasion of malignant glioma cells. Cancer research *68*, 5267-5272.
44. Lindqvist, A., Rodriguez-Bravo, V., and Medema, R.H. (2009). The decision to enter mitosis: feedback and redundancy in the mitotic entry network. The Journal of cell biology *185*, 193-202.
45. Lowery, D.M., Lim, D., and Yaffe, M.B. (2005). Structure and function of Polo-like kinases. Oncogene *24*, 248-259.
46. Macurek, L., Lindqvist, A., Lim, D., Lampson, M.A., Klompmaker, R., Freire, R., Clouin, C., Taylor, S.S., Yaffe, M.B., and Medema, R.H. (2008). Polo-like kinase-1 is activated by aurora A to promote checkpoint recovery. Nature *455*, 119-123.

47. McKenzie, L *et al.* (2010). p53-dependent repression of polo-like kinase-1 (PLK1). Cell Cycle *9*, 4200-4212.
48. Michal, A.M., So, C.H., Beeharry, N., Shankar, H., Mashayekhi, R., Yen, T.J., and Benovic, J.L. (2012). G Protein-coupled receptor kinase 5 is localized to centrosomes and regulates cell cycle progression. The Journal of biological chemistry *287*, 6928-6940.
49. Mistry, S.J., Bank, A., and Atweh, G.F. (2005). Targeting stathmin in prostate cancer. Molecular cancer therapeutics *4*, 1821-1829.
50. Mitra, M., Kandalam, M., Sundaram, C.S., Verma, R.S., Maheswari, U.K., Swaminathan, S., and Krishnakumar, S. (2011). Reversal of stathmin-mediated microtubule destabilization sensitizes retinoblastoma cells to a low dose of antimicrotubule agents: a novel synergistic therapeutic intervention. Investigative ophthalmology & visual science *52*, 5441-5448.
51. Molli, P.R., Li, D.Q., Bagheri-Yarmand, R., Pakala, S.B., Katayama, H., Sen, S., Iyer, J., Chernoff, J., Tsai, M.Y., Nair, S.S., and Kumar, R. (2010). Arpc1b, a centrosomal protein, is both an activator and substrate of Aurora A. The Journal of cell biology *190*, 101-114.
52. Ohashi, S., Sakashita, G., Ban, R., Nagasawa, M., Matsuzaki, H., Murata, Y., Taniguchi, H., Shima, H., Furukawa, K., and Urano, T. (2006). Phospho-regulation of human protein kinase Aurora-A: analysis using anti-phospho-Thr288 monoclonal antibodies. Oncogene *25*, 7691-7702.
53. Perry, J.A., and Kornbluth, S. (2007). Cdc25 and Wee1: analogous opposites? Cell division *2*, 12.
54. Persico, A., Cervigni, R.I., Barretta, M.L., Corda, D., and Colanzi, A. (2010). Golgi partitioning controls mitotic entry through Aurora-A kinase. Molecular biology of the cell *21*, 3708-3721.
55. Piehl, M., and Cassimeris, L. (2003). Organization and dynamics of growing microtubule plus ends during early mitosis. Molecular biology of the cell *14*, 916-925.

56. Polager, S., and Ginsberg, D. (2003). E2F mediates sustained G2 arrest and down-regulation of Stathmin and AIM-1 expression in response to genotoxic stress. The Journal of biological chemistry *278*, 1443-1449.
57. Reinhardt, H.C *et al.* (2010). DNA damage activates a spatially distinct late cytoplasmic cell-cycle checkpoint network controlled by MK2-mediated RNA stabilization. Molecular cell *40*, 34-49.
58. Rieder, C.L. (2011). Mitosis in vertebrates: the G2/M and M/A transitions and their associated checkpoints. Chromosome research : an international journal on the molecular, supramolecular and evolutionary aspects of chromosome biology *19*, 291-306.
59. Rieder, C.L., and Cole, R. (2000). Microtubule disassembly delays the G2-M transition in vertebrates. Current biology : CB *10*, 1067-1070.
60. Ringhoff, D.N., and Cassimeris, L. (2009). Stathmin regulates centrosomal nucleation of microtubules and tubulin dimer/polymer partitioning. Molecular biology of the cell *20*, 3451-3458.
61. Santamaria, A., Wang, B., Elowe, S., Malik, R., Zhang, F., Bauer, M., Schmidt, A., Sillje, H.H.W., Korner, R., and Nigg, E.A. 2011. The Plk1-dependent phosphoproteome of the early mitotic spindle. Molecular and Cellular Proteomics. *10,* M110.004457.
62. Sardon, T., Pache, R.A., Stein, A., Molina, H., Vernos, I., and Aloy, P. (2010). Uncovering new substrates for Aurora A kinase. EMBO reports *11*, 977-984.
63. Scheffner, M., Werness, B.A., Huibregtse, J.M., Levine, A.J., and Howley, P.M. (1990). The E6 oncoprotein encoded by human papillomavirus types 16 and 18 promotes the degradation of p53. Cell *63*, 1129-1136.
64. Scutt, P.J., Chu, M.L., Sloane, D.A., Cherry, M., Bignell, C.R., Williams, D.H., and Eyers, P.A. (2009). Discovery and exploitation of inhibitor-resistant aurora and polo kinase mutants for the analysis of mitotic networks. The Journal of biological chemistry *284*, 15880-15893.

65. Seki, A., Coppinger, J.A., Jang, C.Y., Yates, J.R., and Fang, G. (2008). Bora and the kinase Aurora a cooperatively activate the kinase Plk1 and control mitotic entry. Science *320*, 1655-1658.
66. Sellin, M.E., Holmfeldt, P., Stenmark, S., and Gullberg, M. (2008). Global regulation of the interphase microtubule system by abundantly expressed Op18/stathmin. Molecular biology of the cell *19*, 2897-2906.
67. Song, B., Liu, X.S., and Liu, X. (2012). Polo-like kinase 1 (Plk1): an Unexpected Player in DNA Replication. Cell division *7*, 3.
68. Soung, N.K., Park, J.E., Yu, L.R., Lee, K.H., Lee, J.M., Bang, J.K., Veenstra, T.D., Rhee, K., and Lee, K.S. (2009). Plk1-dependent and -independent roles of an ODF2 splice variant, hCenexin1, at the centrosome of somatic cells. Developmental cell *16*, 539-550.
69. Steegmaier, M., Hoffmann, M., Baum, A., Lenart, P., Petronczki, M., Krssak, M., Gurtler, U., Garin-Chesa, P., Lieb, S., Quant, J., Grauert, M., Adolf, G.R., Kraut, N., Peters, J.M., and Rettig, W.J. (2007). BI 2536, a potent and selective inhibitor of
70. Toya, M., Terasawa, M., Nagata, K., Iida, Y., and Sugimoto, A. (2011). A kinase-independent role for Aurora A in the assembly of mitotic spindle microtubules in Caenorhabditis elegans embryos. Nature cell biology *13*, 708-714.
71. Trunnell, N.B., Poon, A.C., Kim, S.Y., and Ferrell, J.E., Jr. (2011). Ultrasensitivity in the Regulation of Cdc25C by Cdk1. Molecular cell *41*, 263-274.
72. Tsvetkov, L., and Stern, D.F. (2005). Phosphorylation of Plk1 at S137 and T210 is inhibited in response to DNA damage. Cell Cycle *4*, 166-171.
73. Van Horn, R.D., Chu, S., Fan, L., Yin, T., Du, J., Beckmann, R., Mader, M., Zhu, G., Toth, J., Blanchard, K., and Ye, X.S. (2010). Cdk1 activity is required for mitotic activation of aurora A during G2/M transition of human cells. The Journal of biological chemistry *285*, 21849-21857.
74. Wang, R., Dong, K., Lin, F., Wang, X., Gao, P., Wei, S.H., Cheng, S.Y., and Zhang, H.Z. (2007). Inhibiting proliferation and enhancing chemosensitivity to taxanes in osteosarcoma cells by RNA interference-mediated downregulation of stathmin expression. Mol Med *13*, 567-575.

75. Xu, D., and Dai, W. (2011). The function of mammalian Polo-like kinase 1 in microtubule nucleation. Proceedings of the National Academy of Sciences of the United States of America *108*, 11301-11302.
76. Yuan, H., Wang, Z., Zhang, H., Roth, M., Bhatia, R., and Chen, W.Y. (2012). Overcoming CML acquired resistance by specific inhibition of Aurora A kinase in the KCL-22 cell model. Carcinogenesis *33*, 285-293.
77. Zhang, H.Z., Wang, Y., Gao, P., Lin, F., Liu, L., Yu, B., Ren, J.H., Zhao, H., and Wang, R. (2006). Silencing stathmin gene expression by survivin promoter-driven siRNA vector to reverse malignant phenotype of tumor cells. Cancer biology & therapy *5*, 1457-1461.
78. Zou, J., Luo, S.D., Wei, Y.Q., and Yang, S.Y. (2011). Integrated computational model of cell cycle and checkpoint reveals different essential roles of Aurora-A and Plk1 in mitotic entry. Molecular bioSystems *7*, 169-179.

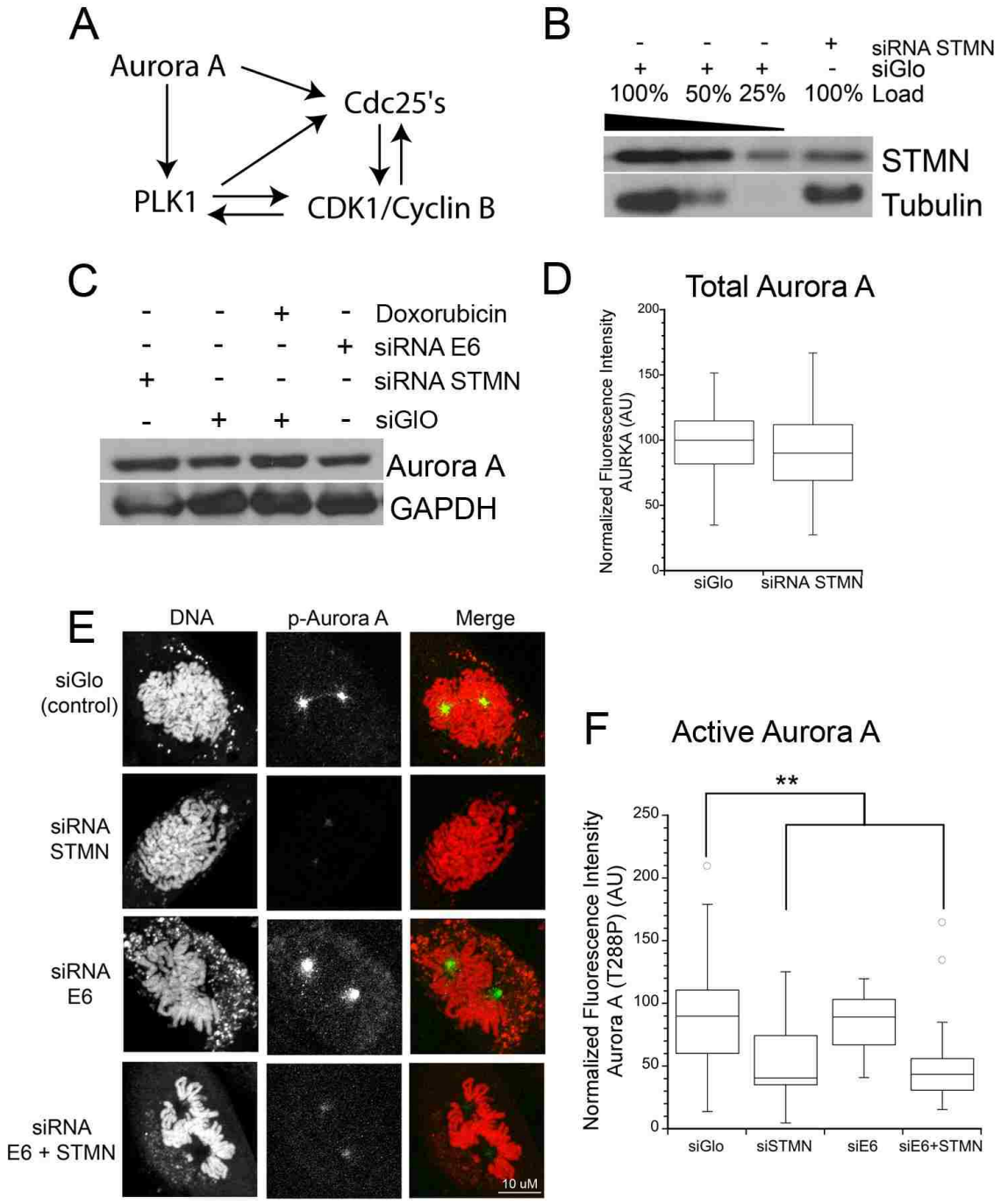

Figure 2.1: **Active Aurora A at the centrosome is reduced in stathmin-depleted Hela cells.** (A) Outline of AURKA and Plk1 activation of CDC25 and/or CDK1 at mitotic entry and feedback between these proteins (reviewed in Lindqvist et al. 2009). (B)

Stathmin level was reduced by ~ 75% by siRNA compared to siGLO-transfected control cells. Western blot for stathmin, reprobed for tubulin as a loading control. See also (Carney and Cassimeris 2010, Carney *et al.*, 2012). Lysates were isolated 48 hr after transfection, but depletion was equally evident at 24 hr. (C) Western blot for total AURKA protein, reprobed for GAPDH as a loading control. Neither stathmin depletion, nor p53 expression, changed AURKA expression (see Supplemental Figure 2 for p53 restoration by depletion of HPV protein E6). (D) Box plot of the relative fluorescence intensity of total AURKA at the centrosomes of prophase cells measured from immunofluorescent images. (E) Representative images of maximum intensity projections of Z-stacks of active Aurora A at prophase centrosomes. Fixed cells were stained with an antibody against Aurora A phospho-T288 (green in merged images) and propidium iodide to stain DNA (red in merged images). (F) Box plot of the relative fluorescence intensity of active AURKA (T288P) at the centrosomes of prophase cells measured from immunofluorescent images. For (D and F) images were analyzed for fluorescence staining intensity as described in Methods. Values for each cell were normalized to the average of control cells and statistical significance determined using a student's t-test. Plots represent normalized data pooled from three independent experiments, at least 7 cells per treatment/experiment. * * denotes $p<0.01$.

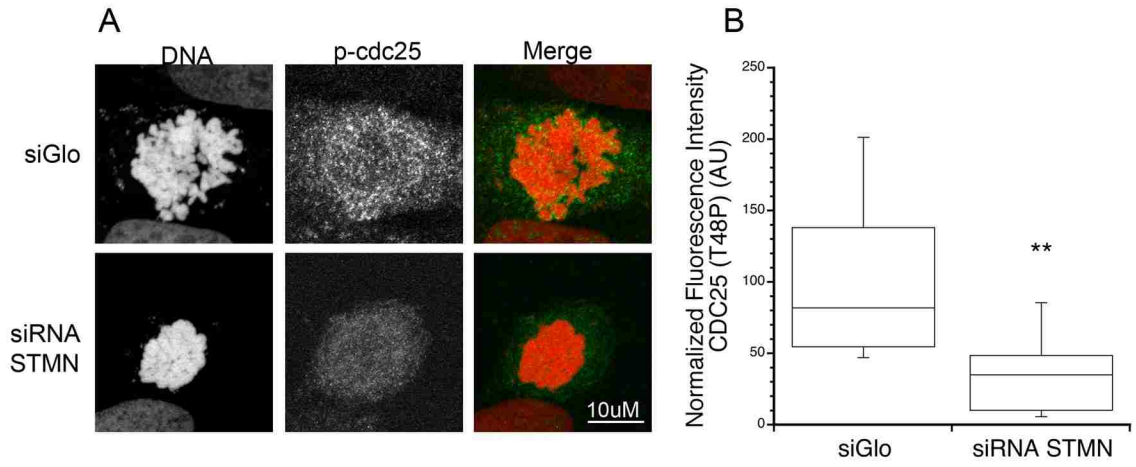

Figure 2.2: Stathmin depletion from Hela cells decreased the level of active CDC25. Hela cells were transfected with siGlo control siRNA, or siRNA targeting stathmin mRNA. Cells were fixed at 48 hours post transfection and stained with an antibody recognizing active CDC25 (T48P) (green in merged images) and propidium iodide to stain DNA (red in merged images). (A) Representative images of maximum intensity projections of Z-stacks of active CD25 (T48P) at mitotic entry. Images were analyzed for fluorescence intensity of CDC25 staining. (B) Box plot of relative fluorescence intensities of active CDC25. Values for each cell were normalized to the average of control cells and statistical significance determined using Student's t-test. Data shown was pooled from two independent experiments, at least 7 cells per treatment/experiment. * * denotes $p<0.01$.

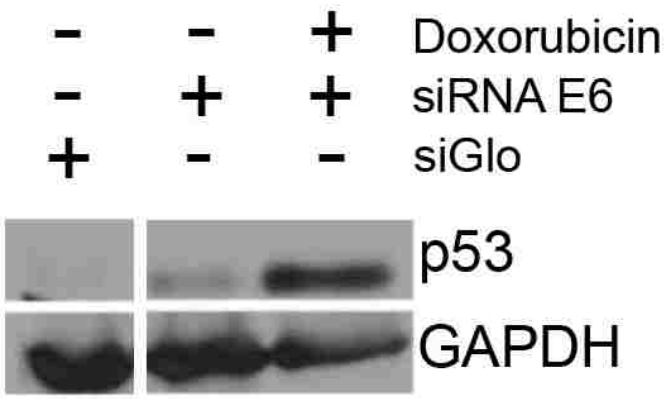

Figure 2.3: P53 was restored by depletion of HPV E6 protein from Hela cells. Western blot depicts p53 protein level, reprobed for GAPDH as a loading control. Doxorubicin treatment was included in one sample to induce p53 stability, increasing detectability by blot (see also Carney and Cassimeris, 2010). A sample unrelated to this experiment was cropped from the blots. The position of the removed lane is shown as a vertical white line.

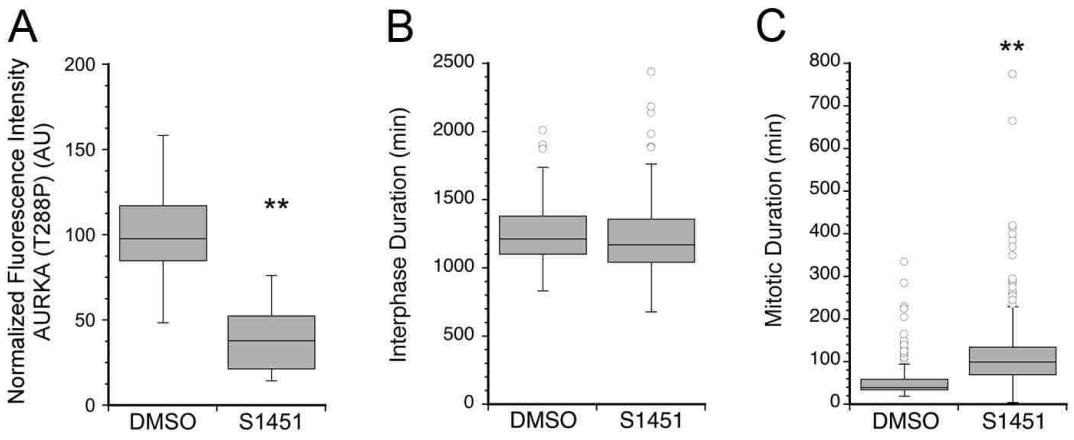

Figure 2.4: **Inhibition of AURKA does not delay mitotic entry**. (A) Hela cells were treated for 16 hours with either DMSO as the vehicle control or AURKA inhibitor, S 1451 (300 nM). Cells were fixed and stained with an antibody to AURKA phosphor-T288 and fluorescence intensity of centrosomal AURKA T288P measured as described in Methods. AURKA inhibition decreased active AURKA by ~50%. Values for each cell were normalized to the average value of DMSO-treated cells to allow pooling of independent experiments. Statistical significance was determined using Student's t-test. Box plot represents normalized data pooled from two independent experiments, at least 7 cells per treatment/experiment. (B, C) Hela cells treated with DMSO or S 1451 (300 nM) were followed by live cell imaging. Cell fates were determined from phase contrast image series as described in Methods. Box plots are shown, summarizing data from >100 cells and three independent experiments per condition. (B) S 1451 shortened interphase by 0.7 h. (C) S 1451 increased mitotic duration compared to DMSO treated controls. ** denotes $P<0.01$

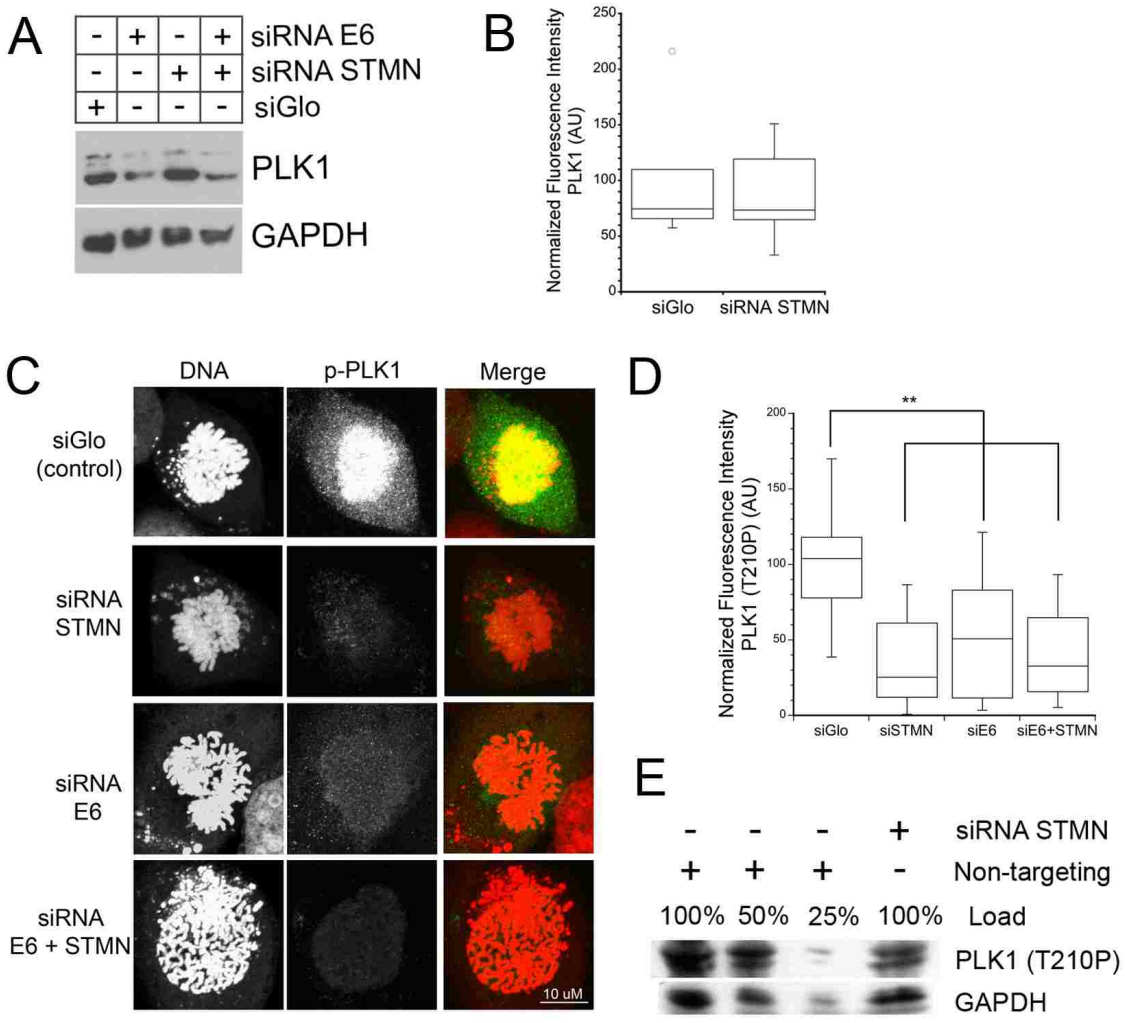

Figure 2.5: Active Plk1 on chromatin is decreased in stathmin-depleted cells. Hela cells were transfected with siGlo control siRNA, or siRNA targeting stathmin, HPV E6 or both mRNAs. Cells were either fixed at 48 hours post transfection or whole cell lysates were prepared for western blot. (A) Western blot of total Plk1 protein and reprobed with GAPDH as a loading control. Restoring p53 by depletion of E6 (see Supplemental Figure 2) led to decreased expression of Plk1. Stathmin depletion did not effect Plk1 expression. (B-D) Fixed cells were stained with an antibody against Plk1 or Plk1 phospho-T210 (green in merged images) and propidium iodide to stain DNA (red in merged images).

Fluorescence intensities were measured and normalized as described in Methods. (B) Box plot of Plk1 levels within the nucleus of prophase cells. (C) Representative images of maximum intensity projections of active Plk1 (T210P) in prophase cells. Staining intensity of active Plk1 is reduced in cells depleted of stathmin, E6, or both proteins. (D) Quantitation of active Plk1 (T210P) measured as described in Methods. Depletion of stathmin, E6 or both proteins reduced the level of active Plk1 on chromatin. For cells depleted of E6 to restore p53, the decreased level of active Plk1 is likely a consequence of reduced Plk1 expression. For graphs in B and D, data pooled from three independent experiments, at least 7 cells per treatment/experiment. * * denotes $p<0.01$. (E) Western blot of Plk1 (T210P) protein reprobed with GAPDH as a loading control. Plk1 (T210P) level is decreased ~50% by stathmin depletion.

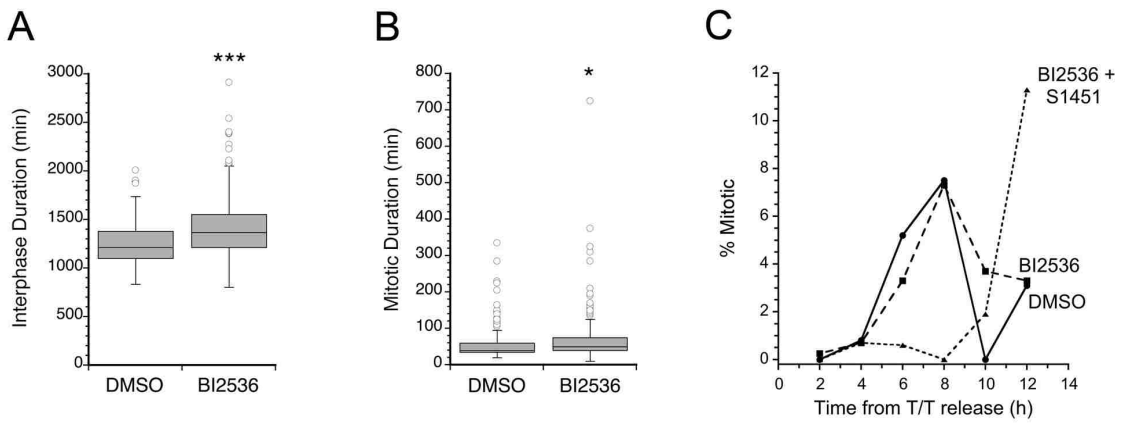

Figure 2.6: Partial inhibition of both AURKA and Plk1 delays mitotic entry. (A,B) Hela cells were treated with DMSO as vehicle control or chemical inhibitor 0.8 nM BI 2536 followed by live cell imaging. Cell fates were determined from phase contrast image series as described in Material and Methods section. Box plots are shown, summarizing data from >100 cells and three independent experiments per condition. BI 2536 increased interphase duration by 2.6 h (A) and mitotic duration (B) compared to DMSO-treated cells. * denotes $p<0.05$, *** denotes $p<0.001$ (C-D) Hela cells untransfected, or transfected with non-targeting or siRNA targeting stathmin mRNA and synchronized by a double thymidine block were released into media containing DMSO, BI 2536 (0.8 nM) or BI 2536 (0.8 nM) and S 1451 (300 nM). Mitotic index was determined from propidium iodide stained cells fixed at 2-hour intervals following release. The graphs are representatives from at least two independent experiments with >100 cells per treatment group in each replicate.

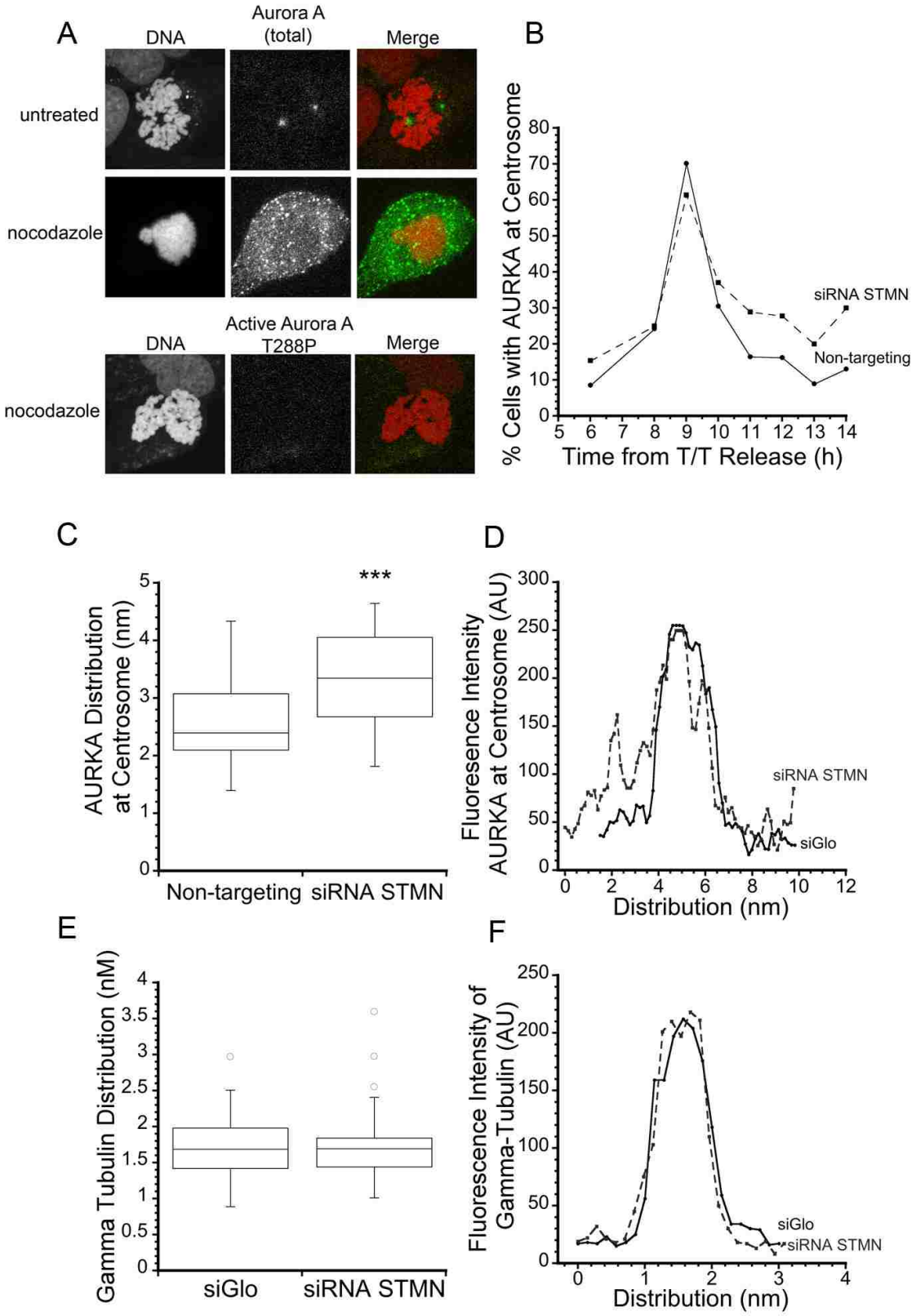

Figure 2.7: MTs are required for AURKA activation. (A) Hela cells were treated with

either DMSO or 33 μM nocodazole for 3h and then fixed with PFA and stained with antibody against AURKA or phospho-AURKA (T288) (green in merge) and propidium iodide to stain DNA (red in merge). Representative images are shown of AURKA and AURKA (T288P) in prophase cells, demonstrating that MTs are required for AURKA localization and activation at the centrosome. (B) The timing of AURKA recruitment to the centrosome is independent of stathmin depletion. Centrosomes staining positive for AURKA were counted at times after release from a double thymidine block. Graph is a representative from two independent experiments with >100 cells per treatment group in each replicate. (C-F) Stathmin-depletion broadens the distribution of AURKA near the centrosome. (C) Box plot of the width of AURKA centrosomal staining, measured as described in Methods. *** denotes $p<0.001$. (D) Representative line scans of AURKA fluorescence intensity near the centrosome. (E, F) The distribution of g-tubulin is unaffected by stathmin depletion.

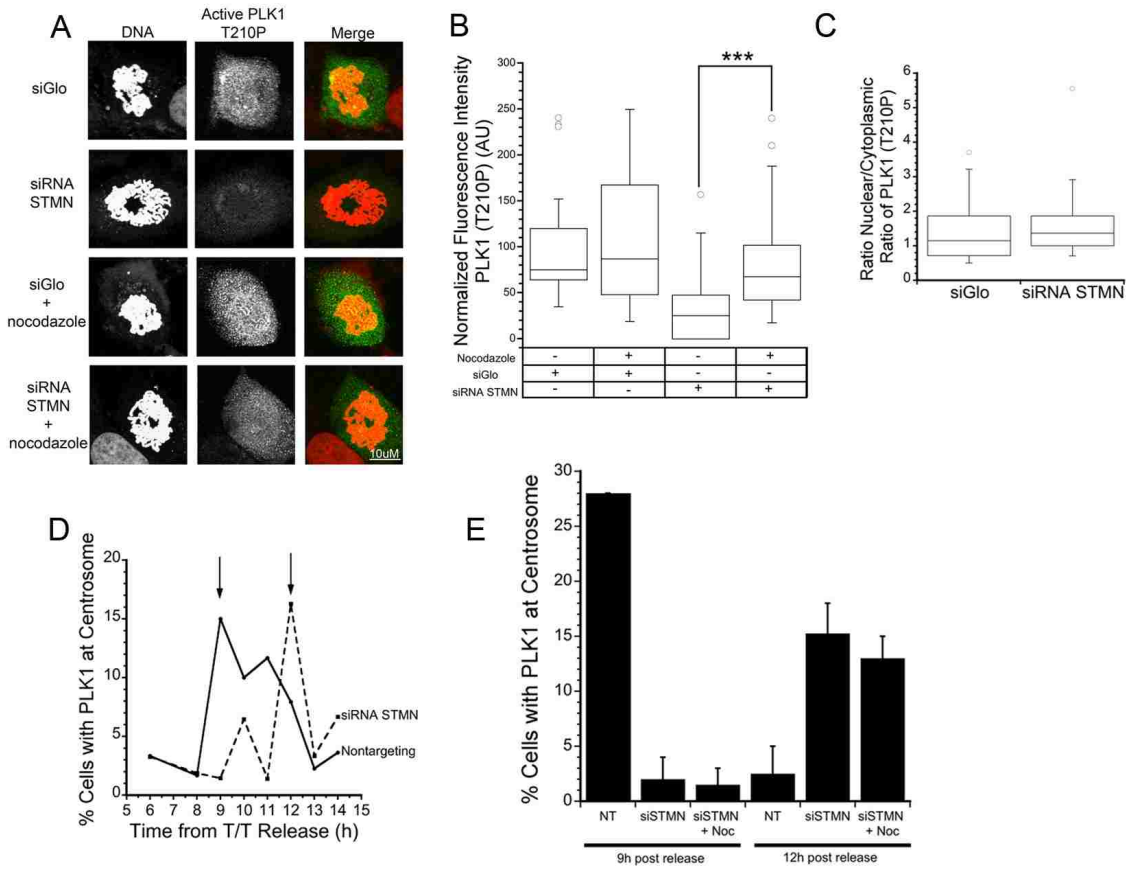

Figure 2.8: MT depolymerization restores active Plk1 in stathmin-depleted cells without reversing the delay in Plk1 localization to centrosomes. (A) Approximately 45 hours after siRNA transfection, Hela cells were incubated with DMSO or 33µM nocodazole for 3 hours. Cells were then fixed 3 h later and stained with an antibody against Plk1 phospho-T210 (green in merged images) and propidium iodide to stain DNA (red in merged images). Representative images of maximum intensity projections of Z-stacks of active Plk1 were analyzed for fluorescence intensity. Values for each cell were normalized to the average of control cells and statistical significant determined using Student's t-test. (B) Box plot represents normalized data pooled from three independent

experiments, at least 7 cells per treatment/experiment. MT depolymerization restored active Plk1 level to nearly that measured in siGLO control-transfected cells *** denotes $p<0.001$. (B) The reduction in active Plk1 measured within nuclei of stathmin-depleted cells does not result from a failure to localize to the nucleus. The ratio of fluorescence intensities for active Plk1 in the nucleus/cytoplasm were unchanged by stathmin depletion. (C) Stathmin depletion delays Plk1 localization to the centrosome. Cells were stained with antibodies to Plk1 and g-tubulin at times after release from a double thymidine block and the percent Plk1 positive centrosomes are shown. (D) MT depolymerization with 33 μM nocodazole did not restore the timing of Plk1 recruitment to the centrosome in stathmin-depleted cells. Cells were fixed 9 and 12 h after release from a double thymidine block. Data shown are the average of two experiments and > 100 cells per time point, per experiment.

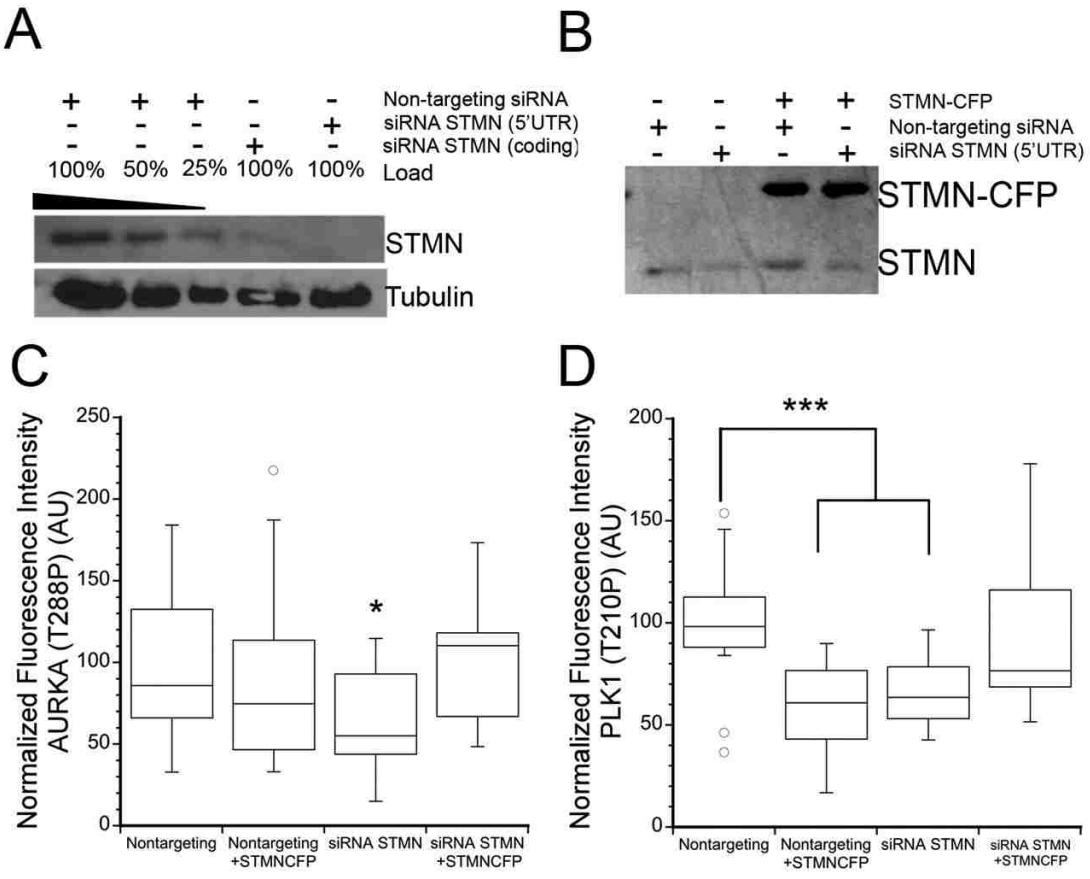

Figure 2.9: Stathmin overexpression decreased Plk1, but not AURKA, activation level. Hela cells were transfected with non-targeting control siRNA, or siRNA targeting 5' UTR of stathmin, and/or plasmid containing stathmin-CFP. Fixed cells were stained with propidium iodide to stain DNA and antibodies against either AURKA phospho-T288 or PLK1 phospho-T210. For stathmin-CFP transfected cells, only those cells expressing CFP were used for imaging and analysis. (A) Western blot demonstrating stathmin knockdown with the 5'UTR-targeted sequence. (B) Western blot of stathmin and/or stathmin-CFP expression as noted. (C) Box plot of the relative fluorescence intensity of AURKA (T288P) at the centrosomes of cells entering mitosis. (D) Box plot of Plk1 (T210P) levels within the nucleus of prophase cells. Values for each cell were

normalized to the average of control cells and statistical significance determined using Student's t-test. Box plot represents normalized data pooled from two independent experiments, at least 7 cells per treatment/experiment. * denotes $p<0.05$, *** denotes, $p<0.001$.

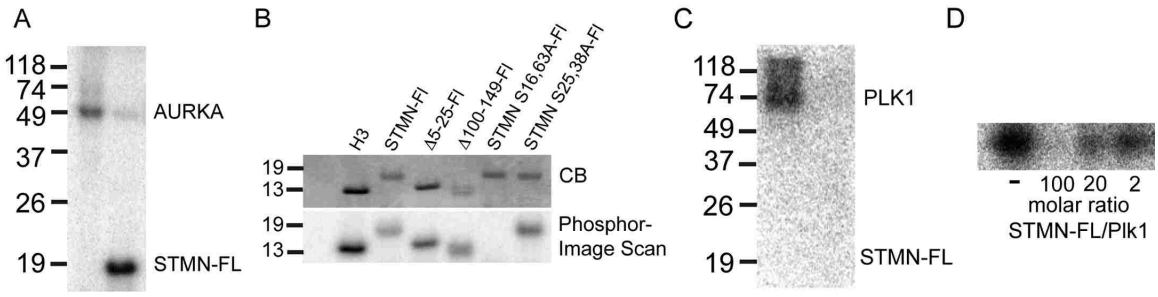

Figure 2.11: Stathmin is phosphorylated by AURKA and inhibits Plk1 autophosphorylation in vitro. Bacterially-expressed and purified stathmin-FLAG or mutants (also FLAG-tagged) were incubated with active AURKA and [32P]-ATP as described in Methods. (A) PhosphorImager scan showing phosphorylation of stathmin. AURKA was also capable of autophosphorylation. The lesser AURKA autophosphorylation in the sample containing stathmin was not consistently observed. (B) AURKA phosphorylation was abolished by mutation of S16 and S63 to alanine. Histone H3 (H3) served as a positive control for kinase activity. CB, Coomassie Blue. (C) Stathmin was not phosphorylated by Plk1 in vitro, but stathmin significantly reduced Plk1 autophosphorylation. (D) Stathmin inhibits Plk1 autophosphorylation in a dose dependent manner. The molar ratio of stathmin to Plk1 is given below each lane.

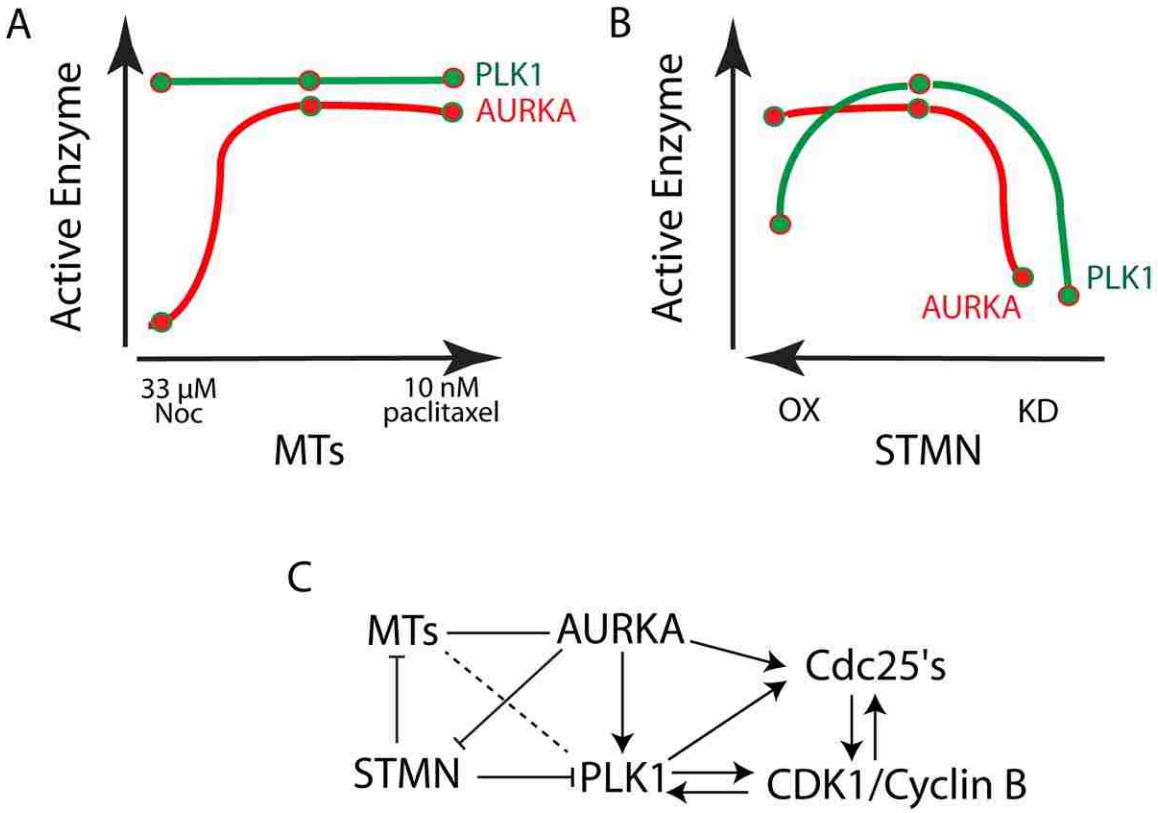

Figure 2.12: Summary of MT and stathmin regulation of AURKA and Plk1 activation. (A, B) Schematic representations of active AURKA and Plk1 after manipulation of MTs (A) and stathmin level (B). Note that stathmin level is diagrammed from high to low (left to right). A delay in mitotic entry is only observed when both AURKA and Plk1 are inhibited, which is only present in stathmin-depleted cells. (C) Outline of where MTs and stathmin MTs interact with enzymes driving mitotic entry. Arrows represent direct activation, the line connecting MTs and AURKA represents the MT requirement for AURKA localization to centrosomes, the dashed line between MTs and Plk1 represents the ability of MT depolymerization to restore Plk1 activity after stathmin depletion.

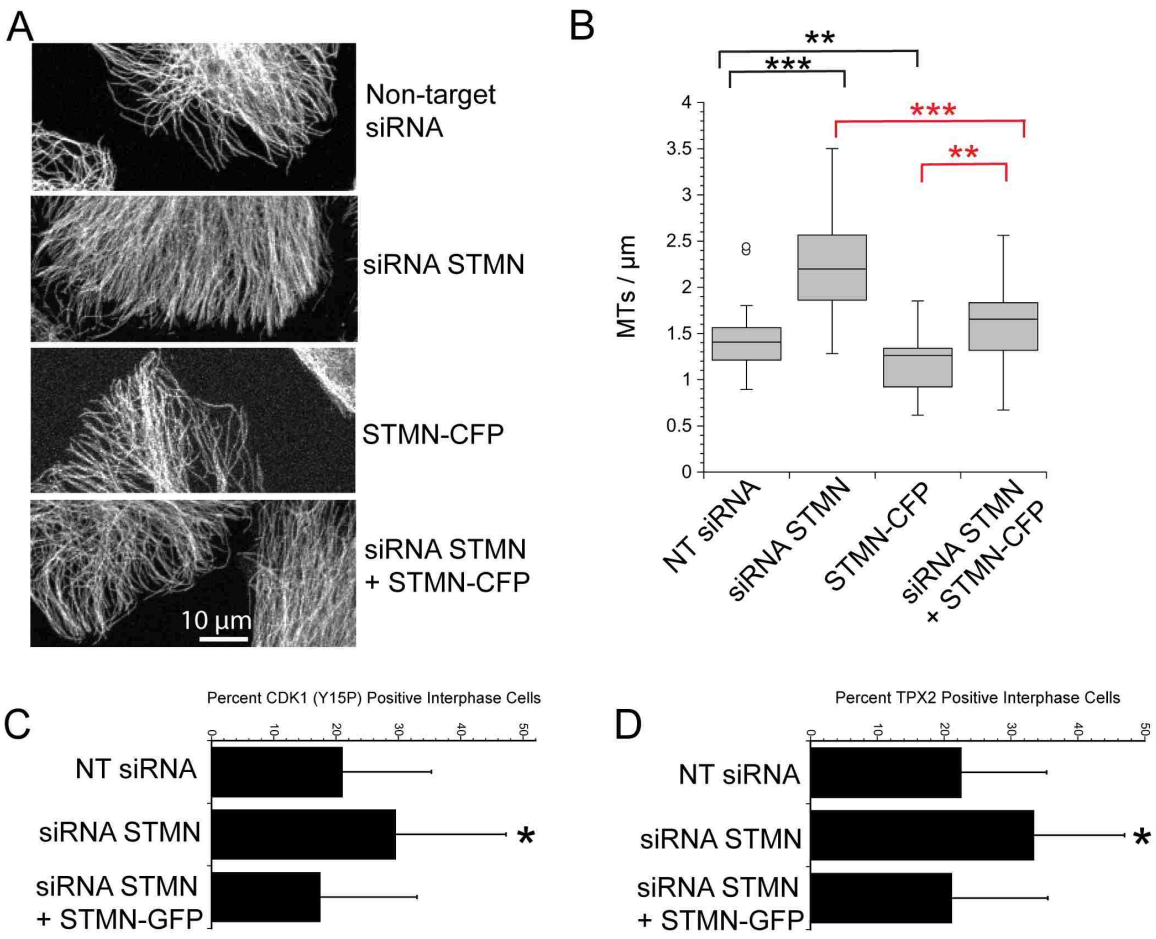

Figure 2.10: Exogenous stathmin expression restores normal MT number and mitotic entry timing. Hela cells were transfected with non-targeting control siRNA, or siRNA targeting 5' UTR of stathmin, and/or plasmid containing stathmin-CFP or STMN-GFP. (A) Representative images of MTs are shown for depletion and/or expression of stathmin (STMN) tagged with GFP or CFP. (B) MT numbers were counted for all detectable ends within 5 µm of the cell periphery and reported as MTs per µm of cell circumference. Box plot represents pooled data from 4 independent experiments with at least 19 cells per treatment. (C-D) Percent of cells staining positive for (C)CDK1 (Y15P) or (D) TPX2. *, **, *** denotes $p<0.05$, $p<0.01$ and $p<0.001$ respectively.

Chapter 3

Mechanistic basis for p53-deficient cell death triggered by a mitotic entry delay.

Introduction

Mutations or loss of the tumor suppressor gene, p53, are the most prevalent and catastrophic gene alterations in cancer, present in over half of all human cancers (Soussi 2006, Green and Kroemer 2009). P53 acts as a master regulator in normal cells, facilitating responses to stress and DNA damage, cell cycle progression, metabolism and mitochondrial integrity (Green and Kroemer 2009, Matoba 2006, Nantajit 2010). Great efforts have been made to restore p53 function in cancer cells by viral delivery of WT p53, inhibition of nonsense mediated RNA decay to promote read through of premature stop codons or small molecule inhibition of mutant copies of p53. However, such therapies have yet to successfully make it out of clinical trials in the U.S. (Vecil and Lang 2003, Prabhu 2012, Martin 2014).

In addition to restoring p53 function, there has also been much research toward finding selective targets for cells with missing or mutated p53. Indeed p53-deficient cells are more vulnerable to ATR/Chk1 inhibition with DNA damage, serine/threonine kinase inhibition as well as PLK1 inhibition (Reaper 2011, Schoppy and Brown 2012, Jemaa 2012, Liu 2006, Sur et al.2008). However, these treatments, despite favoring p53 deficient cells, still lead to significant cell death in non-transformed cells.

A microtubule regulator, stathmin, is overexpressed in a number of cancers and thus represents a potential therapeutic target (Mistry 2005, Belletti 2011). Stathmin acts as a microtubule destabilizer by binding soluble tubulin dimers and promoting catastrophe of existing microtubules. Depletion of stathmin slows proliferation and

increase cell death in cancer-derived cell lines (Mistry 2005, Zhang 2006, Wang, 2007) and in some studies death was observed only in p53 deficient cells (Alli 2002, Alli 2007, Carney and Cassimeris 2010). The effect of stathmin loss on proliferation occurs at least in part via changes in microtubule dynamics that delay mitotic entry by slowing the kinetics of CDK1 activation (Carney et al. 2012, Silva and Cassimeris 2013).

However, the mechanism by which stathmin loss leads to cell death is unknown. We set out to determine whether cell death in stathmin-depleted cells was directly triggered by a mitotic entry delay, by some other consequence of altered microtubule stability or the result of a novel function of stathmin loss. Additionally, we wanted to identify the role p53 plays in survival for these cells. Here we describe results demonstrating that a mitotic entry delay triggers caspase 8 dependent apoptosis selectively in cells without functional p53. Caspase 8 activation is inhibited by cFLIP, a protein that can form heterodimers with procaspase 8 and is normally present in low levels in p53 deficient cells. We find that restoration of cFLIP level rescues viability of stathmin-depleted p53 deficient cells. These findings reinforce the potential of stathmin modulation as a therapeutic strategy and suggest that mitotic entry disruption can selectively cause cell death in the majority of cancers lacking a functional p53 protein.

Results:

A 4 hour G2 delay is sufficient to induce cell death in p53-deficient cells

To determine if a mitotic entry delay was initiating death in stathmin-depleted cells, we induced a mitotic entry delay using a combination of enzyme inhibitors. We had previously found (Silva and Cassimeris, 2013) that stathmin depletion reduces the

activity of mitotic entry kinases, AURKA and PLK1, slowing kinetics of CDK1 activation to produce an approximate four hour delay in mitotic entry (Silva and Cassimeris 2013). We used a combination of chemical inhibitors to both AURKA (inhibitor S1451) and PLK1 (inhibitor BI2536) to delay mitotic entry in Hela cells first synchronized with a double thymidine block. Approximately 6 hours following release from the block, we added either a combination of S1451 and BI2536 or DMSO as a vehicle control for four hours and then replaced drug-containing medium with regular DMEM. The cells were then followed over the next 72 hours via live cell imaging. From these videos we determined the percent of cells that died. Cell death was marked by cell retraction and formation of apoptotic bodies (Figure 3.1, A). We found that the group of cells treated with both AURKA and PLK1 inhibitors had a three fold increase in cell death over DMSO treated control cells and these increases were statistically significant (Figure 3.1, B). In order to know whether cell death occurs during a distinct point after a mitotic entry delay or at a particular stage of the cell cycle, we also tracked when cell death occurred respective to both start of imaging and from that cell's last mitosis. We observed that cells die anywhere from hours to days following an initial mitotic entry delay and that death can occur at any point of the cell cycle (Figure 3.1 C).

To confirm that the cell death was due to a delay in mitotic entry and not some off target effect of AURKA and PLK1 inhibition, we repeated these experiments using a CDK1 inhibitor (RO3306) at a concentration (10uM) sufficient to arrest cells in G2. We also found that cell death in the group treated with the CDK1 inhibitor for 4 hours was significantly higher than DMSO controls, a four-fold increase (Figure 3.1, B). Additionally, we confirmed that the increase in cell death was due to inhibition of CDK1

specifically prior to mitotic entry and not elsewhere in the cell cycle. We treated asynchronously growing Hela or HCT116 p53 $^{-/-}$ cells with CDK1 inhibitor (RO3306) for four hours and assessed viability 48 hours following treatment by trypan blue exclusion (Figure 3.1, D). We found no increase in cell death over DMSO treated controls indicating that CDK1 inhibition only prior to mitotic entry causes cell death.

Since it was previously shown that stathmin depletion leads to death only in cells lacking p53 (Alli et al. Oncogene 2007, Carney and Cassimeris 2010), we next asked whether the death induced by a 4 hour delay in mitotic entry was also dependent on the absence of p53. Using isogenic colorectal cancer cell lines differing in p53 genotype, HCT116 p53$^{+/+}$ and p53 $^{-/-}$, we synchronized cells with a double thymidine block and pulsed with either DMSO or 10uM RO3306 for four hours beginning 6 hours after release from the block. At 48 hours after drug pulse, a time at which we observed the most death in the time-lapse imaging experiments, we assayed viability by a trypan blue exclusion assay. We found that only the HCT116 p53 $^{-/-}$ line pulsed with RO3306 exhibited a significant decrease in viability compared to DMSO pulsed control cells (Figure 3.1, E). We previously used these cell lines to confirm the p53 dependence for stathmin depletion induced death (Carney and Cassimeris, 2010).

Given that the percent of cells that die from stathmin depletion is greater than a single 4 hour delay produces, it was possible that stathmin depletion causes some other effect outside of mitotic entry that also contributes to cell death. To test whether stathmin depletion induces cell death by delaying mitotic entry or by a mechanism independent of the cell cycle delay, we next compensated for reduced AURKA and PLK1 in these cells to eliminate the delay in G2 by inhibiting Wee 1 kinase. Since Wee1 normally inhibits

CDK1 activation, we hypothesized that inhibition of Wee1 would alleviate the mitotic entry delay in stathmin-depleted cells. To test this hypothesis we synchronized control and stathmin-depleted Hela cells with a double thymidine block and released cells into a Wee1 inhibitor (10nM MK1775) or DMSO. Mitotic index was determined at timepoints following release for all groups. For stathmin depletion, Hela cells were transfected with siRNA targeting stathmin, which reduces stathmin protein levels to approximately 25% of control cells (Silva and Cassimeris, 2013, Carney et al. 2013, Carney and Cassimeris, 2010; See Chapter 2). We observed that stathmin-depleted cells treated with MK1775 entered mitosis with normal timing following release from a thymidine block (Figure 3.2, A).

Since Wee 1 inhibition restores normal mitotic entry timing in stathmin-depleted cells, we were able to assess whether reduced stathmin level could induce death in the absence of a cell cycle delay. We synchronized control and stathmin-depleted Hela cells released into either MK1775 or DMSO and measured cell viability 48 hours following release. We found that Wee 1 inhibition restored viability in stathmin-depleted cells to that of control cells indicating that the mitotic entry delay from stathmin depletion is the major trigger of cell death (Figure 3.2, B). Given that we observed cell death occurring at various times following a mitotic entry delay from treatment with AURKA and PLK1 inhibitors, we wanted to know if stathmin-depleted cells also die randomly. Using live cell imaging we followed stathmin-depleted Hela cells for 72 hours and tracked when these cells die respective to their last mitosis. We found that similar to treatment with AURKA and PLK1 inhibitors, there is no apparent pattern to when death occurs (Figure 3.2, C). Microtubule targeting drugs that block cells in mitosis also have a similar

phenotype, where many cells die at various times after slipping out of the mitotic arrest (Gascoigne and Taylor, 2009).

Mitotic Entry Delay induced death is caspase 8 dependent

Since a mitotic entry delay is sufficient to trigger cell death, we then wanted to know by what mechanism cell death occurs. We had previously determined that stathmin-depleted cells were undergoing apoptotic cell death based on cell morphology changes, caspase 3 activation and the presence of cleaved PARP (Carney and Cassimeris, 2010). We then asked which apoptotic pathway(s) were activated in these cells. We had hypothesized that cell death from stathmin depletion was occurring via the intrinsic death pathway and caspase 9 activation since others have found that prolonged CDK1 activity during mitotic arrest leads to caspase 9 dependent death. Cell lysates from stathmin-depleted and non-targeting siRNA transfected control cells were prepared on days 2-5 following transfection and probed for (active) cleaved Caspase 8 and (active) cleaved Caspase 9 via western blot. Initially, we did not detect an increase in either form of active caspase. Since the observed death in these cells is modest and the time frame from initiator caspase cleavage to cell death is on the order of minutes (Green, 2005), we repeated the experiment with the addition of z-VAD, a broad caspase inhibitor, to allow accumulation of active caspases. Since caspase 8 and 9 are initiator caspases, z-VAD would bind these caspases as soon as they were active thereby stopping the death cascade and allowing accumulation of active initiator caspases. Stathmin-depleted Hela cells treated with z-VAD had an increased amount of cleaved caspase 8 compared to control cells treated with z-VAD (Figure 3.3, A) whereas there was no detectable activation of

caspase 9 (data not shown). We also detected increased cleaved caspase 8 in both Hela cells and HCT116 p53 $^{-/-}$ cells delayed for 4 hours at mitotic entry with CDK1 inhibitor, RO3306 (Figure 3.3, A and B).

To confirm that caspase 8 activation was triggering cell death, we blocked caspase 8 activity with a specific caspase 8 inhibitor, Z-IETD. We treated Hela and HCT -/- p53 cells with 4 hour pulses of RO3306 or DMSO as described above and then added either Z-IETD or DMSO for 48 hours and measured viability. We found that in both cell lines, treatment of RO3306 pulsed cells with Z-IETD restored viability to that of control cells, confirming the requirement for caspase 8 activity to activate a death pathway following a mitotic entry delay (Figure 3.3, C and D). Consistent with caspase 8 activation, we also observed an increase in active (active) NFκB and active ERK, which are downstream targets of caspase 8 activity (Figure 3.3, E and F).

Programmed cell death can also be driven by caspase 8 activity via interaction with stress induced adaptor kinase RIP1, a mechanism called necroptosis (Festjens 2007, Tenev 2011). We probed whether a RIP1 inhibitor, necrostatin, could alleviate cell death following stathmin-depletion. We added necrostatin (1uM) at a concentration that is double the recommended IC50 (EMD Millipore) to stathmin-depleted Hela cells for 72 hours following transfection and observed no rescue in cell viability (data not shown). From these data we conclude that stathmin depletion, via a mitotic entry delay, leads to caspase 8 dependent cell death that is likely apoptosis and not necroptosis.

CDK1 inhibition decreased caspase 8 phosphorylation

A key modulator of apoptosis inhibition during mitosis is CDK1 activity. CDK1 has been shown to phosphorylate a number of caspases, including caspase 8 (Andersen 2009, Matthess 2010). Phosphorylation by CDK1 on caspases at or near interdomain sites prevents caspase activation (Andersen, 2009). Since caspase 8 has been shown to be a substrate for CDK1, we hypothesized that decreased CDK1 activity as seen in stathmin-depleted cells would be accompanied by a decrease in procaspase 8 phosphorylation at Serine 387 (Ser387P), which protects against caspase 8 autoproteolysis (Matthess 2010). We probed lysates of Hela cells via western blot and found procaspase 8 (S387P) to be greatly reduced after either stathmin depletion or CDK1 inhibitor treatment (Figure 3.4, A and B).

cFLIP level is dependent on p53

Given that cell death is only observed following stathmin depletion or a mitotic entry delay in cells lacking p53,we hypothesized that it is likely that a regulator of caspase 8 is influenced by p53 status. A strong candidate protein is cFLIP, an endogenous caspase 8 inhibitor, whose expression or protein stability requires p53 (Fukazawa 2010, Galligan 2005). We hypothesized that cFLIP levels were reduced in p53 deficient cells. We probed cFLIP levels in Hela cell lysates depleted of stathmin and/or HPV protein E6 to restore p53 (see Carney and Cassimeris 2010, Figure 3.4, C). We found that restoring p53 greatly increased cFLIP protein levels and surprisingly, stathmin depletion alone further reduced already low levels of cFLIP in Hela cells (Figure 3.4, D). In order to know whether decreased cFLIP in stathmin-depleted cells was contributing to caspase 8

activation and therefore cell death, we restored cellular cFLIP levels by transient expression of FLAG tagged cFLIP (Figure 3.4, E). As others have reported (Chang 2002), cells are sensitive to both lower and higher levels of cFLIP and we found that our typical transfection protocol using 1ug plasmid DNA lead to high level over-expression of FLAG-cFLIP which on its own induced cell death. Transfection with a lower plasmid amount, 100ng, did not induce cell death and was sufficient to restore viability in stathmin-depleted to the level of control cells (Figure 3.4, F).

Discussion:

The requirement for stathmin in survival of cancer cells lacking p53 has been poorly understood. It was known that stathmin depletion leads to mitotic entry delay as well as cell death, but whether these two phenotypes were linked was unknown. Here we set out to determine if a mitotic entry delay initiates cell death and by what mechanism cell death occurs. We established that a four hour delay in mitotic entry triggers cell death via caspase 8 activation. However, the possibility of caspase 9 involvement in mitotic entry delay induced apoptosis cannot be ruled out. Caspase 8 is known to trigger cytochrome C release and therefore downstream apoptosome formation and caspase 9 activation (Kruidering and Evan 2000). The time from caspase 9 activation to cell death occurs on the order of minutes (Green, 2005). Considering the potentially small time window of caspase 9 activity and the random timing of individual cell death, it is possible that increases in cleaved caspase 9 are too small to detect. However, if there is a role for caspase 9, it would be occurring downstream of caspase 8 activation.

In order to know why a mitotic entry delay contributes to caspase 8 activity, we considered the biochemical differences between a delayed and normal mitotic entry timing and how these differences relate to what is known about how cells survive a prolonged mitosis (a delay in mitotic exit). For example, it is proposed that during mitosis, cells require increased protection against cell death because factors such as loss of adhesion signaling or leakage of cytochrome c during mitochondrial fission (Andersen 2009) make mitotic cells particularly vulnerable to activation of apoptosis. CDK1 is a key mediator of this protection, phosphorylating a number of caspases to inhibit their activation. During a mitotic entry delay, such as that induced by stathmin depletion, CDK1 activity remains below threshold for an atypically long duration, estimated to be at or greater than four hours. These data are consistent with a model where decreased CDK1 activity during prolonged mitotic entry leads to loss of protective phosphorylation of caspase 8 and lowers the threshold for caspase 8 activation, which may make these cells more vulnerable to apoptotic stimuli.

In order to know if phosphorylation of Ser387 on caspase 8 actually confers resistance to apoptosis, we expressed a pseudophosphorylated form of caspase 8, with Ser387 mutated to Glutamic Acid (S387E) with the hypothesis that it might act as a dominant negative form of caspase 8 in cells. Expression of S387E did not increase viability of stathmin-depleted cells (data not shown). It is possible that the phospho-mimetic mutant of caspase 8 does not act as a dominant negative version of the caspase or that there is already sufficient endogenous caspase 8 concentration for activation. Therefore, the functional significance of phospho-Ser387 on caspase 8 is still unknown.

Since a mitotic entry delay only activates caspase 8 in the absence of p53, we hypothesized that caspase 8 inhibitor is regulated by p53. We measured levels of a known caspase 8 inhibitor, cFLIP, and found it to be reduced in the absence of p53 (Figure 3.4, D), consistent with previously published results (Bartke 2001). Based on these observations, we hypothesized that p53 deficient cells are more susceptible to death due to decreased levels of cFLIP protein. This hypothesis was supported by experiments to over-express cFLIP, which restored viability to stathmin-depleted or mitotic entry delayed cells. Taken together, the combination of CDK1 inhibition and loss of p53 culminates in loss of two sources of caspase 8 inhibition, phosphorylation of Ser387 on caspase 8 and decreased cFLIP levels. Decreased phosphorylation at Ser387 and lower cFLIP levels are potentially sufficient for caspase 8 activation in the absence of any other death stimuli.

The timing and small percentage of cell death observed in our experiments (Figure 3.1,C and Figure 3.2, C) is consistent with the above model. We determined that cell death occurs at various times following mitotic exit and therefore in the absence of cell cycle specificity, other than an initiating event in G2. If caspase 8 activation in stathmin-depleted, p53-deficient cells were stochastic, cell death would occur randomly following an initial mitotic entry delay and this is precisely what we observe. The trigger for caspase 8 activation remains unknown, but several possible mechanisms are discussed next.

It is possible that CDK1 inhibition and decreased cFLIP allow increased caspase 8 sensitivity to some unknown external death signal, produced in response to cell stress caused by a mitotic entry delay. Alternatively, an intracellular trigger may promote

assembly of a caspase 8 activating platform, such as the Ripoptosome (Tenev 2011) without requiring engagement of a death receptor. In either case, we expect that the normal balance between pathways that activate and inhibit caspase 8 activation are altered to favor activation. Understanding the trigger mechanism will be difficult given its transient and stochastic formation.

Regardless of the death-triggering mechanism, it is clear that p53 deficient cells, because of decreased cFLIP levels, are more vulnerable to caspase 8 activation. Disrupting mitotic entry is an attractive therapeutic strategy since normal cells do not appear to be effected by a small delay such as that achieved by partial PLK1 and AURKA inhibition. Stathmin inhibition, either via small molecules or RNA interference, would be an ideal means to delay mitotic entry without disrupting normal mitotic progression. Avoiding abnormal mitosis would alleviate some of the harmful effects, such as aneuploidy and massive cell death in normal tissues, caused by microtubule disrupting agents. (Gascoigne and Taylor 2009). Most importantly stathmin inhibition and slowing of mitotic entry represents the only treatment known thus far to selectively cause death only in p53 deficient cells.

Materials and Methods:

Cell Culture and Plasmid Transfections: Hela and HCT 116 ($p53^{+/+}$ and $p53^{-/-}$ lines (gift of Dr. Volgelstein, Johns Hopkins School of Medicine) cells were grown in DMEM (Sigma) supplemented with 10% fetal bovine serum (FBS; Invitogen) and 1X antibiotic/antimycotic (Sigma). In some experiments, cells were synchronized through a double thymidine block by overnight incubation in 5mM thymidine (in DMEM), 8 h

release in DMEM after 5 washes in warm PBS and then 16 h incubation in 5mM thymidine (in DMEM). Cells were transferred to DMEM following 5 washes with warm PBS and used for Trypan Blue exclusion assays and/or cell lysate preparation 48-72 hours following release.

In some experiments Hela cells were transfected with plasmids for expression of FLAG-tagged-cFLIP or an empty vector encoding FLAG, or an empty vector encoding GFP using X-tremeGene HP DNA Transfection Reagent (version 1.0; Roche Diagnostics, Indianapolis, IN) according to the manufacturer's protocol. Cells were transfected approximately four hours following siRNA transfections and cell viability was assessed approximately 48 hours following initial transfection.

Indirect Immunofluorescence and confocal microscopy: Hela cells were grown on glass coverslips and treated as described above. They were either fixed with 4% Paraformaldehyde/20% glycerol in PBS, pH 7.3 (PFA, Electron Microscopy Services) for 10 minutes at room temperature or with methanol supplemented with 1mM EDTA at -20^{o}C for 10 minutes. Cells fixed with PFA were permeabilized with methanol at -20^{o}C for 10 minutes. Fixed cells were incubated with blocking reagent (10% FBS in phosphate buffered saline, PBS) for 30 minutes at 37^{o}C followed by a 45 minute incubation with primary antibody at 37^{o}C. Cells were then washed with PBS and incubated with secondary antibody and 1.5 μM propidium iodide for an additional 45 minutes at 37^{o}C. Antibodies used included: anti-phospho NFkB (Ser536)(1:1000, Cell Signaling), anti-NFkB (T288) (1:1000, Cell Signaling), anti-phospho-ERK 1/2 (Thr218Tyr220) (1:1000, Cell Signaling), anti-ERK (1:100, Cell Signaling), and Goat anti-mouse or anti-rabbit

Alexa Fluor 488 (1:50, Invitrogen). Coverslips were then washed with PBS and mounted on slides with Vectashield (Vector Labs). Cells were imaged as described previously (Piehl and Cassimeris, 2003) using 63X/1.4 numerical aperture plan apo objective on an inverted microscope (Zeiss Axiovert 200M). For synchronized cells mitotic index was determined by staining with propidium iodide and counting cells with condensed chromatin as a percent of total cells. At least ten fields (coverslip positions, > 100 cells per time point) were counted for each treatment group for each independent experiment.

Drugs and Reagents: Chemical inhibitors to PLK1 (BI 2536, Grinshtein *et al,*. 2011), AURKA (S 1451, Yuan *et al.,* 2011), and Wee1 (MK1775, Hirai et al, 2009) were purchased from Selleckchem. Chemical inhibitor to CDK1 (Vassilev 2006) and pan-caspase inhibitor, Z-VAD-FMK were purchased from Tocris Bioscience. Caspase 8 specific inhibitor, Z-IETD was purchased from Millipore. All other reagents were from Sigma unless noted otherwise.

RNA Interference and Transient Transfection: Cells were grown in 35mm dishes and transfected with siRNAs 1-2 days after plating using GeneSilencer (Genlantis) according to the manufacturer's protocol. Cells were serum starved from the time of transfection to four hours post-transfection to improve efficiency. siRNA oligonucleotides (Thermoscientific/Dharmacon) used were SMTN1 (Op18-443), 5'-CGUUUGCGAGAGAAGGAUAdtdt-3'. siGenome non-targeting siRNA (Thermoscientific/Dharmacon) was used as control siRNA sequences for these experiments (Silva and Cassimeris 2013, Carney et al. 2012).

Western Blotting: Soluble cell extracts were prepared as described previously (Carney and Cassimeris, 2010) and protein concentrations were measured by Bradford assay. Lysates were diluted in PAGE sample buffer, 40 μg total protein per lane was typically loaded and resolved in 10% polyacrylamide gels and transferred to Immobilon Membranes (Millpore, Billerica, MA). Membranes were blocked with 5% non-fat milk or 5% BSA (depending on manufacturer recommendation) in Tris-buffered saline with 0.1% Tween and then probed with primary antibodies: anti cleaved Caspase 8 (1:1000; Cell Signaling), phospho-Caspase 8 (1:1000, gift from Klaus Strebhardt, J.W. Goethe University, Matthess et al. 2010), anti-cleaved Caspase 9 (1:1000;Cell Signaling), or cFLIP (1:1000, Cell Signaling), followed by secondary antibodies, anti-mouse (1:2000; Abcam) or anti-rabbit (1:10,000, BD Biosciences) horseradish peroxidase-linked IgG. Immunoreactive bands were developed using enhanced chemiluminscence (GE Amersham). Membranes were reprobed with anti-α-tubulin (1:1000, Sigma) or GAPDH (1:1000, Abcam) as a loading control.

Live Cell Imaging: To follow cell fates over several days, Hela cells were plated on Mattek dishes and imaged using a Nikon Biostation IM as described previously (Silva and Cassimeris, 2013; Carney *et al.,* 2012). Cells were imaged with phase contrast optics using a 20X objective and images were collected at 5 minute intervals for 24-72 hours. Cell fates were tracked from image series. Cell death was determined by changes in cell morphology characterized by cell retraction and blebbing of the plasma membrane.

Cell Viability Measurements: For synchronization experiments, cells were allowed to grow for two days following pulses with kinase inhibitors. For cells transfected with siRNA and/or plasmids, cells were allowed to grow asynchronously for three days following transfection. On the day of measurement, cells were trypsinized and resuspended in PBS with 0.2% Trypan Blue and counted using a hemocytometer to determine viability via Trypan Blue exclusion.

Data Analysis: Statistical analysis of fluorescence intensity and cell cycle durations were performed using unpaired t-tests with GraphPad Software (www.graphpad.com/quickcalcs/ttest1.cfm).

References:

1. Soussi T (2000) The p53 tumor suppressor gene: from molecular biology to clinical investigation. Annals of the New York Academy of Sciences 910:121-137; discussion 137-129.
2. Green DR & Kroemer G (2009) Cytoplasmic functions of the tumour suppressor p53. Nature 458(7242):1127-1130.
3. Matoba S, et al. (2006) p53 regulates mitochondrial respiration. Science 312(5780):1650-1653.
4. Nantajit D, et al. (2010) Cyclin B1/Cdk1 phosphorylation of mitochondrial p53 induces anti-apoptotic response. PloS one 5(8):e12341.
5. Vecil GG & Lang FF (2003) Clinical trials of adenoviruses in brain tumors: a review of Ad-p53 and oncolytic adenoviruses. Journal of neuro-oncology 65(3):237-246.
6. Prabhu VV, et al. (2012) Therapeutic targeting of the p53 pathway in cancer stem cells. Expert opinion on therapeutic targets 16(12):1161-11
7. Martin L, et al. (2014) Identification and characterization of small molecules that inhibit nonsense mediated RNA decay and suppress nonsense p53 mutations. Cancer research.
8. Reaper PM, et al. (2011) Selective killing of ATM- or p53-deficient cancer cells through inhibition of ATR. Nature chemical biology 7(7):428-430.
9. Schoppy DW & Brown EJ (2012) Chk'ing p53-deficient breast cancers. The Journal of clinical investigation 122(4):1202-1205.

10. Jemaa M, et al. (2012) Selective killing of p53-deficient cancer cells by SP600125. EMBO molecular medicine 4(6):500-514.
11. Liu X, Lei M, & Erikson RL (2006) Normal cells, but not cancer cells, survive severe Plk1 depletion. Molecular and cellular biology 26(6):2093-2108.
12. Mistry SJ, Bank A, & Atweh GF (2005) Targeting stathmin in prostate cancer. Molecular cancer therapeutics 4(12):1821-1829.
13. Belletti B & Baldassarre G (2011) Stathmin: a protein with many tasks. New biomarker and potential target in cancer. Expert opinion on therapeutic targets 15(11):1249-1266.
14. Zhang HZ, et al. (2006) Silencing stathmin gene expression by survivin promoter-driven siRNA vector to reverse malignant phenotype of tumor cells. Cancer biology & therapy 5(11):1457-1461.
15. Alli E, Bash-Babula J, Yang JM, & Hait WN (2002) Effect of stathmin on the sensitivity to antimicrotubule drugs in human breast cancer. Cancer research 62(23):6864-6869.
16. Wang R, et al. (2007) Inhibiting proliferation and enhancing chemosensitivity to taxanes in osteosarcoma cells by RNA interference-mediated downregulation of stathmin expression. Mol Med 13(11-12):567-575.
17. Alli E, Yang JM, Ford JM, & Hait WN (2007) Reversal of stathmin-mediated resistance to paclitaxel and vinblastine in human breast carcinoma cells. Molecular pharmacology 71(5):1233-1240.

18. Carney BK & Cassimeris L (2010) Stathmin/oncoprotein 18, a microtubule regulatory protein, is required for survival of both normal and cancer cell lines lacking the tumor suppressor, p53. Cancer biology & therapy 9(9):699-709.
19. Silva VC & Cassimeris L (2013) Stathmin and microtubules regulate mitotic entry in HeLa cells by controlling activation of both Aurora kinase A and Plk1. Molecular biology of the cell 24(24):3819-3831.
20. Carney BK, Caruso Silva V, & Cassimeris L (2012) The microtubule cytoskeleton is required for a G2 cell cycle delay in cancer cells lacking stathmin and p53. Cytoskeleton (Hoboken) 69(5):278-289.
21. Green DR (2005) Apoptotic pathways: ten minutes to dead. Cell 121(5):671-674.
22. Andersen JL, et al. (2009) Restraint of apoptosis during mitosis through interdomain phosphorylation of caspase-2. The EMBO journal 28(20):3216-3227.
23. Matthess Y, Raab M, Sanhaji M, Lavrik IN, & Strebhardt K (2010) Cdk1/cyclin B1 controls Fas-mediated apoptosis by regulating caspase-8 activity. Molecular and cellular biology 30(24):5726-5740.
24. Fukazawa T, et al. (2001) Accelerated degradation of cellular FLIP protein through the ubiquitin-proteasome pathway in p53-mediated apoptosis of human cancer cells. Oncogene 20(37):5225-5231.
25. Galligan L, et al. (2005) Chemotherapy and TRAIL-mediated colon cancer cell death: the roles of p53, TRAIL receptors, and c-FLIP. Molecular cancer therapeutics 4(12):2026-2036.

26. Grinshtein N, et al. (2011) Small molecule kinase inhibitor screen identifies polo-like kinase 1 as a target for neuroblastoma tumor-initiating cells. Cancer research 71(4):1385-1395.
27. Hirai H, et al. (2009) Small-molecule inhibition of Wee1 kinase by MK-1775 selectively sensitizes p53-deficient tumor cells to DNA-damaging agents. Molecular cancer therapeutics 8(11):2992-3000.
28. Vassilev LT, et al. (2006) Selective small-molecule inhibitor reveals critical mitotic functions of human CDK1. Proceedings of the National Academy of Sciences of the United States of America 103(28):10660-10665.
29. Sur, S., Pagliarini, R., Bunz, F., Rago, C., Diaz, L.A., Jr., Kinzler, K.W., Vogelstein, B., and Papadopoulos, N. (2009). A panel of isogenic human cancer cells suggests a therapeutic approach for cancers with inactivated p53. Proceedings of the National Academy of Sciences of the United States of America 106, 3964-3969.
30. Gascoigne, K.E., and Taylor, S.S. (2008). Cancer cells display profound intra- and interline variation following prolonged exposure to antimitotic drugs. Cancer cell 14, 111-122.
31. Festjens, N., Vanden Berghe, T., Cornelis, S., and Vandenabeele, P. (2007). RIP1, a kinase on the crossroads of a cell's decision to live or die. Cell death and differentiation 14, 400-410.

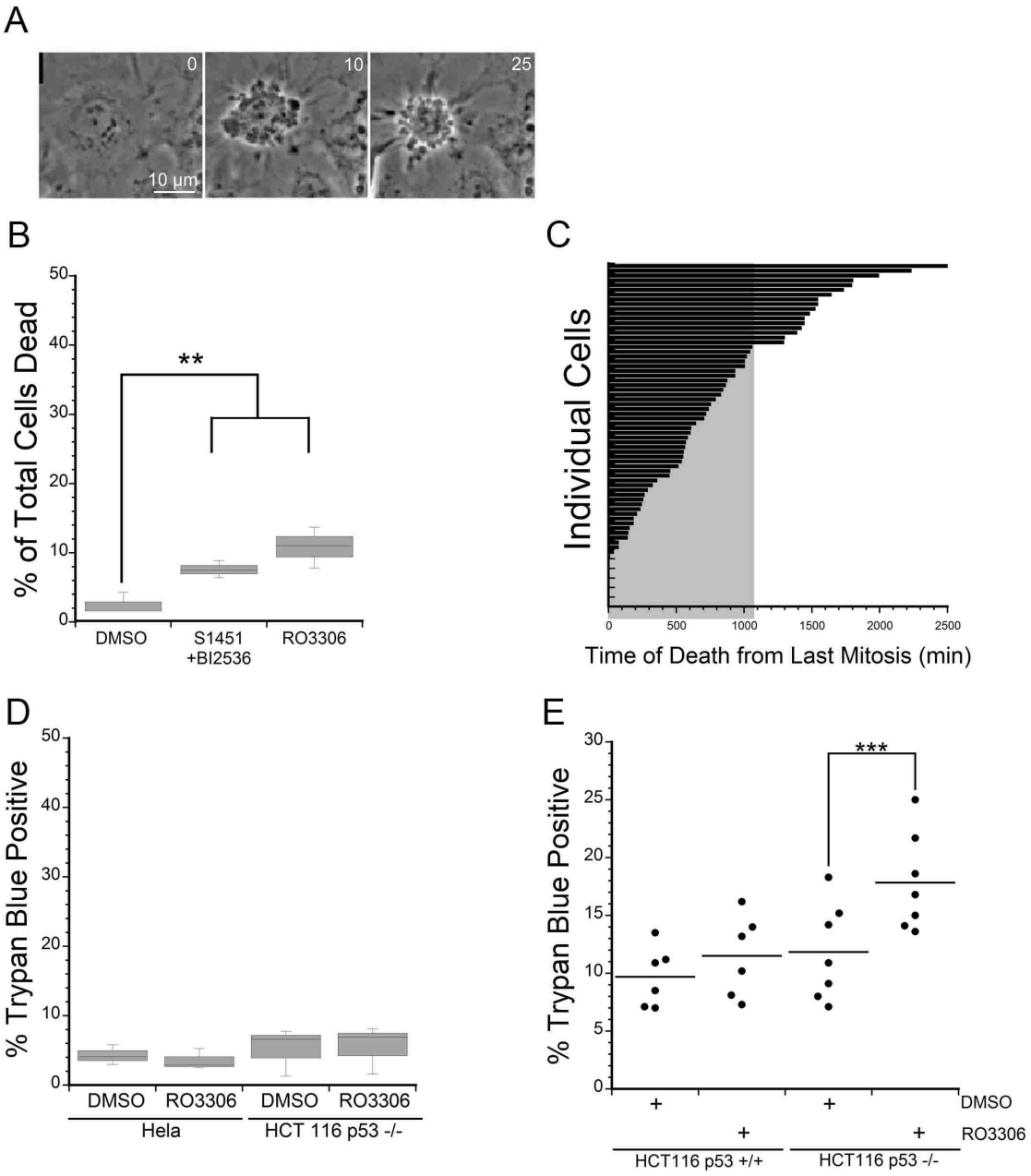

Figure 3.1: A mitotic entry delay triggers cell death in p53 deficient cells. Live cell recordings of Hela cells synchronized with double thymidine block, released and pulsed with DMSO, S1451 and BI2536 or RO3306 for four hours at 6 hours from release. (A)

Representative images of a cell undergoing apoptosis following a mitotic entry delay. (B) Cells and progeny were followed for 72 hours and percent of total cell death calculated. The mitotic entry delay induced by these inhibitors (BI2536 and S1451) increased cell death which occurred at various times following each cell's last mitosis (C). Four hour pulse of inhibitors in asynchronous Hela and HCT116 $p53^{-/-}$ cells (D) followed by live cell recordings as in (A, B). Treatment with AURKA and PLK1 or CDK1 inhibitors in an asynchronous population does not decrease cell viability, demonstrating that the drugs are not toxic throughout the cell cycle. (E) Synchronized HCT116 $p53^{+/+}$ and $p53^{-/-}$ cell lines synchronized and pulsed with RO3306 as in (A). Viability was assayed 48 hours post inhibitor treatment via trypan blue exclusion. Mitotic entry delay via CDK1 inhibition decreased cell viability only in the p53 knockout cell line. Graphs are representative of at least three independent experiments with >300 cells/experiment. ** denotes $p<0.01$, *** denotes $p<0.001$.

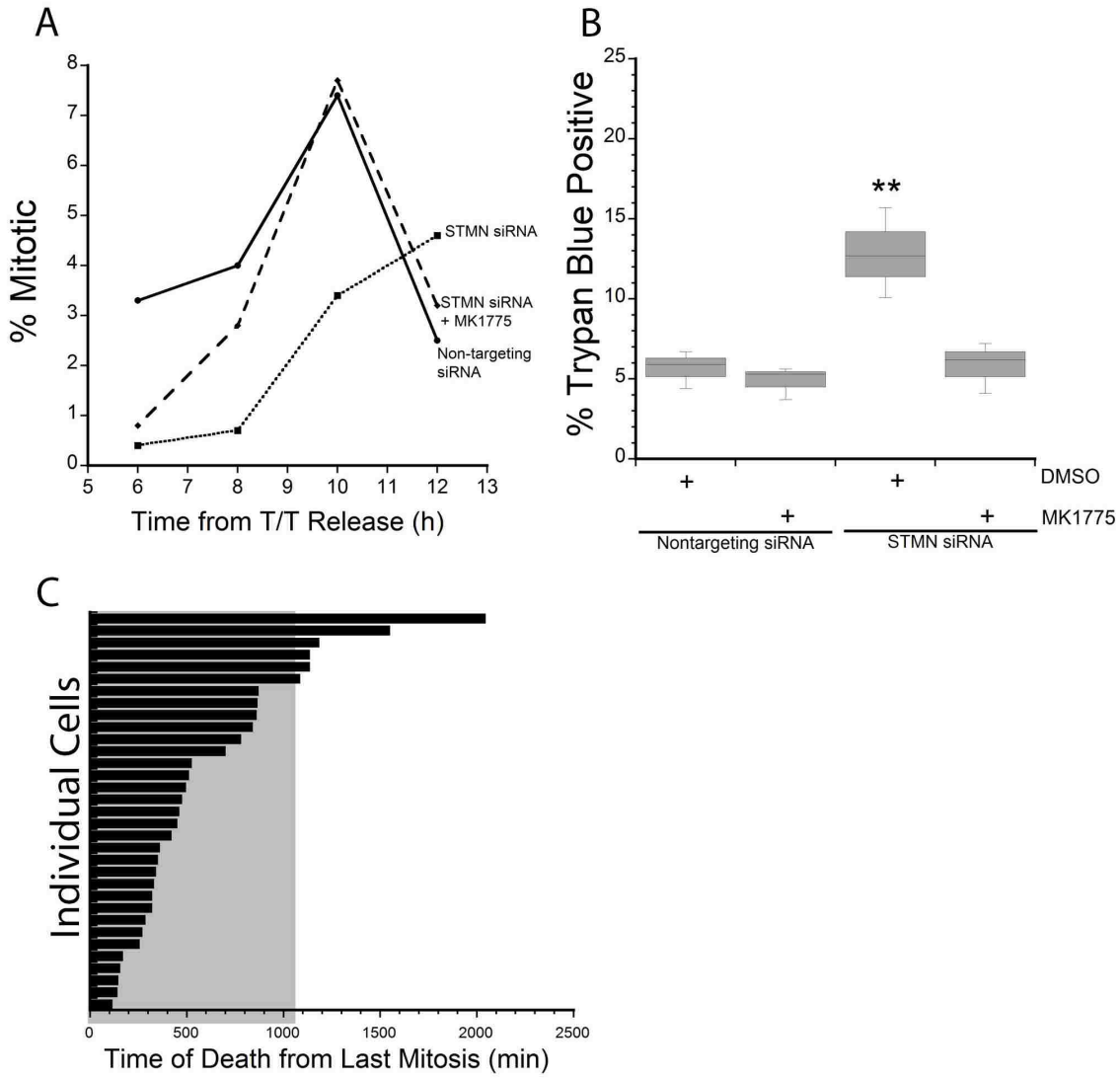

Figure 3.2: A Wee 1 inhibitor relieved both the stathmin depletion-induced cell cycle delay and cell death. Hela cells were synchronized with a double thymidine block and transfected with non-targeting siRNA or siRNA to stathmin were released into medium containing DMSO or the Wee 1 inhibitor MK1775. (A) Mitotic index was determined at 2 hour intervals for 12 hours following release. Wee1 inhibition restored mitotic entry timing in stathmin-depleted cells to that of control treated cells. (B) Viability was assayed at 48 hours following release via trypan blue exclusion. Relieving the mitotic

entry delay in stathmin-depleted cells restored viability to that of control treated cells. (C) Timing of cell death from the last mitosis recorded for individual Hela cells depleted of stathmin. See Figure 3.1C for similar plot for inhibitor BI2536 and S1451 treated cells. Death occurs at variable times following last mitosis. ** denotes $p<0.01$

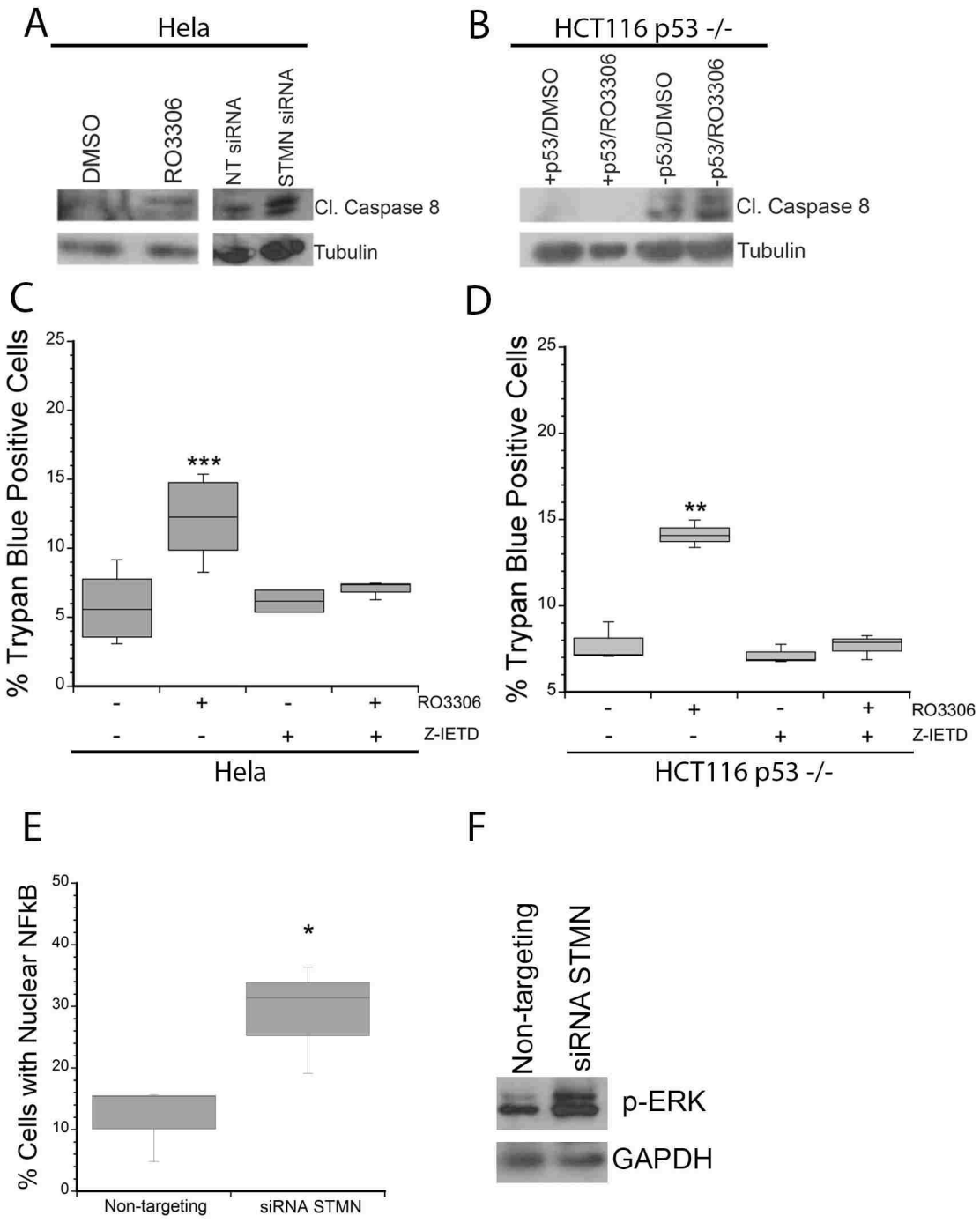

Figure 3.3: A mitotic entry delay triggers caspase 8 activation. Western blot for cleaved caspase 8, reprobed for tubulin as a loading control. (A, left) Hela cells or (B)

HCT116 synchronized with double thymidine block and pulsed with RO3306 for four hours upon release or (A, right) transfected with non-targeting or siRNA to stathmin and treated with Z-VAD. Lysates made 48 hours following transfection or inhibitor pulse. Stathmin depletion or a pulse of CDK1 inhibitor to lengthen G2 increased the level of cleaved caspase 8. (C, D) Hela cells (C) or HCT116 -/-p53 cells (D) were synchronized with a double thymidine block and pulsed with RO3306 for four hours. Following RO3306 inhibitor washout, cells were incubated with medium containing DMSO or Z-IETD for 48 hours and assayed for viability via trypan blue exclusion. Caspase 8 inhibition with Z-IETD restores viability in RO3306 treated cells. (E) Representative graph of immunofluorescence experiments in stathmin-depleted Hela cells stained for NFkB and DNA. Percent of cells with nuclear NKκB staining was determined. Stathmin depletion increased levels of phospho-NFκB consistent with caspase 8 activation. (F) Western blot for phospho-ERK, reprobed for GAPDH as a loading control. Lysates from Hela cells transfected with non-targeting or siRNA to stathmin. Representative images of western blots shown, each experiment was performed at least twice. Graphs are representative of at least three independent experiments. * denotes $p<0.05$, ** denotes $p<0.01$, *** denotes $p<0.001$.

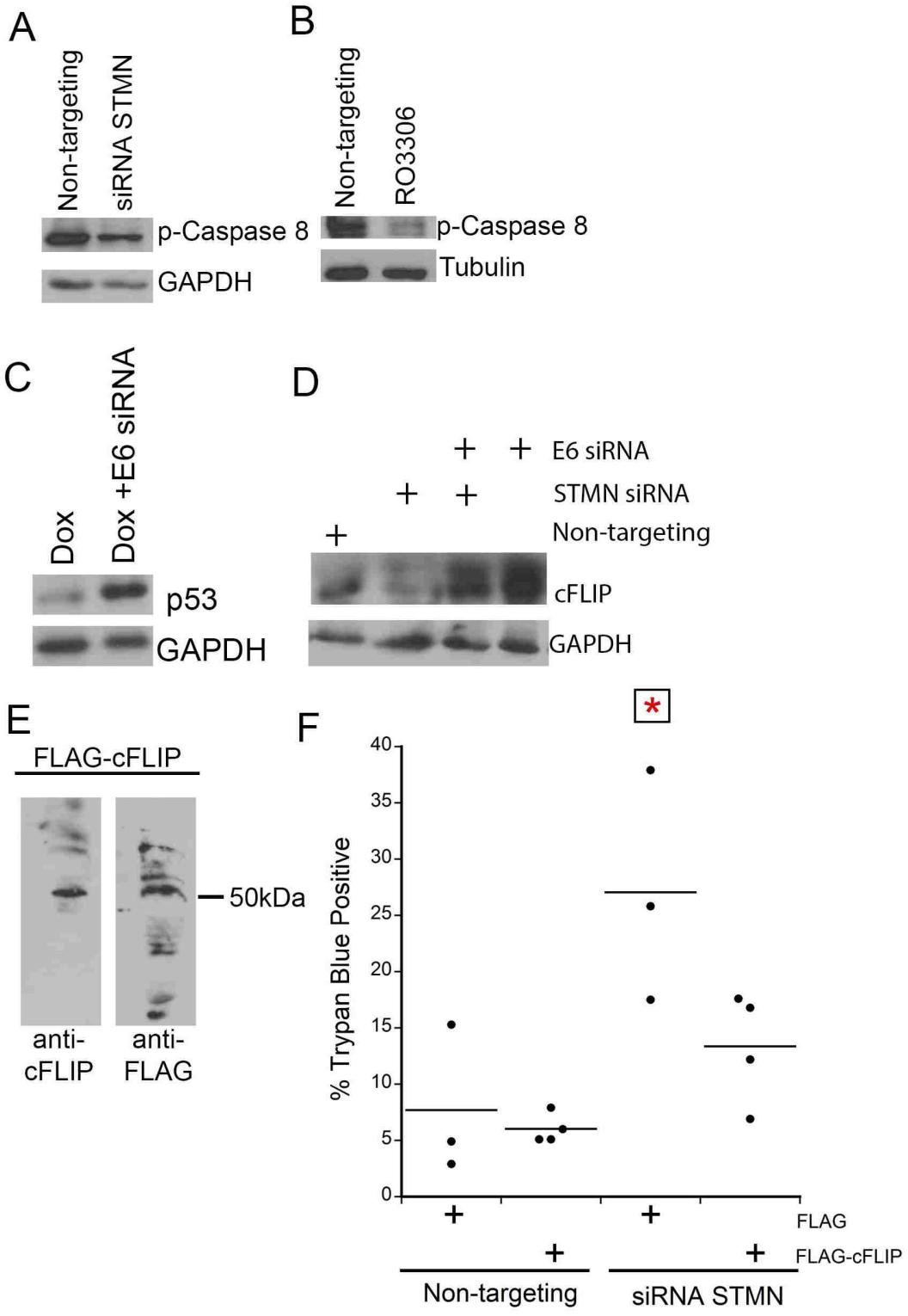

Figure 3.4: Stathmin depletion and cFLIP regulate caspase 8 activity. Western blot for phospho-caspase 8 (Ser387), reprobed for GAPDH or tubulin as a loading control.

Hela cells (A) transfected with non-targeting or siRNA to stathmin or (B) synchronized and pulsed with RO3306 for four hours. Stathmin loss or a pulse of CDK1 inhibitor reduced the level of phospho-caspase 8. (C) Western blot for p53. Lysates were prepared from Hela cells either untransfected or transfected with siRNA targeting HPV protein E6 and treated with Doxorubicin (included to stabilize p53) for 6 hours at 42 hours following transfection. siRNA knockdown of E6 restores p53 level. (D) Western blot for cFLIP, reprobed with GAPDH as a loading control. Hela cells were transfected with non-targeting siRNA, or siRNA to stathmin and/or E6. Cells lacking p53 have decreased cFLIP protein levels compared to Hela cells transfected with E6 to restore endogenous p53. Stathmin depletion reduced the cFLIP level relative to control siRNA-transfected cells. (E) Western blots of lysates from Hela cells transfected with FLAG-tagged cFLIP. Antibodies to FLAG (top) and cFLIP (bottom) produce bands at 55kDA, the approximate molecular weight of cFLIP. (F) Hela cells were transfected with non-targeting siRNA or siRNA to stathmin and a plasmid containing FLAG-tagged cFLIP or empty FLG vector, as noted on the plot. Viability was assayed by trypan blue exclusion at 48 hours following transfection. Exogenous cFLIP expression rescued viability in stathmin-depleted cells to that of control cells. Representative images of western blots shown, each experiment was performed at least twice. Graphs representative of at least three independent experiments. * denotes $p<0.05$.

Chapter 4: Conclusions and Future Directions

Future Directions

Work described in this dissertation lays out the general mechanism by which stathmin depletion leads to a mitotic entry delay that is sufficient to trigger caspase 8 dependent death selectively in cells lacking p53. However, further investigation needs to be done in order to understand how stathmin, both independently and via microtubules, alters AURKA distribution and PLK1 recruitment and activation at centrosomes. Additionally, although stathmin-depleted cells undergo a p53 dependent cell death due to caspase 8 activity, it is unknown whether caspase 8 activation is the result of some unknown death ligand signaling or a stochastic consequence of reduced inhibitors. The following proposed models and experiments would further define the exact pathways and mechanisms affected by loss of stathmin and p53.

Stathmin and PLK1 recruitment

In Drosophila, PLK1 is found associated with microtubules throughout interphase and during cytokinesis. This recruitment and stable association of PLK1 with microtubules was found to be dependent on MAP205, Drosophila homolog to human MAP4 (Archambault 2008). MAP205 tethers PLK1 strongly to microtubules in interphase and phosphorylation by CDK1 on MAP205 relieves interaction of PLK1 and MAP205 and allows PLK1 to move to centrosomes (Archambault 2008). Stathmin-depleted cells have increased microtubules and potentially more MAP4 bound which may translate into more microtubule bound PLK1, decreasing the pool available to localize to centrosomes. Additionally, decreased CDK1 activity may further inhibit release of

tethered PLK1 from MAP4 and microtubules. This may explain the two-part activation scheme for PLK1. MT depolymerization restores the amount of active PLK1 in prophase cells perhaps by untethering Map4 and PLK1 from microtubules. However, Plk1 activation may require dissociation of PLK1 from MAP4, which likely still requires CDK1 activity. Our inability to detect PLK1 at centrosomes with normal timing after nocodazole treatment may be the result of PLK1/MAP4 interactions that hinder PLK1 docking at centrosomes. Alternatively, since MT depolymerization rescues mitotic entry timing and restores levels of active PLK1 in prophase cells, it is possible that PLK1/MAP4 interactions may mask antibody recognition while still allowing PLK1 recruitment that was not detectable by immunofluorescence. This may explain how microtubule depolymerization rescues the mitotic entry delay and accumulation of active PLK1 around chromatin but not levels of centrosome associated PLK1.

To test whether PLK1 is tethered to microtubules in interphase we have looked for co-localization of PLK1 with α- tubulin via indirect immunofluorescence. PLK1 was not visible on microtubules in Hela cells using PLK1 and tubulin antibodies. However, expression of PLK1-GFP as done by Archambault et al. may reveal co-localization of PLK1 on MTs. Using a GFP tagged construct may alleviate issues with masking of antibody binding sites and provide a more robust fluorescence signal. Alternatively, microtubule co-pelleting assays may reveal association of PLK1 with polymerized tubulin. If this model is correct, stathmin depletion is predicted to increase both Map204 and PLK1 association with microtubules either via immunofluorescence or co-pelleting assay. Furthermore, if MAP4 tethering of PLK1 to MTs inhibits PLK1 centrosomal localization, depletion of MAP4 would rescue the PLK1 activation in stathmin-depleted

cells by increasing the cytoplasmic pool of PLK1 available for centrosome recruitment. Similarly, over expression of MAP4 would likely mimic PLK1 recruitment defect seen with stathmin-depletion.

Stathmin and AURKA Distribution

We observe a wider distribution, equivalent to a roughly two-fold increase in volume, of total and active AURKA in stathmin-depleted cells. We hypothesized that a wider distribution of AURKA had a dilution effect on the kinase's concentration at the centrosome. Since AURKA needs to dimerize in order to autophosphorylate, a dilution of monomers would decrease dimer formation and limit autoactivation, which has been demonstrated *in vitro* (Joukov 2010). Using known kinetics of AURKA activation from computational modeling, a two fold dilution of AURKA concentration is predicted to yield a 50% decrease in active kinase which is precisely the decrease in activity measured upon stathmin depletion (Zou 2011, Silva and Cassimeris *unpublished*). The mechanism behind a wider distribution of AURKA is not simply due to a wider distribution of gamma-tubulin since that centrosome marker retains its normal size in stathmin-depleted cells. Instead, increased microtubule nucleation could spread AURKA beyond the centrosome. Depletion of stathmin not only leads to increased microtubule stability but also increased nucleation of new microtubules. AIR1, a *C. elegans* homolog of AURKA, has been shown to localize to the base of nascent microtubules as well as to other molecular scaffolds within the centrosome. Increased nucleation may provide increased binding area for AURKA on newly nucleated microtubules, leading to a dilution of total AURKA concentration. To test this model, nucleation could be increased by some other

method such as BRCA1 inhibition, as BRCA1 directly inhibits centrosomal microtubule nucleation (Sankaran 2007). Similarly, overexpression of EB1, a microtubule plus tip binding protein, may also increase nucleation by conferring increased microtubule stability (Holzbaur 2003). If this model is correct, increased nucleation by any means should also result in a wider distribution of AURKA as well as decreased AURKA activation. Similarly, it would also be expected that decreasing or eliminating nucleation such as depolymerizing microtubules would rescue AURKA activation. However, we found that, in the absence of microtubules, AURKA is unable to localize at centrosomes and remains inactive (Silva and Cassimeris 2013). This suggests that AURKA requires MT for centrosome recruitment but that there must be some normal density of microtubules to facilitate both AURKA recruitment and proper centrosomal concentration.

Caspase 8 Activation

Death ligand independent

Stathmin depletion or partial inhibition of AurA and PLK1 at mitotic entry decreases cell viability due to stochastic caspase 8 activation and apoptosis (Chapter 3). It is possible that cell death occurs in a ligand independent mechanism. There are precedents for caspase 8 induced death in the absence of death receptor ligand binding such as from genotoxic stress or loss of caspase 8 inhibitors (Tenev 2011, Day 2008). Under certain conditions a caspase-activating platform composed of RIP1/FADD/caspase 8, called a ripoptosome, assembles spontaneously, independent of ligand signaling (Tenev 2011). Ripoptosome activation is accompanied by NFκB mediated production of

autocrine TNF and depletion of cIAPs (cellular inhibitors of apoptotic proteins) followed by caspase 8-dependent death (Tenev 2011).

Since we observed robust NFκB activation following stathmin depletion, suggesting that the cell death observed in the current study is apoptosome dependent. To test if NFκB is mediating autocrine TNF signaling, further experiments might include assaying levels of TNFα in media of stathmin-depleted cells or clustering of TNFα receptors in the plasma membrane. Conversely, a complementary approach is to test whether NFκB prevents cell death. To test the role of NFκB activation in stathmin depletion triggered cell death, we can express dominant negative IκB, cellular inhibitor of NFκB, and look for rescue of cell viability.

The role NFκB signaling is not fully understood and can result in contradictory outcomes, promoting either survival or cell death depending on stimuli and circumstances (Fan 2002). It is possible that NFκB signaling in stathmin-depleted cells promotes survival but in a p53 dependent fashion. NFκB has been shown to upregulate cFLIP to inhibit full caspase 8 activity and cell death (Kreuz 2001). However, both the protein and mRNA of cFLIP is short lived. Upon treatment with cyclohexamide (a protein synthesis inhibitor) or Actinomycin D (RNA synthesis inhibitor) cFLIP levels become nearly undetectable after 1 hour treatment and cells are sensitized to TNF stimulated death (Fulda 2000). This suggests that cells are particularly sensitive to cFLIP levels and any small changes can produce significant shifts in cell programming.

It has been suggested that p53 also positively regulates cFLIP levels via transcription and protein stability (Bartke 2001). Therefore in the absence of p53, despite

NFκB upregulated transcription, cFLIP levels may still be decreased. In order to fully understand how p53 regulates cFLIP level, we should measure changes in cFLIP mRNA with or without stathmin and/or p53. If mRNA is unchanged by p53 status, it would suggest cFLIP protein level is altered by decreased protein stability. In p53 deficient cells, inhibiting protein degradation might restore cFLIP level and rescue the death phenotype.

In the absence of death ligand-signaling, caspase 8 activation may result solely from decreased cFLIP level. For example, cFLIP knockdown in MCF-7 breast cancer cells was shown to be sufficient to induce caspase 8 activation and cell death (Day 2008). cFLIP acts as a decoy receptor for caspase 8 and loss of cFLIP increases the likelihood of caspase 8 homodimerization and activation. If this model is correct, immunoprecipitation of caspase 8 in p53 deficient cells should show increased association of caspase 8 homodimers with death inducing signaling complex, DISC components. Caspase 8 homodimerization coupled with loss of protective phosphorylation at Serine 387, as seen with decreased CDK1 activity, may be sufficient to allow full caspase 8 proteolysis in the absence of cFLIP inhibition.

Death Ligand Dependent

It is possible that caspase 8 activation in stathmin-depleted or CDK1 inhibited cells is triggered by autocrine or paracrine release of a death ligand. Preliminary tests exposing naïve cells to conditioned media from stathmin-depleted cells failed to increase cell death (Silva and Cassimeris *unpublished*). This result does not exclude paracrine signaling since such signals are likely to be transient and ligands are likely bound to their

respective receptors shortly after secretion. It is possible that the resulting extracellular concentrations of death ligand are insufficient to induce death in naïve cells. More detailed examination of conditioned media, such as by Liquid Chromatography-Mass Spectrometry or 2-Dimensional Nuclear Magnetic Resonance may reveal differences in cytokine or other death ligand levels.

Death receptors only cluster upon ligand binding. Examination via immunofluorescence for coupling of various death receptors such as TNFR, FasR and TRAILR could provide evidence for paracrine or autocrine signaling that is not detectable with conditioned media experiments. Given high NFkB activation, signal transduction through TNF receptor is likely. For example, under certain stimuli, cIAPs are recruited to ligand-boundTNF receptor clusters initiating signal cascades that result in NFκB activation and MAPK signaling which both increase survival. Interestingly, we have observed both increased activation of NFkB and ERK with stathmin depletion. It is possible that an external signal activates a TNF mediated survival signal that is inhibited by some other effect of stathmin or p53 loss, such as decreased cFLIP levels.

Conclusions

Work described in this dissertation outlines a previously unknown mechanism regulating mitotic entry timing via both stathmin and microtubules. Timely activation of AURKA and PLK1 requires both spatial and temporal control that is organized in part by changes in microtubule stability that occur at the G2/M transition. Mitotic cells depend on active anti-apoptotic signaling, conferred in part by CDK1 activity. Delaying mitotic onset by slowing activation kinetics of CDK1, such as by stathmin depletion, increases

vulnerability to cell death after division. In cells without functional p53 slowing mitotic entry, shifts the balance of apoptotic signaling to increase the odds of cell death and represents a potent and selective strategy for treating the majority of cancer cell types.

References:

1. Archambault, V., D'Avino, P.P., Deery, M.J., Lilley, K.S., and Glover, D.M. (2008). Sequestration of Polo kinase to microtubules by phosphopriming-independent binding to Map205 is relieved by phosphorylation at a CDK site in mitosis. Genes & development 22, 2707-2720.
2. Joukov, V., De Nicolo, A., Rodriguez, A., Walter, J.C., and Livingston, D.M. (2010). Centrosomal protein of 192 kDa (Cep192) promotes centrosome-driven spindle assembly by engaging in organelle-specific Aurora A activation. Proceedings of the National Academy of Sciences of the United States of America 107, 21022-21027.
3. Zou, J., Luo, S.D., Wei, Y.Q., and Yang, S.Y. (2011). Integrated computational model of cell cycle and checkpoint reveals different essential roles of Aurora-A and Plk1 in mitotic entry. Molecular bioSystems 7, 169-179.
4. Sankaran, S., Crone, D.E., Palazzo, R.E., and Parvin, J.D. (2007). Aurora-A kinase regulates breast cancer associated gene 1 inhibition of centrosome-dependent microtubule nucleation. Cancer research 67, 11186-11194.
5. Ligon, L.A., Shelly, S.S., Tokito, M., and Holzbaur, E.L. (2003). The microtubule plus-end proteins EB1 and dynactin have differential effects on microtubule polymerization. Molecular biology of the cell 14, 1405-1417.
6. Silva, V.C., and Cassimeris, L. (2013). Stathmin and microtubules regulate mitotic entry in HeLa cells by controlling activation of both Aurora kinase A and Plk1. Molecular biology of the cell 24, 3819-3831.

7. Tenev, T., Bianchi, K., Darding, M., Broemer, M., Langlais, C., Wallberg, F., Zachariou, A., Lopez, J., MacFarlane, M., Cain, K., and Meier, P. (2011). The Ripoptosome, a signaling platform that assembles in response to genotoxic stress and loss of IAPs. Molecular cell 43, 432-448.
8. Day, T.W., Huang, S., and Safa, A.R. (2008). c-FLIP knockdown induces ligand-independent DR5-, FADD-, caspase-8-, and caspase-9-dependent apoptosis in breast cancer cells. Biochemical pharmacology 76, 1694-1704.
9. Fan, C., Yang, J., and Engelhardt, J.F. (2002). Temporal pattern of NFkappaB activation influences apoptotic cell fate in a stimuli-dependent fashion. Journal of cell science 115, 4843-4853.
10. Kreuz, S., Siegmund, D., Scheurich, P., and Wajant, H. (2001). NF-kappaB inducers upregulate cFLIP, a cycloheximide-sensitive inhibitor of death receptor signaling. Molecular and cellular biology 21, 3964-3973.
11. Fulda, S., Meyer, E., and Debatin, K.M. (2000). Metabolic inhibitors sensitize for CD95 (APO-1/Fas)-induced apoptosis by down-regulating Fas-associated death domain-like interleukin 1-converting enzyme inhibitory protein expression. Cancer research 60, 3947-3956.
12. Bartke, T., Siegmund, D., Peters, N., Reichwein, M., Henkler, F., Scheurich, P., and Wajant, H. (2001). p53 upregulates cFLIP, inhibits transcription of NF-kappaB-regulated genes and induces caspase-8-independent cell death in DLD-1 cells. Oncogene 20, 571-580.

Victoria Caruso Silva
Department of Biological Sciences
111 Research Drive
Lehigh University
Bethlehem, PA 18210
vic208@lehigh.edu

ACADEMIC PREPARATION

2008-Present **LEHIGH UNIVERSITY** Bethlehem, PA

Doctoral Candidate, Cell and Molecular Biology
Cumulative GPA: 3.9

2001-2005 **SETON HALL UNIVERSITY** South Orange, NJ

Bachelor of Science, Biology; Classical Studies (Minor)
Cumulative GPA: 3.9

RESEARCH AND PROFESSIONAL EXPERIENCE

2008- Present **LEHIGH UNIVERSITY** Bethlehem, PA

Research Assistant, Department of Biological Sciences

- Thesis work explores the molecular mechanism by which loss of a microtubule regulator, stathmin, delays mitotic entry via decreased cdk1 activation and the mechanism by which a decrease in cdk1 activity selectively triggers caspase 8 dependent death selectively for cells missing p53.

2006 - 2008 **SANOFI-AVENTIS** Bridgewater, NJ

Assistant Scientist, General Toxicology/Molecular and Cellular Toxicology

- Served as a Study Coordinator on Preclinical Safety studies (General Toxicology) and assisted in discovery research (Molecular Toxicology) characterizing the role of the antioxidant response elements (PXR, NRF2) in oxidative stress.

2003 – 2004 **SETON HALL UNIVERSITY** South Orange, NJ

Undergraduate Research Assistant- Biology Honors Program, Neuroimmunology Lab

- Examined the effect of opiates on brain metabolites in a model of endotoxin tolerance via proton NMR.

RESEARCH EXPERIENCE

- Experienced with microtubules/cytoskeleton, mammalian cell cycle, apoptosis, pharmacokinetics and basic pharmacology.

TECHNICAL EXPERTISE

- Experienced with phase, widefield and confocal fluorescence microscopy (including photobleaching and bifluorescence techniques) of fixed and live specimens.
- Additional skills include: tissue preparation/ fixation for microscopy, mammalian cell culture, molecular cloning (including PCR and primer design), flow cytometry, Bradford protein assay, SDS PAGE/Western blot, agarose electrophoresis, DNA/RNA transfection, proliferation and viability assays (trypan blue exclusion, propidium iodide uptake, MTS, cell-titer glo),.

TEACHING EXPERIENCE

2011- 2012	**Lehigh University**	*Teaching Assistant*
2009 - 2011	**Lehigh Valley STEM**	*NSF Teaching Fellow*
2005 – 2006	**University of Maryland**	*Teaching Assistant*
2005	**Seton Hall University**	*Teaching Assistant/Tutor*

AWARDS AND HONORS

2013	Marjorie Nemes Fellowship
2012	Lehigh Dept. of Biological Science Spotlight Graduate Student
2012	Lehigh University College of Arts and Science Travel Award
201	Lehigh Graduate Student Senate Travel Award
2010	Lehigh University Graduate Open House Poster Competition
2009-2011	NSF- Lehigh Valley STEM Fellowship
2008-2009	Lehigh University Fellowship
2004	Clare Booth Luce Summer Research Grant
2001-2005	Seton Hall University Full Tuition Scholarship

PROFESSIONAL MEMBERSHIPS

American Society for Cell Biology

Pennsylvania Academy of Science

PUBLICATIONS

Silva VC and Cassimeris L. 2014. Delayed mitotic entry leads to caspase 8 dependent death in p53 deficient cells via reduced CDK1 activity and cFLIP levels. *PNAS* (*in prep*)

Silva VC and Cassimeris L. 2014. CAMSAPs Add to the Growing Microtubule Minus End Story. *Developmental Cell* 28(3): 221-222.

Silva VC and Cassimeris L. 2013 Stathmin and microtubules regulate mitotic entry in Hela cells by controlling activation of both Aurora A and Plk1. *Molecular Biology of the Cell* (24):3819-31.

Carney BK, Caruso Silva V, Cassimeris L. 2011. Stathmin depletion delays cell cycle progression via increased microtubule stability in cells lacking p53. *Cytoskeleton* 60(5):278-289.

Cassimeris L, Silva VC, Tong Q, Miller E, Molnar C, Fong J. 2012. Fueled by Microtubules: does tubulin/dimer partitioning regulate intracellular metabolism? *Cytoskeleton* 69(3): 133-43.

ABSTRACTS/POSTER PRESENTATIONS

2013 American Society for Cell Biology 53rd Annual Meeting New Orleans, LA

Victoria Caruso Silva and Lynne Cassimeris. "Stathmin and microtubules regulate mitotic entry in Hela cells by controlling activation of both Aurora Kinase A and Plk1"

2012 American Society for Cell Biology 52nd Annual Meeting San Francisco, CA

Victoria Caruso Silva and Lynne Cassimeris. "Stathmin regulates mitotic entry in Hela cells by controlling activation of both Aurora A and Plk1"

2010 American Society for Cell Biology 50th Annual Meeting Philadelphia, PA

Victoria Caruso and Lynne Cassimeris "Stathmin depletion in cancer cells: An Arresting Phenomenon"

2012 Penn Muscle Institute 19th Ann. Retreat and Symposium Philadelphia, PA

Victoria Caruso Silva, Bruce Carney and Lynne Cassimeris. "Building Cellular Complexity Two Molecules at a Time: Loss of a Microtubule Destabilizer, Stathmin, and p53 synergize to Delay the Cell Cycle"

2004 Seton Hall University Petersheim Academic Exposition South Orange, NJ

2003 Society for Neuroscience 33rd Annual Meeting

Chang S., Chen R., Silva J., Caruso V., Malellari L. "Mu Opioid Receptor, Cell Death, and Pro- Inflammatory Cytokine Expression in the Brain of Rats Following Treatment with Lipopolysaccharide"

2003 Seton Hall University Graduate Medical Education Colloquium South Orange, NJ

PROFESSIONAL CONFERENCES

2013 American Society for Cell Biology Annual Meeting New Orleans, LA

2012 American Society for Cell Biology Annual Meeting San Francisco, CA

2012 Pennsylvania Muscle Institute Retreat and Symposium Philadelphia, PA

2012 Biophysical Society Pennsylvania Network Meeting Bethlehem, PA

2010 Pennsylvania Muscle Institute Retreat and Symposium Philadelphia, PA

2010 American Society for Cell Biology Annual Meeting Philadelphia, PA

TALKS

2013 BioScience in the 21st Century (Invited Lecture) Lehigh University
"The Cell Cycle and Cancer" Bethlehem, PA

2013 Biological Sciences Colloquium Seminar Lehigh University
"In the symphony of survival, timing is everything" Bethlehem, PA

2009 Lehigh Valley STEM Group Meeting Bethlehem, PA
"The World of Microtubules"

2005 Seton Hall University Undergraduate Honors Thesis South Orange, NJ
"Changes in brain metabolites induced by chronic morphine and acute LPS measured by H^1 NMR"

COCURRICULAR ACTIVITIES

2012-2013 Biological Society of Graduate Students (B.O.G.S., *Secretary*)
2008-2012 B.O.G.S. (*Student Liaison to the Graduate Committee*)
2001-2005 Seton Hall University Biology Society
2001-2005 Seton Hall University Biology Journal Club
2002-2005 Seton Hall University Classics Club (*President*)
2001-2005 Seton Hall University Power Choir

GRADUATE COURSEWORK

Elements of Biochemistry I and II
Advanced Cell Biology
Molecular Genetics
Molecular Cell Biology II
Eukaryotic Signal Transduction
Virology
Methods in Molecular Genetics
Pharmacology and Toxicology
Select Topics: Cancer Cell Biology
Select Topics: Microtubules and Cellular Metabolism